ORIGIN AND MINERAL RESOURCE POTENTIAL OF ROSEDALE DISTRICT, SOCORRO COUNTY, NEW MEXICO

By

William T. Zutah

Department of Mineral Engineering
New Mexico Institute of Mining and Technology

Submitted as partial fulfillment of the
Requirement for Degree of
Masters of Science in Mineral Engineering
Fall 2017

ABSTRACT

The Rosedale volcanic-epithermal mining district lies in the northern region of the Mogollon-Datil volcanic field, which is a part of a late Eocene-Oligocene volcanic province that extends from west-central New Mexico south to Chihuahua, Mexico. The district is located on the northeastern slope of the San Mateo Mountains, about 25 miles south of Magdalena, New Mexico.

The Rosedale district, an important gold-producing district in Socorro County, was discovered in 1882 and produced an estimated total value of metals of $500,000 from 28,000 oz gold and 10,000 oz silver (McLemore, 2017). The Rosedale and Bell are the main patented claims with mines that yielded ore from underground workings along parallel fault zones. An estimated historic resource amount of 1.5-2 Mt containing 0.3 oz/ton gold is reported to remain in the district (Perry, Knox and Kaufman, Inc., 1975). The Rosedale district is one of the few gold-rich, silver-poor volcanic-epithermal districts in New Mexico.

Mineralization and alteration in the Rosedale district was probably developed shortly after eruption and deposition of the 27.4 Ma South Canyon Tuff (McIntosh et. al., 1992a). Argillic alteration comprising generally clays, sanidine, and quartz, cross-cuts fault zones that juxtapose altered and unaltered rock. Structurally controlled mineralization is hosted in well-developed breccia and sheared rhyolite porphyry and is locally cemented by banded bluish-white quartz. The shear-zone mineralization extends into a footwall of white rhyolite porphyry. The veins carry free-milling gold and are usually associated with hematite and manganese oxides occurring as replacements of pyrite grains and stringers, and as coatings on fracture surfaces. Oxidized sulfide, as pyrite now replaced by hematite and goethite as shown by electron microprobe analyses, exist above the current phreatic level (depth approximately 723 feet below shaft elevation). Replacement of magmatic or late magmatic biotite is common.

Electron microprobe analyses reveal elevated gold content, with little or no silver, within hematite grains. Sphalerite was found in nominal amounts in a sample from the Rosedale mine and was generally replaced by hematite through oxidation. A copper phase, which occurs in trace amounts, is associated with the sample that had elevated whole-rock gold concentrations (3.61 ppm Au, ROSE004, from the Rosedale mine).

Most of the waste rock piles surrounding the mine are suitable for backfill material because they are thoroughly oxidized and contain only nominal residual pyrite. In addition, a borrow pit was used as cover for the Rosedale tailings, and no ARD has been observed from this material; as such, this material would be suitable for backfill material. Regarding potential environmental issues with Rosedale district waste rock piles and tailings, the study shows that only one sample plotted in the "uncertain" field on the usual ARD diagrams; all other samples plotted as nonacid-forming. Notably, the Rosedale samples contain low concentrations of all metals.

It is concluded that the Rosedale district has a high mineral-resource potential with a high level of certainty for gold-silver as low-sulfidation, quartz-dominant, low base metal, volcanic-epithermal vein deposit with an unknown mineral-resource potential with a low degree of certainty for base metals at depths below the present precious-metal workings.

ACKNOWLEDGEMENTS

My ultimate appreciation goes to my advisors and committee members, Dr. Virginia McLemore, Dr. Navid Mojtabai, Dr. William X. Chavez, and Dr. Ingar Walder for their technical support, commitment, encouragement and constructive and earnest assessment. I greatly appreciate the assistance from John Asafo-Akowuah, Ashlynne Winton, Marcus Silva, Joseph Blais, Bon Durica, John Durica, and Benjamin Sears who supported field activities during the study. My appreciation also goes to the mine owners of the Rosedale mine, Mr. and Mrs. Holley, who allowed access to the Holley-Rosedale Exploration project area for mapping and sampling of mine features. All the historical information received were scanned into digital formats and archived in the New Mexico Bureau of Geology and Mineral Resource (NMBGMR) database. My appreciation to Amy Trivitt-Kracke for making all these data accessible for the project work. Virgil W. Lueth and Kelsey C. McNamera provided support in the XRD lab while Lynn Heizler helped at the electron microprobe lab during sample analysis.

This work is part of the economic geology research by NMBGMR to evaluate the mineral resources potential in New Mexico. This project was funded by Energy Minerals and Natural Resources Department (Abandoned Mine Lands Bureau) and the U.S. Department of the Interior, Office of Surface Mining and Reclamation (OSMRE). Additional funding of my research was by the New Mexico Bureau of Geology and Mineral Resources (NMBGMR), Mineral Engineering Department of New Mexico Tech, Society for Mining, Metallurgy and Exploration (SME), and New Mexico Geological Society (NMGS). The Cameca SX-100 electron microprobe at NMIMT was partially funded by NSF Grant STI-9413900.

TABLE OF CONTENT

LIST OF FIGURES

LIST OF TABLES

APPENDICES

CHAPTER ONE: INTRODUCTION

The volcanic-epithermal deposits in the Rosedale district are in hydrothermal quartz-rich breccia veins along faults cutting the South Canyon Tuff. The district was one of the important gold-producing districts in Socorro County, and the Rosedale and Bell mines were the only two major properties that produced Au-Ag in the district. The Rosedale mine was discovered in 1882 but mining did not start until 1886 and operations finally ceased in 1941. The Bell mine, located about a mile southwest of the Rosedale mine and which has a history roughly paralleling, produced a small amount of gold and silver in the early 1900's but detailed history of operations is currently unknown.

The veins system and mineralization association in the Rosedale district was examined previously and some conclusions from these studies are summarized below -

During middle Tertiary time eruptions of rhyolite, andesite, and basalt latite took place and extensive areas are covered by these flows. These volcanic, in some places, contain gold and silver bearing veins. Mineralization also exists in porphyritic rhyolite flows and breccias (Lindgren et. al, 1910).

Lasky (1932) recognized that, the brecciated and sheared rhyolite is partly cemented by banded bluish-white quartz. After re-fracturing of these rocks, the entire mass has been recemented with glassy vein quartz. Examination of footwalls and hanging-wall of mineralized zones have been silicified, and the outcrop stands out clearly. The rhyolite in the few higher ridges shows more evidence of flow banded structures than that in the vein walls and may indicate different sequence of flow. Observations appears to hypothesize that the mineralized veins have been covered by a later flow. This can be an important feature, since there may be a number of workable veins in the district, which do not outcrop (Lasky, 1932).

Much of the north-central part of the Rosedale volcanic-epithermal gold district is underlain by areas of altered and mineralized intra-cauldron South Canyon Tuff. Areas affected by intense argillic alteration of varying degrees are concentrated along the north-northwest trending faults between North Canyon and Big Rosa Canyon. Mineralization and alteration in the Rosedale district was probably shortly after emplacement of the South Canyon Tuff. The driving force for the epithermal gold system within the district is mostly likely associated with a sub-caldera pluton (Ferguson, 1986).

These above observations clearly indicate the potential of mineralization associated with volcanic epithermal vein system. Other volcanic epithermal deposits have also been discovered in mining districts in New Mexico, such as Red River in Taos County; Cochiti in Sandoval County; Socorro and Mill Canyon in Socorro County, Mogollon in Catron County; Apache, Black Range, and Hillsboro in Sierra County; and Steeple Rock and Kimball in Grant County and are similar to the Rosedale. Other than North and McLemore (1986, 1988) and McLemore (1996), very little comparison between these districts has been attempted.

Purpose of the Investigation

The objectives of my investigation are to determine the origin of Au-Ag mineralization within Rosedale district and examine the relationships with similar ore deposit types within New Mexico. This research will present an evaluation of the mineral resource potential of the study area. The following are the primary purpose and important goals for this research: -

1. Understanding the ore relationships at the Rosedale mining district, provides data for correlating rock types between the Rosedale district and other areas within Socorro County, and other parts of New Mexico, where new exploration for undiscovered deposits could occur.
2. An understanding of the structural correlation can be used to locate other types of associated deposits.
3. The overall relationships between stratigraphy, structure, mineralization and the distribution on intrusive rocks are important in evaluating the mineral resource potential of the study area.
4. This investigation will improve the geologic models for volcanic-epithermal vein deposits in Mogollon-Datil volcanic field in New Mexico.
5. Characterization of the waste rock piles will assist to determination the suitability of these piles as a backfill in the ongoing AML program.

Location and Accessibility

The Rosedale mining district is located in Socorro County, New Mexico and lies within the Grassy Lookout quadrangle, at the northeastern slope of the San Mateo Mountains, which is about 25 miles south of Magdalena, New Mexico.

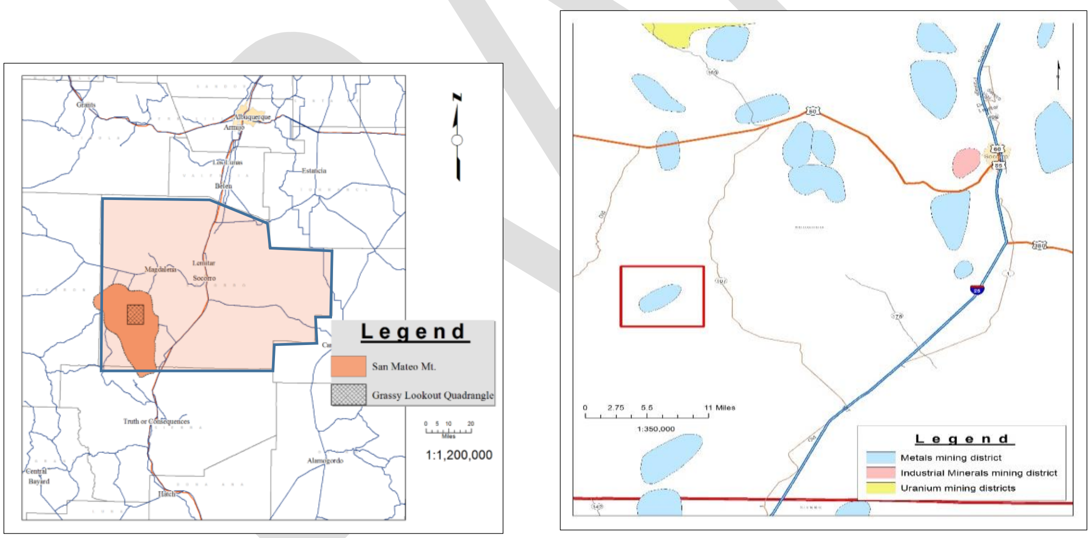

Figure 1:Rosedale mining district is located on Grassy Lookout quadrangle, Socorro County, NM

The Rosedale and Bell mine are the two (2) main mines, situated about two miles east-southeast of Withington Wilderness and they can be accessed via U.S. Highway 60 from Socorro, 30 miles west to Magdalena and about 30 miles on southwest dirt road leading from State Highway 107 to Forest Service Road 330. The district is situated about 7 miles on Forest Service Road 330 from State Highway 107 (Fig. 1).

Previous Investigations

Reconnaissance investigation of the Rosedale district in San Mateo Mountains by Lindgren et. al., (1910) revealed Au veins are hosted by mainly rhyolite with breccias, tuff, and devitrified glass. General characteristics of the deposits observed contain principally free-milling ore in a gangue of bluish-white quartz, carrying in places where small amounts of oxide of iron and manganese oxide appear to be associated with the richer grades of ore. Lindgren et al (1910), also observed from the Rosedale mine that the ore occur in a well-marked fissure vein in the rhyolite having a strike of about N. 20° W. and dips at a high angle (80°) toward the east. The width of the veins is usually from 3 to 5 feet at the surface but was said to reach a width of 12 feet at depth. From underground observation, two (2) ore shoots were located and they appear to merge at depth. Above the groundwater level, a depth of 726 feet, the ore is predominantly oxidized and contains free-milling gold.

Lasky (1932) confirmed most of the observation made by Lindgren et. al. (1910) in the earlier studies. But further deduced a structural relation of the ore in a tunnel found at the Rosedale. An interesting feature at the Rosedale tunnel is the fact that the width of the veins becomes smaller as the dip of the veins steepens, and accompanying this change is the diminishing amount of manganese present. The change for the amount of manganese may be referred in part to the depth of oxidation, but it is significant that this change accompanies a marked change in both the physical character and attitude of the vein. It is probable that this circumstance indicating the location of the ore shoot was controlled by the warp that is indicated by the change in dip along the fault surface. Similar warps may have caused the localization of other shoots. From the surface, the mineralized veins are traceable for some distance to the north and south but it may have been covered by a later flow. The Robb and Lane mine located at the south and north of the Rosedale mine respectively shows very similar signature in many respects to the Rosedale veins. Bell mine also shows similar vein systems and lies on a parallel structure to the Rosedale veins. If this hypothesis is true, then there may be a number of workable veins in the district that do not outcrop. The Bell mine also shows similar vein systems and lies on a pararell structure to the Rosedale veins (Lasky, 1932).

The Rosedale and Bell gold are hosted in the South Canyon Tuff formation. At these mines, according to Neubert (1983), mineralized veins are parallel to basin and range faults that trend N340^{o} and dip about 75^{o} to the west. Argillic alteration, associated with the mineralization, is found parallel to or adjacent to faults throughout the area (Ferguson, 1990; Fig. 11). Zones of alteration are defined by sanidine phenocrysts with white and chalky coloration and occurs along the Lemitar-South Canyon contact on the west side of North Canyon. Along this contact, alteration is most advanced in thin poorly welded tuff just below the vitrophyre, which is the South Canyon Tuff Formation. Alteration extends downward about 98 feet into the Lemitar Tuff, but upward only about 32 feet into the South Canyon vitrophyre.

The geological history can be divided into three (3) main sequences: 1) the late Oligocene formation of the Mt. Withington caldera. 2) Late Oligocene episode of thin-skinned style extension within the caldera. 3) Miocene through present phase of thick-skinned basin and range style extension (Ferguson, 1990). Ferguson (1990) observed that much of the north-central part of the area is underlain by large areas of altered and mineralized intracaldera South Canyon Tuff. The most intense alteration is concentrated along the north-northwest trending faults between North Canyon and Big Rosa Canyon. Mineralization and alteration in the Rosedale district was probably shortly after emplacement of the South Canyon Tuff. Argillic alteration typically overprints and cross-cuts fault zones attributed to the late Oligocene thin-skinned phase of extension, but younger basin and range style high-angle faults sometimes juxtapose altered and unaltered rock. The driving force for the epithermal system was most likely a sub-caldera pluton. Ferguson (1986) also indicated that the South Canyon Tuffs are crystal-poor to crystal-rich quartz, sanidine bearing rhyolite ash-flow Tuff. It fills a structural basin (Mt. Withington Caldera) in the north-central part of the study area, where it is at least 600m thick. At the thickest areas, South Canyon Tuff is invaded by epithermal gold veins and associated zones of argillic alteration in the Rosedale mining district. Mineralization occurs along basin and range faults, which trend about N30°E (Fig. 2)

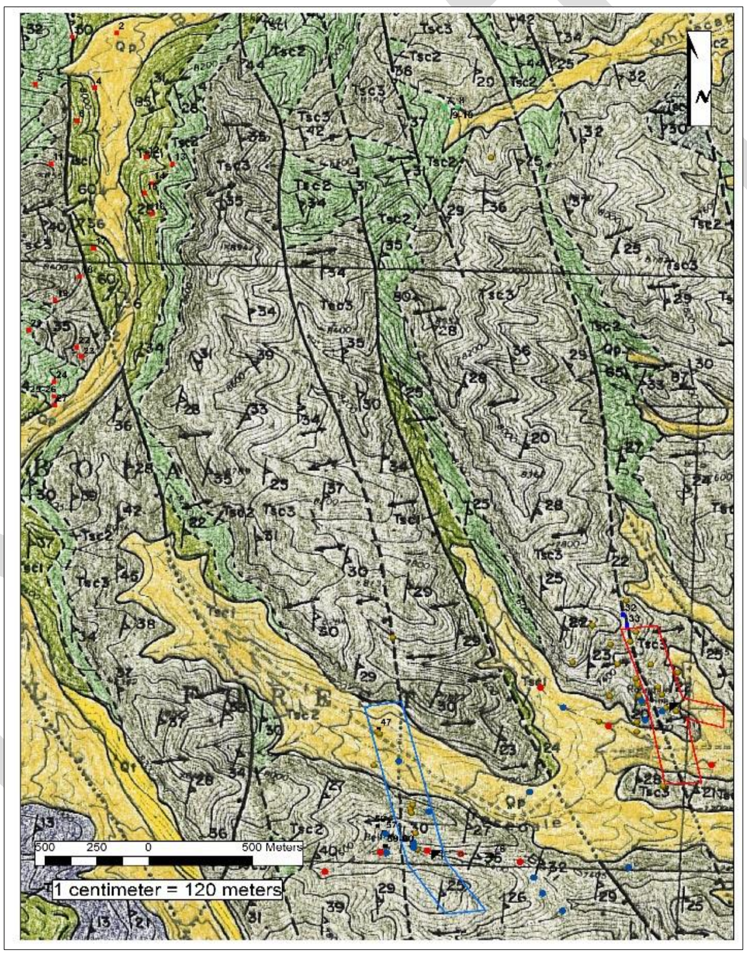

Figure 2: Geological map of the Grassy Lookout 7’5 quadrangle, Socorro County, New Mexico. Modified from Ferguson, June 1990, NMBGMR open file report 336 plate.

McLemore (1996) compared and contrasted the geologic, mineralogical, and the geochemical characteristics of volcanic-epithermal, precious metal deposits of New Mexico to offer some theories concerning structural controls, origin and resource potential of these deposits. The report concluded that volcanic-epithermal, precious metals deposit in the New Mexico are formed in response to episodic and waning volcanic activity and subsequent development of local hydrothermal system in structurally controlled areas of high heat flow produced by multiple intrusions. Mineralization for low-sulfidation volcanic-epithermal deposits such as Rosedale occurs typically as veins and is controlled by complex structures in the vicinity of a volcanic activity. Geologic and geochemical data also suggested that mineralization occurred in multiple pulses in shallow hydrothermal environment (McLemore, 1996).

Exploration and Mining History

Gold was discovered in the district in 1882 and, because of the rich gold content of the deposit, it created a rush to the area (Jones, 1904). The only properties within the Rosedale district developed to any major extent are the Rosedale and Bell mines. In 1886, the Rosedale mine (on the Great London and Rothchild claims) was started by the Rosedale Mining Company and operated until management problems forced closure in 1911. The company also constructed a 10-stamp mill in 1891 and a cyanide plant in 1899 but was approved for patent in 1900. Ore was first processed in a wood-fired, steam-operated 10-stamp mill using amalgamation and cyanide treatment (Fig. 3 and 4). The 50-ton capacity cyanide plant processed approximately 450 short tons of ore monthly with four to five cords of wood, 13 pounds of cyanide, three pounds of zinc, oil, and other incidentals (Batchelder, 1910). In total, the company produced about 8,200 troy ounces (255,020 g) of gold by amalgamation and cyanidation (Lindgren et. al., 1910). The property was then sold in 1913. The new owners operated the mine until 1916, when fire destroyed the mill and spread to the whole mine causing a second shutdown. The Rosedale mine was resold in 1930 and in 1934, the Black Bear Mining Co. shipped 58 tons of ore to the El Paso smelter for refining. Early in 1935 the property was sold to the Rosedale Mining and Milling Co. and operated once more from 1935 to 1937. This company completed a mill and treated 2,972 short tons of ore that year. Production was increased to 16,000 tons the following year, and in 1937, 30,513 short tons of ore treated between March 15 and December 2, when the mine closed down in 1941. The most recent production from the district came in 1941, when a small amount of gold (35 oz) and silver (128 oz) was recovered from the Rosedale mine (Anderson,1957). By June 1942 the Rosedale Mining Company was being advertised for sale in the New Mexico Mining News (1942:3, 6). Inquiries continued to express interest in Rosedale’s gold potential into the 1960s and 1970s (Milligan 1967; Perry, Knox and Kaufman Inc., 1976).

An estimated total value of metals (Au and Ag) produced from Rosedale district between 1882 and 1941 amounted to about $500,000 (North, 1983; McLemore, 2017; Table 1). Three mill tailing facilities were constructed at the Rosedale mine: Longtail (easternmost consolidation), Elizabeth (westernmost) and the Rose (between Longtail and Elizabeth) repository areas (Burney and Scarlata, 2008; Fig. 6). The mine was worked to a depth of 732 feet with an inclined shaft with the first level at 70 feet below the surface and subsequent levels at 50 feet interval. Total development in the main workings was about 5300 feet and all of which was in ore (Fig. 5).

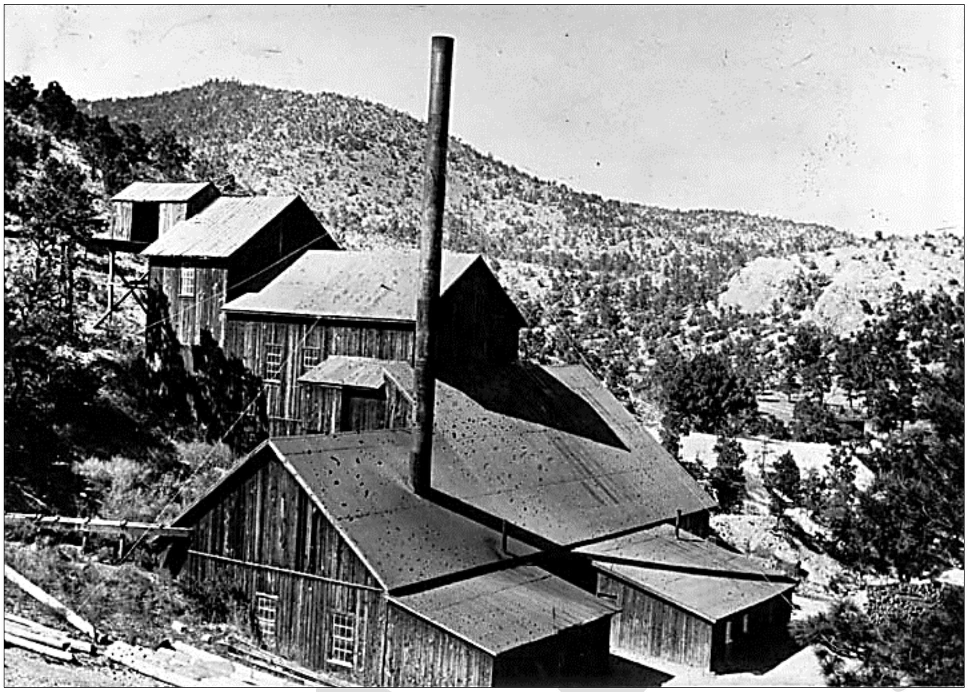

Figure 3: Mill and cyanide plant at the Rosedale mine, looking north about 1905 (NMBGMR historical photos #p-00970).

Figure 4: Foundations of Rosedale Mill near the Rosedale mine, looking northwest.

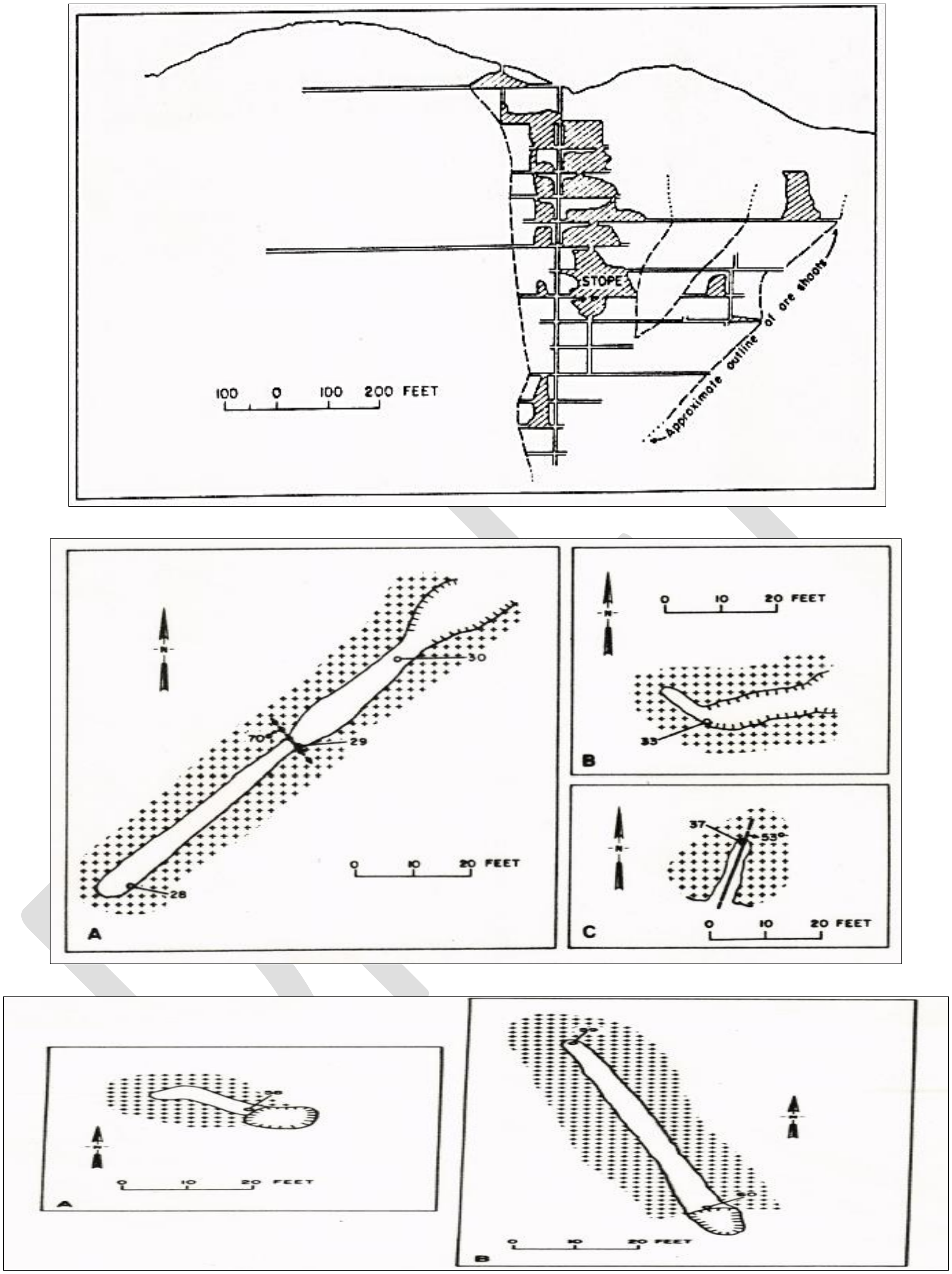

Figure 5: A) Vertical projection of Rosedale Mine, looking N70°E, from Lasky (1932). Map showing adits in the Rosedale and Bell mine; B) North Adit C) Adit about 450 feet south of northern adit D) Western Adit, Neubert (1983)

Figure 6: View across reclaimed Longtail tailings, looking east

Other mining claims were staked in the district but only Bell (Golden Bell) was patented in 1930. The foundation of a small processing plant indicates some production at Bell mine but detailed history of operations is currently unknown (Fig. 7). Other prospects such as the Big Rosa Canyon, Lane mine, Oak Spring Lode, Noon Day Prospect and Robb mine also produced some amount of ore but no production data has been identified. Robb mine, which is located on the claim that adjoins the Rosedale claim on the south, width of mineralized vein is about 10 feet wide, and reported ore valued at $12 a ton at the bottom of a 20-foot winze (Lasky, 1932).

Figure 7: Foundations of Bell processing plant near Bell Adit (NMSO0600), looking southwest.

Table 1: Metals production from the Rosedale mining district, Socorro County (from U.S. Geological Survey, 1902-1927, U.S. Bureau of Mines, 1927-1994; Wells and Wootton, 1940; North, 1983; McLemore, 2017; NMBMMR file data). — = none. ? =unknown production.*Mining and production records are generally poor, particularly for the earliest times, and many early records are conflicting. These production figures are the best data available and were obtained from published and unpublished sources (NMBGMR file data)

YEAR	ORE (short tons)	GOLD (ounces)	SILVER (ounces)	VALUE $	OWNER-OPERATOR
1896	?	47.2	—	976	Rosedale Mining Co.
1898	2,003	510.5	—	10,552	W.H. Martin Co.
1899	4,731	1,367.3	—	28,262	W.H. Martin Co.
1900	5,995	2,188.2	—	45,230	W.H. Martin Co.
1901	3,406	984.3	—	19,601	W.H. Martin Co.
1903	912	485.2	—	10,029	W.H. Martin Co.
1904	5,471	1,800.0	—	37,206	W.H. Martin Co.
1905	3,252	994.2	—	20,550	W.H. Martin Co.
1909	4,561	1,397.0	—	28,876	W.H. Martin Co.
1910	430	?		?	Rosedale Mining and Milling Co.
1911-1913	?	?	—	?	W.H. Martin Co.
1934	58	13.2	115	535	Rosedale Mining and Milling Co.
1935	2,972	158.1	147	5,641	Black Bear Mining Co.
1936	16,179	1,631.4	2,682	59,174	Rosedale Gold Mines, Ltd.
1937	30,513	1,665.4	2,291	60,062	Rosedale Gold Mines, Ltd.
1941	200	35	128	1,316	Rosedale Gold Mines, Ltd.
Total Reported	80,253	13,277	5,363	328,010	
Estimated Total 1882-1981	100,000	28,000	10,000	500,000	Totals reported by Wells and Wootton (1940) and Koschmann and Bergendahl (1968)

There has been some exploration work reported for the district and they include drilling programs and rock chip surveys carried out by Perry, Knox, and Kaufman Inc. in the 1970's within the Rosedale and Bell claims. From the drilling data, Perry, Knox and Kaufman Inc estimated about 1.5 to 2 Mt containing 0.3 oz/short ton-gold mineral resources remaining in the district. In 1976, during the drilling project, eight holes were drilled with a total depth of 1472 ft. The results of the drilling program showed strong mineralization at the southern portion of the Bell mine. A total of sixty-six (66) samples taken from waste rock piles and exposed veins at Rosedale and Bell showed anomalous amount of Au and Ag (Fig. 8; Blakestad, 1975). Samples of quartz vein material and/or intensely altered hematite coated South Canyon Tuff were collected by Ferguson (1990) in the district and analysis showed some promising geochemical results for Au and Ag around the Lane mine Other exploration programs of rock chip and stream sediment sampling was conducted by students at New Mexico Tech (NMT) under the supervision of Dave Norman for Sunshine Mining Company, Idaho , 1991 at the southern portions of the two major mines and results also showed strong mineralization on these prospects (Scott, 1991). The area, south of Bell mine was the focus of the program and was sampled based on the presence of abundant quartz and Fe/Mn oxides veins showing outcrops of possible mineralization. For a sampling pattern of 200 feet by 250 feet, outcrops were sampled along strike of veins in a NE direction and a total of 215 samples were collected, and these include several waste rock piles from adits and shafts. High geochemical values of gold were located at areas with adits and drainages with quartz breccias. Total of 21-stream sediment sample were collected from streams draining from both the Rosedale and Bell mines (Fig. 8).

Presently, a minimal impact exploration drilling permit have been granted to conduct a drill program near Rosedale mine.

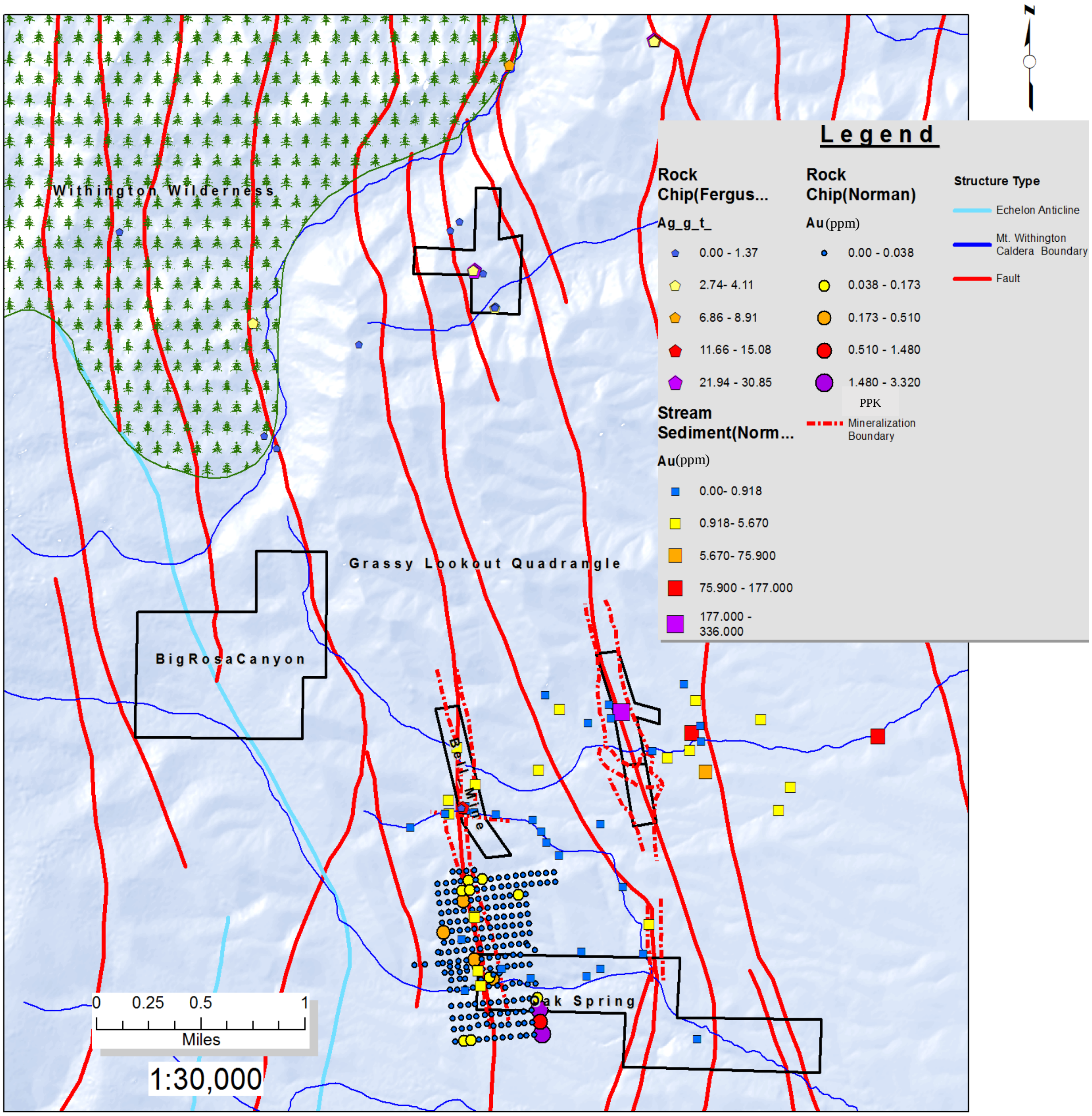

Figure 8: Spatial representation of geochemical results for rock chip and steam sediments sampling, and drilling conducted by Perry, Knox, and Kaufman Inc., Ferguson (1990) and Sunshine Mining Company at the Bell and Rosedale mines

CHAPTER TWO: METHODS OF STUDY

Interpretation of Available Data

To conduct study of the area, an accurate compilation and interpretation of available published and unpublished achieved maps, geological and geochemical reports of mines within the district, and as well as mineral production database (McLemore et al., 2005a, b; McLemore, 2017) were conducted. Mineral databases examined, include the New Mexico Mines Database, U.S. Forest Service Abandoned Mine Lands database, AML (U.S. Bureau of Land Management), and unpublished files at the NMBGMR. Achieved maps covering mineralized and geologic areas, and identified mine features, mineral occurrence, deposits and prospects were georeferenced and digitized in ArcGIS and these were plotted as base maps for field Inspections. Well and spring locations compiled from updated topographical maps in All Topo software and from available literatures were also plotted on the base map used for field observation.

Inventory of mine features, Mapping and Sampling

An inventory form designed to employ procedures from Bureau of Land Management (2014) was used for the collection of data from all mine features during the field examination and inventoried mine features were further compiled in the New Mexico Mines Database (McLemore et al., 2005a, b; McLemore, 2017). From published and unpublished data within the Rosedale district, mining was mostly conducted by employing surface and/or underground methods, which included shaft, adits and/or pit. Field observations of these mine features were conducted by mapping all accessible features and the waste rock piles located around or near the openings of most of these features. Waste rock piles were mapped using a handheld GPS and/or measuring tape and sketches of these dumps were compiled for volume estimation in ArcGIS. A number of sketches and photographs of waste rock piles and their estimated volumes are presented in Appendix1. In order to determine the mineralogy and geochemical signature of the ore deposit, bulk composite sampling of waste rock piles and outcrop sampling at adits and shafts were conducted. All composite samples were collected by employing procedures outlined in Munroe (1999) and the U.S. Geological Survey (Smith et al., 2000b; Smith et al., 2005; McLemore et al., 2014).

Laboratory Analysis

Selected samples from waste rock piles were collected for analysis by a variety of methods to determine the mineralogical composition and paragenesis using standard petrographic techniques, Electron Microprobe, and X-Ray Diffraction (XRD) at the NMBGMR laboratory. Samples were also analyzed for major and trace elements by Induced Coupled Plasma Spectroscopy (ICP) and X-Ray Fluorescence (XRF) at the ALS Laboratory, Reno, Nevada.

Surface Model Interpretation

A surface geologic map was compiled in ArcGIS by using Ferguson's (1986) geologic map of Grassy Lookout quadrangle. 2D interpretation of the surface geology were completed to assist in the analysis of the structural and mineralization controls within Rosedale district. Surface interpretation such as geophysical anomalies to defined area of interest was considered to be out of scope of this study.

Comparison of Volcanic Epithermal Deposit

Compare Rosedale district with other epithermal vein hosted Au-Ag districts within Socorro county and New Mexico.

This report assesses the potential of mineral resources in Rosedale district by considering a number of factors such as evaluation of host-rock favorability, structural controls, evidence of mineralization, previous mining and production, geochemical anomalies, regional geologic setting, time of mineralization, alteration, mineralogy and mineral assemblages, processes affecting mineralization since their formation, and geologic history.

CHAPTER THREE: GEOLOGIC AND TECTONIC SETTING

Introduction

Rosedale district is a volcanic epithermal-vein deposits that lies in a tectonically active and structurally complex area within the Mogollon-Datil volcanic field, which trend from southwestern New Mexico and part of a discontinuous belt of mid-tertiary silicic volcanic fields that extends from the San Juan Mountains in Colorado and southward into Chihuahua, Mexico (McDowell and Claubaugh, 1979; McIntosh et al., 1991, 1992a, b; Chapin et al., 2004; Figure 8). In the Mogollon-Datil field, basaltic andesite to andesite volcanoes were active from about 40 to 36 Ma, followed by episodic bimodal basaltic andesite and silicic activity from 36 to 24 Ma (Elston, 1973; Cather et. al., 1987; McIntosh et. al., 1990). The mid to late Oligocene (27.4 Ma, McIntosh, 1989a) South Canyon Tuff of which underlies the district is the youngest major formation in the northeastern Mogollon-Datil volcanic field. This high-silica bearing sometimes flow-banded rhyolite ash-flow tuff erupted from the Mount Withington caldera, which acts as a "trapdoor" caldera hinged along its southern edge (Mcintosh et. al., 1992). The northwestern boundary of the Mt. Withington caldera trending on a normal fault zone lies at the southeastern portion of the Grassy Lookout quadrangle is considered as the source of South Canyon Tuff (Ferguson, 1990). Timing of the mineralization and alteration in the Rosedale district was probably shortly after emplacement of the late-Oligocene South Canyon Tuff (Ferguson, 1990). The mineralization occurs in well-developed veins that is brecciated and sheared in rhyolite porphyry. The most intense alteration is concentrated along the north-northwest trending faults between North Canyon and Big Rosa Canyon, and along the Lemitar Tuff and the South Canyon Tuff contact near the head of North Canyon (Ferguson, 1990). Generally, the shear zones extend into the walls of rhyolite porphyry and abundant brecciated fragments observed within the veins formed at the hanging wall. This has also been fractured, and the entire mass has been recemented with glassy vein quartz. Silicification of the wall rock clearly stands out (Deal, 1973).

Stratigraphy

The northern part of the Grassy Lookout quadrangle is underlain by as much as 1.8 km of intra-caldera South Canyon Tuff and Rosedale epithermal gold district, which lies at the central section of the quadrangle, is underlain by areas of altered and mineralized intra-cauldron South Canyon Tuff (Ferguson, 1986). In the thickest part of the caldera fill, three distinct zones (herein called the lower, middle, and upper) are recognized primarily on the basis of phenocryst abundances and also because they are usually separated by lithic-rich intervals (Ferguson, 1990; Fig. 9). These zones are defined only within the thickest part of the caldera fill. They do not necessarily correspond to zonal variations of the South Canyon Tuff either near the southeastern caldera margin or in the outflow sheet where the Tuff is significantly thinner. Osburn and Chapin (1983) indicated that there were two stages of the formation of the ash flow Tuff: simple to compound cooling unit of quartz-rich, one felspar Rhyolite Tuff. There was no significant distension between these units so are usually mapped together as a unit. Nine mappable units were recognized in the Grassy Lookout quadrangle of the South Canyon Tuff: two basal unit; two localized lithic breccia units; and five vertical zonations of the main caldera-fill, four of which are volumetrically significant (Ferguson, 1990)

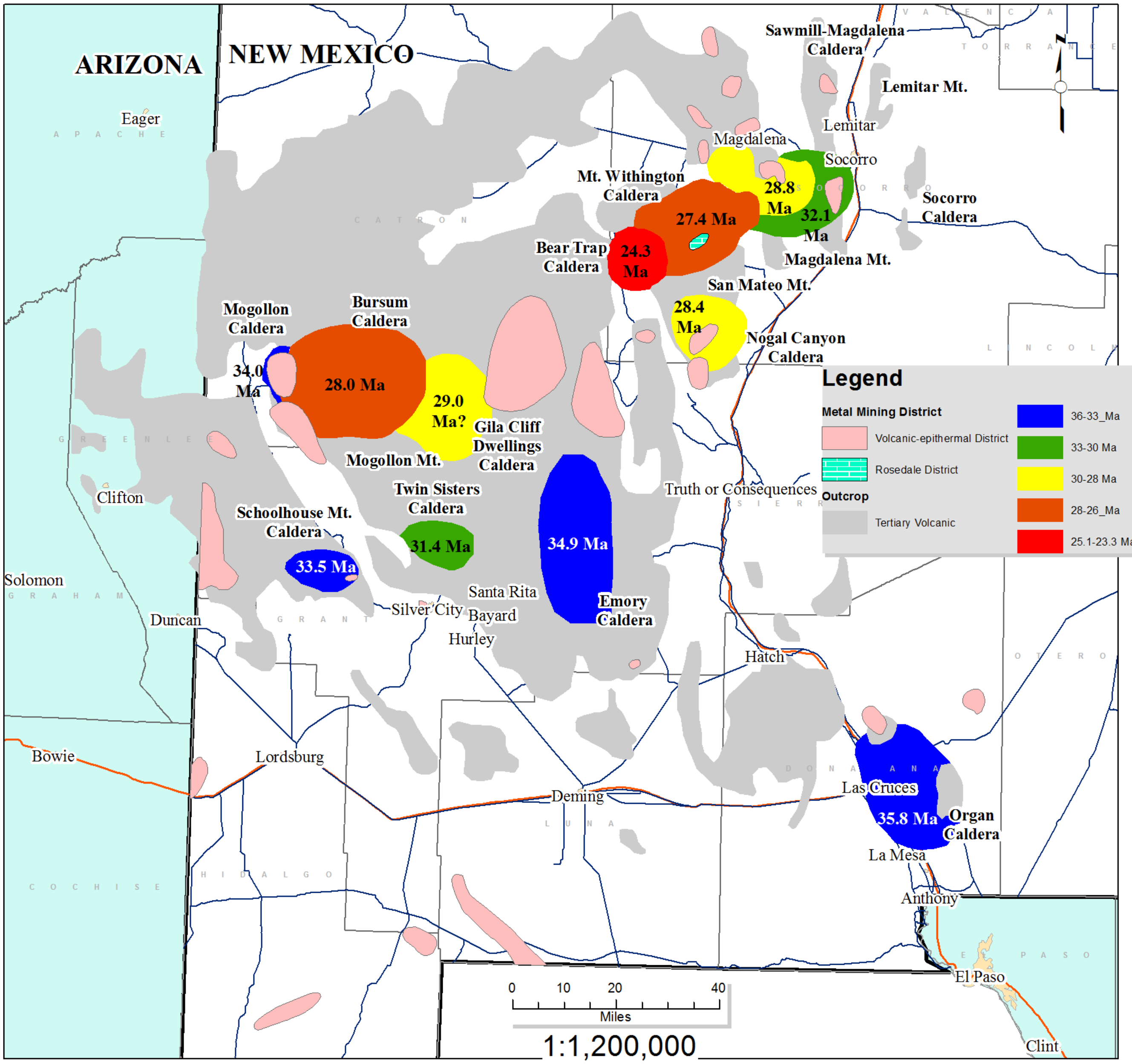

Figure 9: Map of the Mogollon-Datil volcanic field, showing known calderas color coded by age in Ma, modified from Chapin et al., 2004. Shaded areas represent Rosedale mining district which a known volcanic-epithermal vein deposit.

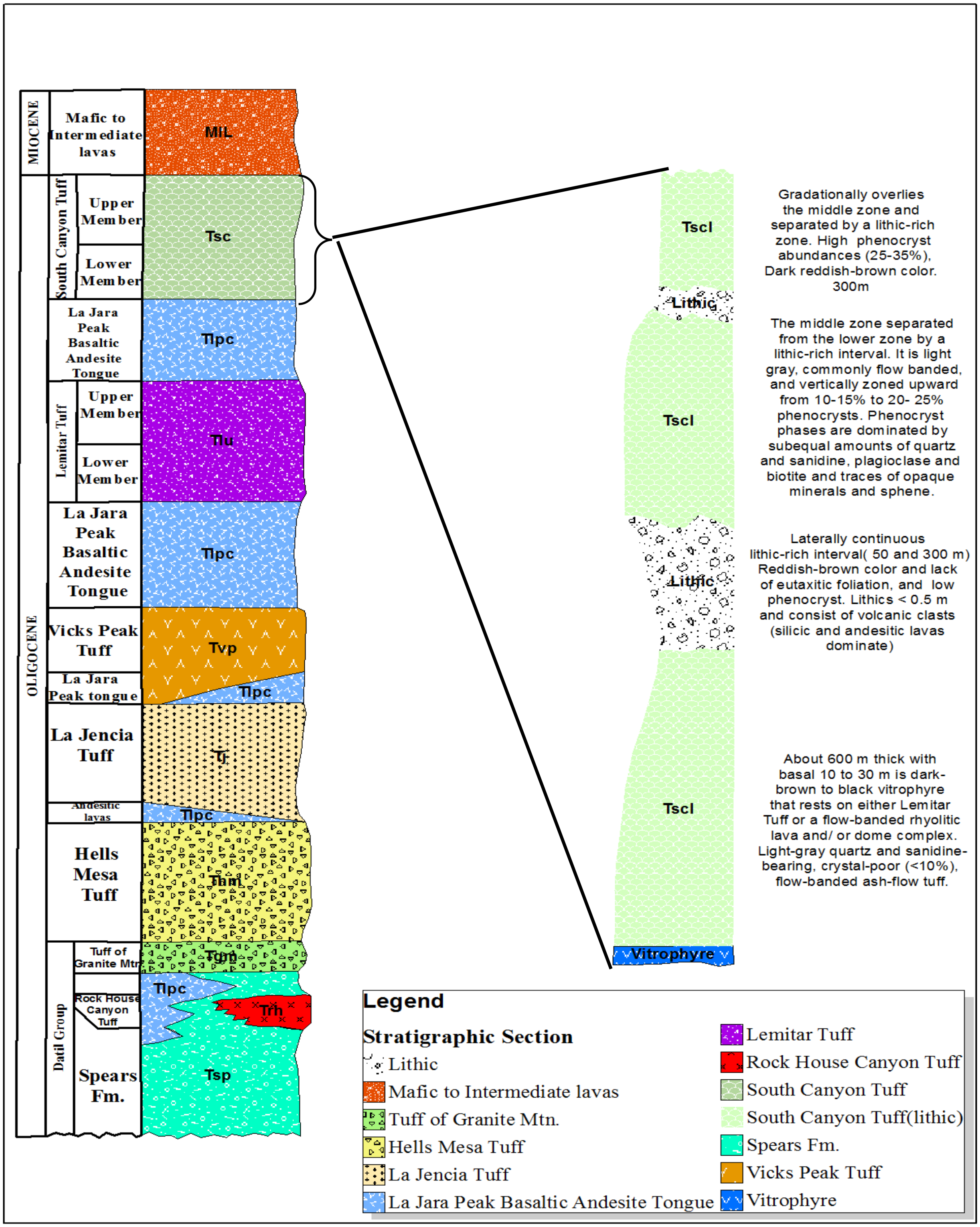

Figure 10: Stratigraphic section of Mogollon-Datil volcanic field (left) with generalized stratigraphic section of the South Canyon Tuff formation (right). The unit of the South Canyon Tuff formation also shows a basal vitrophyre (Blue) and two lithic-rich intervals divided the section into lower, middle and upper zones

Lower zone of the South Canyon Tuff

The lower zone of the South Canyon Tuff is about 600 m thick in the Mt. Withington-A-L Peak area. The basal 10 to 30 m is dark-brown to black vitrophyre that rests on either Lemitar Tuff (Osburn and Chapin, 1983) or a flow-banded rhyolitic lava and/ or dome complex. The main part of the lower zone is light-gray quartz and sanidine-bearing, crystal-poor (<10%), flow-banded ash-flow tuff. The lower zone correlates directly with Deal's (1973) A-L Peak Tuff. The A-L Peak Tuff correlated originally with a texturally similar outflow sheet that later shown to be an older unit now called La Jencia Tuff (Osbum and Chapin, 1983; Mclntosh et al., 1986).

Middle zone of the South Canyon Tuff

The middle zone of the South Canyon Tuff is separated from the lower zone by a lithic-rich interval. It is light gray, commonly flow banded, and vertically zoned upward from 10-15% to 20- 25% phenocrysts. Phenocryst phases are dominated by subequal amounts of quartz and sanidine. Other phases include minor amounts of plagioclase and biotite and traces of opaque minerals and sphene. The middle zone is about 500 m thick in the northern part of the quadrangle and correlates with most of Deal's (1973) Potato Canyon Tuff within the Mt. Withington caldera. Strata mapped by Deal (1973) as Potato Canyon Tuff outside the caldera have been shown since to be several outflow sheets that include the South Canyon Tuff and older tuffs (Ferguson, 1991).

Upper zone of the South Canyon Tuff

The upper zone of the South Canyon Tuff gradationally overlies the middle zone in most areas, and to the northwest it is separated by a lithic-rich interval similar to the one at the base of the middle zone. The upper zone is characterized by high phenocryst abundances (25-35%), and dark reddish-brown color. In the northern part of the caldera it is up to 300 m thick; in the southern part of the caldera it is not present or is significantly thinner (less than 50 m). Phenocrysts in the upper zone are dominated by subequal proportions of quartz and sanidine, between 1% and 5% plagioclase, minor biotite, and traces of sphene and opaque minerals. The zone is unique in that it contains two types of pumice fragments: small (<5 cm) white fragments dominate; larger (>1.0 cm) dark gray-purple fragments that conspicuously lack quartz phenocrysts are rarer. In the northeast corner of the quadrangle, the upper zone grades upward into a medium-gray, moderately crystal-rich (15-20%), feldspar-bearing tuff with little or no quartz phenocrysts (Ferguson, 1991).

Lithic-rich intervals in the South Canyon Tuff

In the thickest part of the caldera fill, two laterally continuous lithic-rich intervals between 50 and 300 m thick are recognized. They are characterized by reddish-brown color, general lack of eutaxitic foliation, and relatively low phenocryst abundances. The low phenocryst content probably reflects dilution by the lithic material and decreased compaction relative to adjacent zones. Lithics are less than 0.5 m and consist of volcanic clasts (silicic and andesitic lavas dominate) that compose 5% to 50% of the tuff (Ferguson 1991). Both lithic-rich intervals are interpreted as caldera-collapse meso-breccias similar to those described in several Tertiary calderas in southern Colorado (Lipman, 1975) and in the Chupadera Mountains near Socorro, New Mexico (Eggleston, 1982). Thickening of the intervals to the north implies derivation from avalanche-like failure of the northwestern caldera wall. Both intervals occur at the base of the middle and upper zones of intracaldera South Canyon Tuff. They are interpreted to be distal equivelents of the clast-supported lithic breccia which consist of fragments mostly of rhyolite lava, Lemitar Tuff, and basaltic andesite lava which rarely exceed 20cm in diameter (Ferguson, 1986). It seems reasonable to link the eruption of these two zones with avalanche events triggered possibly by episodic down-to-the-south fault displacements along the northern margin of the caldera. Lithic-rich intervals near the southeast caldera margin occur as discontinuous lenses characterized by poorly welded to unwelded ash-flow-tuff matrix, lithic abundances to and greater than 50%, larger maximum fragment sizes (to 2 m), and in some cases clast-supported fabrics. The lens-shaped bodies occur vertically throughout the tuff but only within 1 to 2 km of the caldera margin (Ferguson 1991)

Lithologic Descriptions

Rhyolite Porphyry

The most prominent rock in the district is a purplish-brown rhyolite porphyry. Rhyolite lavas are present throughout the Rosedale district below the Lemitar Tuff, but never with any lower constraint. These lavas are correlated chronologically with a dome and flow that occurs between Vicks Peak and Lemitar Tuffs. Rhyolite lavas of this age are widespread and voluminous throughout the central and northern San Mateo Mountains, and a similar sequence, occupying the same stratigraphic position, is found in the northern Black Range (Ferguson, 1986; Figure 12).

Breccia and Tuff

Volcanic breccia and tuff are generally exposed and overlie the rhyolite porphyry series, and these rocks are in turn generally overlain by a coarse porphyritic rhyolite which caps the rounded hills of the district. In some areas a layer of flow rhyolite lies between the tuff and the porphyritic rhyolite. The breccia and tuff are discolored like the underlying rhyolite porphyry and at some places contain cavities up to several inches across lined with irregularly oriented quartz prisms (Lasky, 1932).

Porphyritic Rhyolite

The porphyritic rhyolite that caps the breccia and tuff ranges in color from dove gray to grayish-blue and lavender and is rather soft as compared to the brittle, hard flow-banded rhyolite porphyry. It contains about 20 per cent of medium and coarse-grained idiomorphic feldspar phenocrysts in a somewhat sugary groundmass. Phenocrysts and groundmass are nearly identical in color. Black grains of magnetite are common. This rock also is bleached and discolored in places, particularly in the vicinity of strong faults (Lasky, 1932).

Structural Geology

The central segment, Alamosa to Socorro, is characterized by a north-northeast-trending series of echelon basins separated by complex transverse structures. This segment traverses an area of northeast-trending basement lineaments and crosses 1.4-1.8 Ba-old Precambrian rocks (Hedge et al., 1968) in the north and 1.3 - 1.5 Ba. - old Precambrian rocks (White, 1978) in the south. The southeastern margins of Mount Withington caldera, located about 3 miles from the study area is considered to be relatively simple near vertical fault boundary of very thick intracaldera South Canyon Tuff. At this boundary the South Canyon Tuff occupies a structural depression (Fig. 11). Most part of the study area shows a north to northeast-trending monoclinal structural zone that is least 0.6 miles wide (Deal, 1973; Osburn and Ferguson, 1986). Along the ridge crest of the district, thus in the northern part of the Grassy Lookout quadrangle, intracaldera South Canyon Tuff is gently folded into an anticline trending 345^0 with its axis about 1.2 miles west of the ridge crest (Ferguson, 1986). The fold is cut by set of mostly north-trending very high angle faults which change from east-side-down to west-side-down across the ridge crest. This broad anticline dies out in the west-central part of the study area. Another complex and tighter anticlinal structure continues southward from this area, but it offset as echelon style into the southwest corner of the study area.

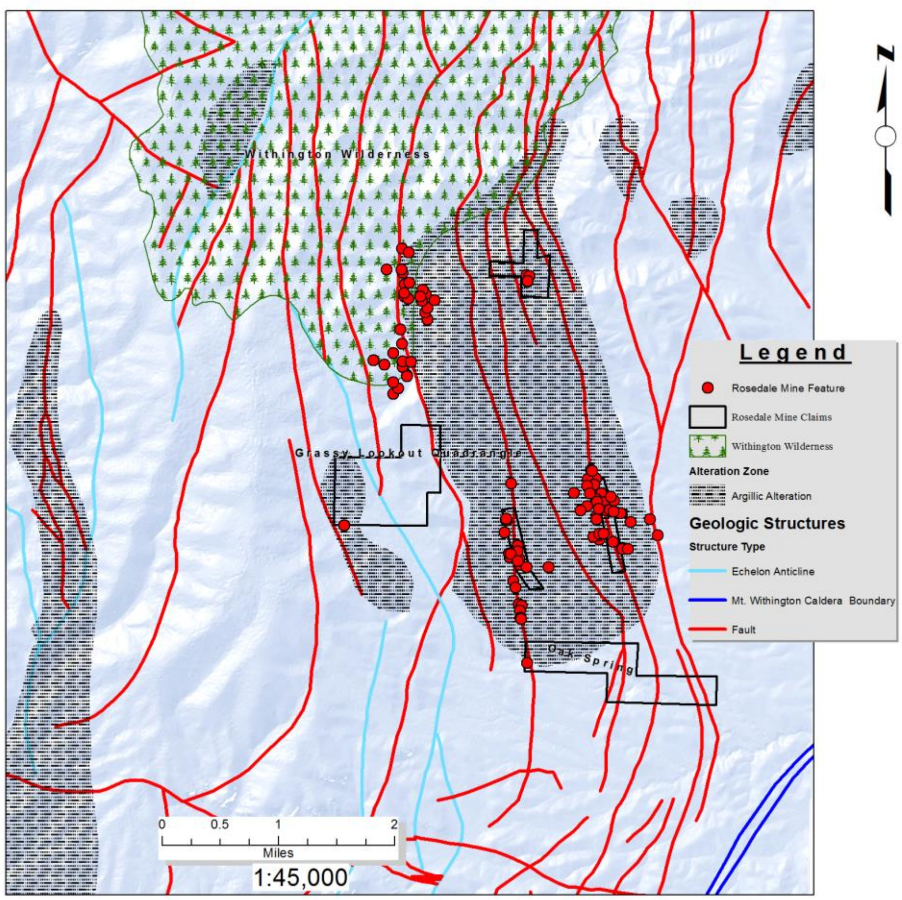

Figure 11: Structures and alterations within Glassy Lookout quadrangle modified from Ferguson (1990). Map depicts the south-eastern margins of Mt. Withington Caldera (blue double lines), faults (Red) and echelon anticlinal folds (Cyan). Also shown are the area of argillic alterations (Shaded zone). The Rosedale district is located in the center of the largest alteration zone.

Chapin (1989) related the structural geology of the northeastern San Mateo Mountains ridge crest to structural patterns of fault blocks within the SAZ farther east. The definition of tilt domains in the Socorro area of the Rio Grande rift is controlled primarily by a transverse boundary (oriented about 070^{o}) called the Socorro accommodation zone (SAZ). However, the northerly trend of the tilt domain transition at the study area is actually more compatible with it being classified as an anticlinal strike-parallel boundary. In addition, four of the five major Oligocene calderas in the Socorro area (including the Mt. Withington caldera) overlap the SAZ. The SAZ probably represents a long-lived crustal flaw coincident or related to the Morenci lineament (Chapin et al., 1978)

Fault patterns, at the eastern portion are dominated by a north to northwest-trending set of mostly parallel and most of echelon moderately dipping west-side-down normal faults. The study area is host to two main deposits (Rosedale and Bell Mine) where their vein mineralization is related to parallel basin and range fault that trends about 340^{o} and dips about 75^{o} to the west (Neubert, 1983). The master fault is a high-angle east-side-down structure that bounds steeply east-tilted blocks to the east from gently east and west-tilted blocks to the west (Ferguson, 1990)

A cross-sectional view developed for the structural margin of the study area is illustrated in Figure 12.

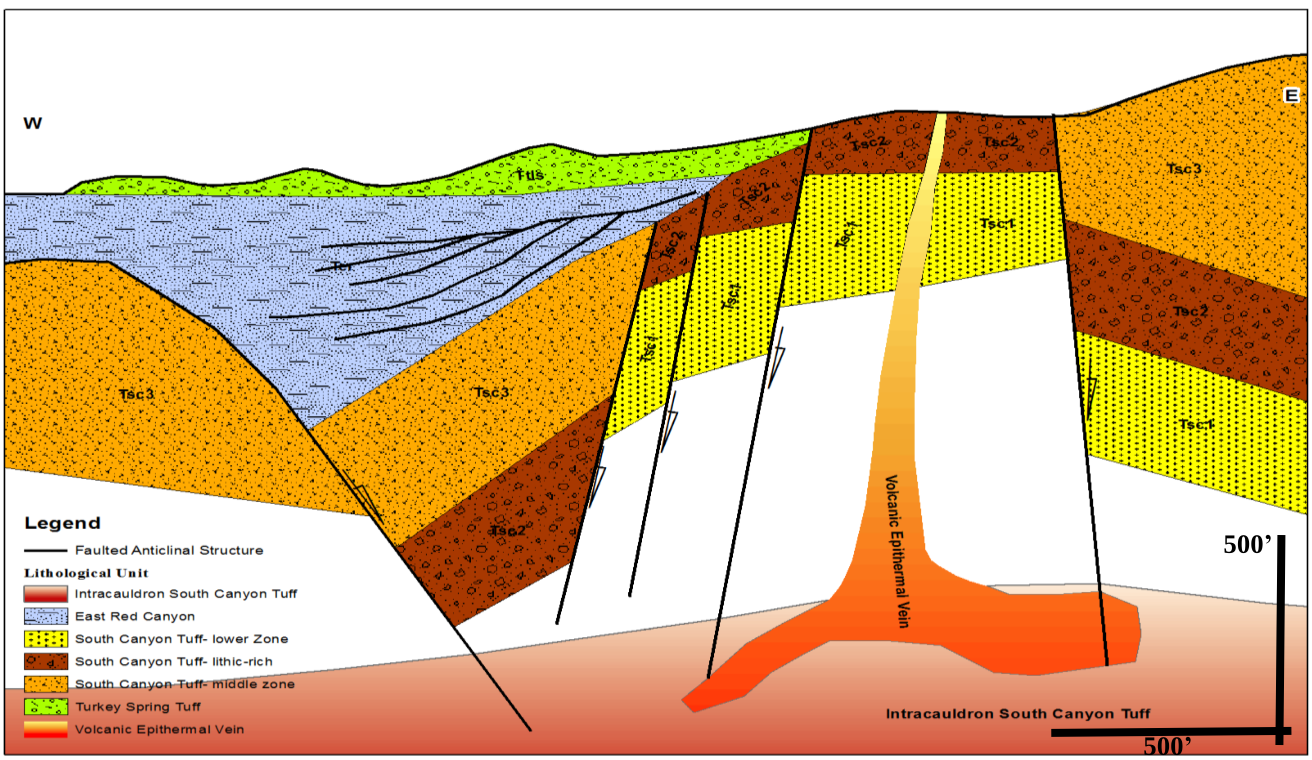

Figure 12: Schematic sketch across the faulted anticlinal structure partially buried by the deposits of the unit of the East Red Canyon (Ter) along the southwest edge of the study area. View is to the north combining field sketches of exposures in Hudson,

spring, and Whitewater canyons. Tsc- undifferentiated South Canyon Tuff, Tsc1-lower zone, Tsc2-lithic-rich interval, Tsc3-middle zone, Tts1-tuff of the Turkey Spring (Modified from Ferguson, 1990)

Alteration

The alteration styles at the Rosedale district provide insight into processes that modified the rocks before, during, and after gold mineralization. In addition, alteration associated with gold mineralization, such as silicification and argillization of rhyolite, reflect the geochemical composition of ore-forming fluids. The gold district is located in the central part of a large alteration zone (Fig. 11).

Oxidation

The most pervasive and apparent alteration style present at Rosedale is oxidation. The sulfide and mineral phases in waste rock piles have been largely destroyed or modified by oxidation. Oxidation has resulted in the formation of iron oxide minerals, such as hematite, as replacement mineral for pyrite on fractured surfaces and veins. Iron oxides are variably colored but are predominantly reddish brown and ubiquitous on nearly all fracture surfaces.

Argillization

Much of the district underlain by large areas of altered and mineralized intracaldera South Canyon Tuff derived from the sub-caldera pluton. Argillic alteration, associated with the mineralization, occurs parallel to and adjacent to faults throughout the area. The most intense alteration occurs along the Lemitar-South Canyon contact on the head of North Canyon and along north-northwest trending faults between North Canyon and Big Rosa Canyon (Ferguson, 1988, 1990). Areas affected by varying degree of argillic alteration are shown on Figure 11. Along the contacts, most advanced alterations are located in the thin poorly welded tuff just below the vitrophyre of the South Canyon Tuff. Alteration extends downward about 30m into the Lemitar Tuff, but upward only about 100 ft into the South Canyon vitrophyre. Argillic alteration typically overprints cross-cuts fault zones and is attributed to the late Oligocene phase of extension, but younger basin and range style high-angle fault juxtapose altered and unaltered rock. (Ferguson, 1990). Alteration of the rhyolitic country rock consist of bleaching which increase in intensity and usually accompanied by variable amount of oxidized pyrite as the veins are approached. Most of the rock units at the study area depicts hematite coatings with stringers of manganese oxide on the South Canyon Tuff because of oxidation.

Silicification

Along the contact between fault zones, irregular thickness of silicification usually marks the end of ore-bearing zones in some places. These silicified sections, which is very dominant at fault zones, consists locally of breccias of the rhyolitic porphyry. The siliceous rock units at certain areas at Rosedale mine contain numerous cavities lined within quartz crystals above the water table. Silicification extends downward along the sides of shear zones into a footwall and the hanging wall of the rhyolite porphyry (Lindgren et al, 1910).

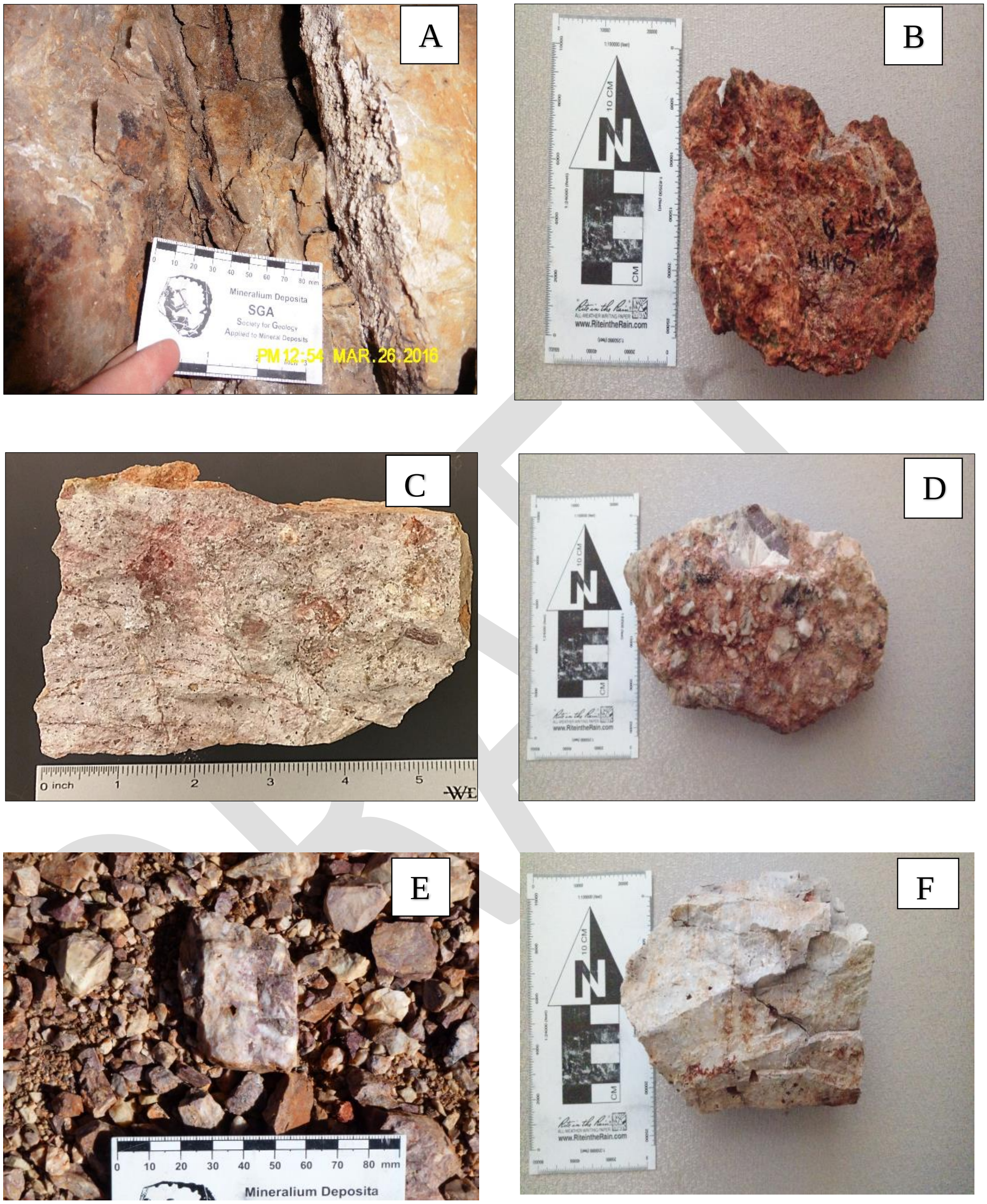

Figure 13: Photographed representative alteration styles in the Rosedale mining district. (A & B) Pervasive hematite alteration of rhyolite from, Rosedale, and Big Rosa Canyon. Pyrite generally replaced with hematite through oxidation. (C) Argillic alteration with hematite overprinted on rhyolitic porphyry from Bell Mine. (D) Silicified breccia units from Rosedale mine adit. E) Glassy quartz veins with vesicles from Rosedale mine. F) Highly fractured rhyolite from Big Rosa Canyon: Likely, close to a Mt. Withington caldera vent.

CHAPTER FOUR: DESCRIPTION OF MINERAL DEPOSIT

Volcanic Epithermal Vein Deposit

The volcanic-epithermal deposits of New Mexico formed largely in faults and fissures in rhyolitic ash-flow tuffs and andesites of Oligocene-Miocene age, commonly within or adjacent to resurgent calderas (Elston, 1978; 1994; Rytuba, 1981; McLemore, 1996; Fig. 13-F). Typical volcanic-epithermal deposits in the state occur as siliceous vein fillings, breccia pipes, disseminations, and replacement deposits along faults and fractures in intermediate to silicic volcanic and volcanoclastic rocks. Two main types of volcanic epithermal deposits: low-sulfidation (quartz-adularia) and high-sulfidation (quartz-alunite) occurs in the Mogollon-Datil field (Cox and Singer 1986, model #25h ; McLemore, 1994). McLemore (1996) classified the Rosedale district as a low-sulfidation volcanic epithermal deposit with dominant gold and low silver content.

South Canyon Tuff of brecciated and sheared rhyolite porphyry invaded by epithermal well-developed gold veins and associated zones of argillic alteration occurs in the Rosedale mining district. Mineralization formed because of development of cross fractures, which allowed the mineral bearing solution more surface on which to deposit and this cross fracturing enhanced erosion to occur. Mineralization occurs along basin and range faults, which trend about N30E and the driving force for the epithermal system was most likely the sub-caldera pluton (Ferguson, 1990). The ores occur in a well-marked fissure vein in the rhyolite having a strike of about N. 20° W. and dipping at a high angle (80°) toward the east. The veins are from 3 to 5 feet wide at the surface but is said to reach in places a width of 12 feet (Lindgren et al, 1910).

The deposits at the Rosedale contain principally free-milling ore in a gangue of bluish-white quartz, carrying in places, an amount of hematite, manganese oxide and some disseminated pyrite (oxidized). The rhyolite shows in hand specimens easily recognized crystals of quartz in a well-crystallized groundmass, giving the rock a granitoid appearance.

Placer Deposit

Placer gold deposits were an important source of gold in New Mexico prior to 1902, but placer production after 1902 has been minor (Johnson, 1972). The deposits generally occur in Late Tertiary to Holocene age alluvial fan deposits, bench or terrace gravel deposits, river-bars, and stream deposits or as residual placers formed directly on top of lode deposits typically derived from Proterozoic, Cretaceous, and Tertiary source rocks. During fluvial events, large volumes of sediment containing free gold are transported and deposited in relatively poorly sorted alluvial and stream deposits. The gold concentrates by gravity in incised stream valleys and alluvial fans in deeply weathered highlands. Native gold and electrum occurs with quartz, magnetite, ilmenite, amphiboles, pyroxenes, pyrite, zircon, garnet, rutile, and a variety of other heavy minerals. Although there has been no reported placer gold production from the Rosedale district, small, irregular, placer gold deposits have been found in Rosedale Canyon.

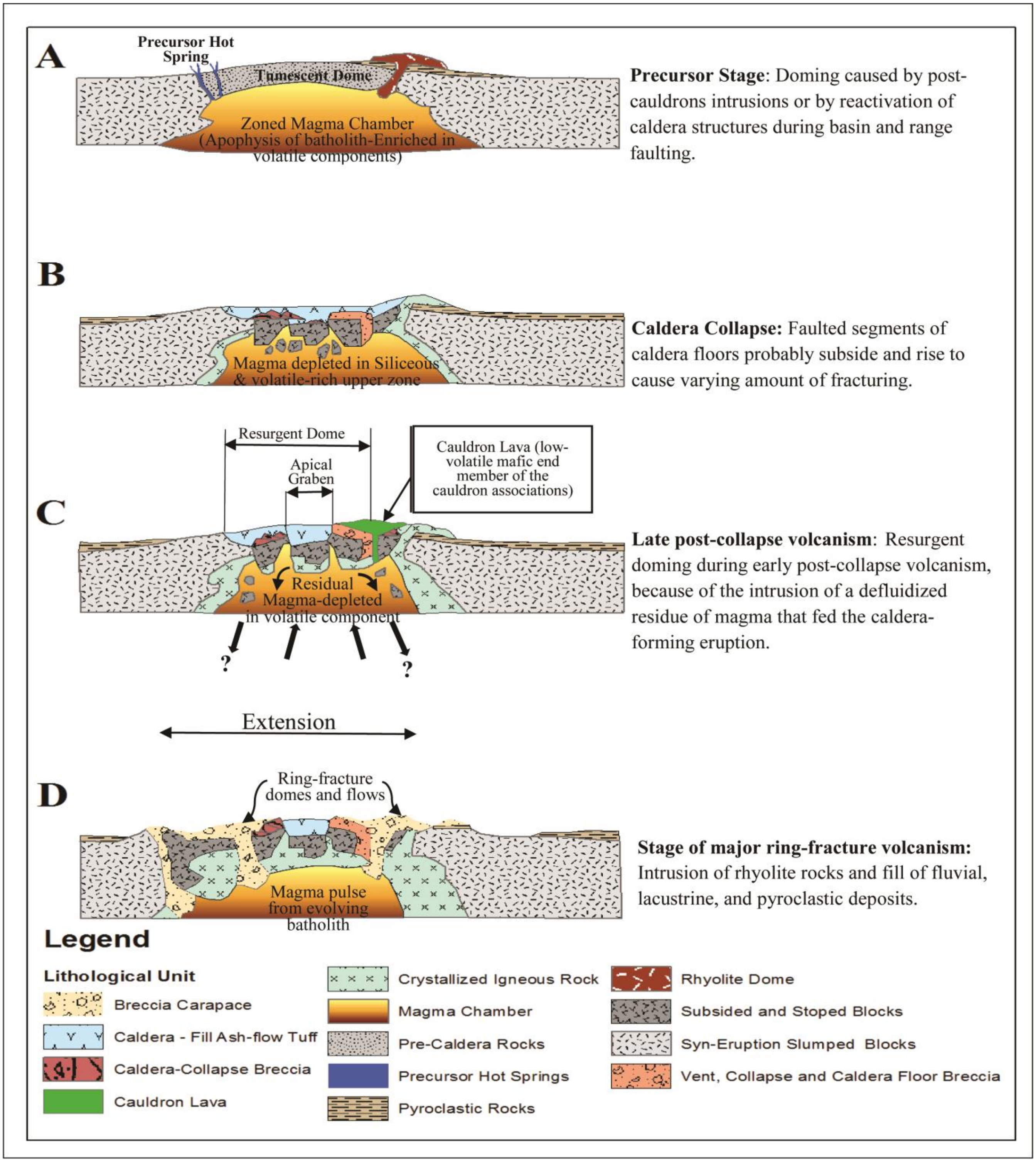

Figure 14: Evolution of typical main-stage resurgent caldera in New Mexico, Vertical exaggeration about 10X. A) Precursor Stage. B) Caldera Collapse C) Early post-collapse volcanism and D) Stage of major ring-fracture volcanism followed by intrusion of rhyolite rocks. Modified from Elston, 1978.

CHAPTER FIVE: PETROCHEMISTRY AND MINERAL PARAGENESIS

Soil Petrography

All sample preparation and analysis were conducted at the NMBGMR Economic Geology lab. Sixteen (16) samples were selected for petrographic analysis based on hand sample observations of alteration and paragenetic relationships at the fault and shear zones and as well as results from whole rock geochemical analyses. Soil petrography was used as a first pass studies to describe the lithology, alteration, and mineralogy of waste rock pile samples through the use of a binocular microscope. Approximately 10g of a representative portion of waste rock pile sample was examined under the microscope prior to sample rinsing to determine the abundance and color of fine material present, cementation, and grain shape of the sample. Test for calcite was conducted by using diluted HCl on the sample and observing the reaction rate. Samples were rinsed in cool tap water to remove fine material and aided in the examination of rock fragment lithology and mineral identification. To limit the dissolution of gypsum and soluble salts, thorough rinsing and long immersion of the samples in water was avoided. Samples were labelled and air-dried on filter paper. The dried samples were examined under reflected light to estimate the percentages of different rock fragments present and described the intensity of alteration, textural and mineralogy composition of the sample. General observation and description of the Rosedale district samples are presented in Appendix 2.

Generally, all samples showed similar lithological and mineralogical composition. The alteration associated with samples indicates a wallrock alteration around veins, shear zones and fractured zones which contains pervasive argillization and silicification. The samples were usually associated moderate amount of hematite and manganese oxides occurring as replacement~~s~~ of dark minerals and stringers, and as coatings on fracture surfaces. Groundmass of the samples analyzed were composed mostly of quartz and plagioclase. However, the quartz fragments observed ranges from glassy to milky massive textures with no apparent orientation of individual mineral grains. Vesicular quartz veins were common with most samples showing leached out mineral.

Geochemistry

Twenty-two (22) bulk composite samples from various waste rock/soil piles and outcrop chip samples from adits and shafts were analyzed for major and trace elements by ALS Laboratory, Reno, Nevada. Trace elements including the full rare earth element suites were analyzed from three digestions with Inductively Coupled Plasma Mass Spectrometry (ICP-MS) finish: a lithium borate fusion for the resistive elements (ME-MS81), a four-acid digestion for the base metals (ME-4ACD81) and an aqua regia digestion for the volatile gold related trace elements (ME-MS42). In this analysis a suite of 50 elements were analyzed in total: Ag, As, Ba, Bi, Cd, Co, Cr, Cs, Cu, Ga, Ge, Hf, Hg, In, Li, Mo, Nb, Ni, Pb, Rb, Re, Sb, Sc, Se, Sn, Sr, Ta, Te, Th, Tl, U, V, W, Y, Zn, Zr, and rare earth elements La, Ce, Pr, Nd, Sm, Eu, Gd, Tb, Dy, Ho, Er, Tm, Yb, and Lu (Appendix 4). Gold (Au) content in all these samples were analyzed separately by fire assay method with Inductively Coupled Plasma-Atomic Emission Spectroscopy (ICP-AES) finish for the accurate determination of total gold content. X-Ray Fluorescence (XRF) were used for the analysis of oxide elements associated with the samples and is considered to be effective for the major rock-forming elements when following a fusion. Elements analyzed include Al_2O_3, BaO, CaO, Cr_2O_3 Fe_2O_3, K2O, LOI, MgO, MnO, Na_2O, P_2O_5, SiO_2, SrO and TiO_2. This analysis was used to chemically characterized waste rock piles and determine the mineral resource potential of these pile materials. The analysis was explored to evaluate geochemical relationships of mineralization (Au) and other trace element and base metals. Geochemical results of some of the element analyzed and their spatial location of samples are indicated in the Table 3. Due to insufficient samples from geochemistry, correlation between gold, base metals and other elements is inconclusive (Fig. 15) but some deduction was analyzed from the results. Gold showed a positive correlation with Ag and Mn however, presented no correlation between K, Na, and the base metals. The results show elevated concentration of Au averaging about 1.21 ppm at the Rosedale Mine and 0.23 ppm at the Bell Mine for waste rock pile material (Table 2)

Table 2: Summary of selected geochemical analysis results for samples from study area. All sample analyzed were oxidized samples from waste rock piles and rock samples from adits and shafts.

Samp. No.	Samp. type	UTM_E	UTM_N	Geochemical ICP Results (ppm)												
				Au	**Sn**	**U**	**Zr**	**Ag**	**Co**	**Cu**	**Li**	**Mo**	**Ni**	**Pb**	**Zn**	**As**
BEL001	Rock	276018	3742604	0.024	4	10.85	153	0.9	3	4	20	1	5	20	49	11.2
BEL002	Soil	276018	3742604	0.403	3	5.84	107	7.5	2	8	70	14	5	24	36	12.8
BEL003	Soil	276018	3742604	0.168	3	7.38	105	6.9	2	8	70	19	6	30	51	13.6
BEL004	Rock	276018	3742604	0.201	2	4.03	83	12.4	1	6	90	24	4	16	25	7.8
BEL005	Soil	276115	3742575	0.006	4	4.23	286	<0.5	3	7	30	1	6	24	53	6.2
BEL006	Rock	276018	3742620	0.283	2	2.51	47	25.2	1	9	100	55	4	8	17	8.3
BEL007	Rock	276018	3742620	<0.001	3	5.11	236	<0.5	1	1	30	1	2	23	68	6.6
BEL008	Soil	275993	3742661	0.397	2	3.7	68	10.2	2	8	100	6	1	65	42	16.2
BEL009	Soil	275989	3742824	0.281	2	5.16	119	9.7	2	8	60	4	1	119	50	17.1
BEL012	Soil	276000	3742845	0.418	3	5.19	119	3.1	2	7	50	3	3	39	57	17.2
ROSE001	Soil	277223	3743363	2.1	2	5.76	82	20.2	2	17	80	6	5	26	64	13.7
ROSE002	Soil	277223	3743363	0.011	4	5.27	311	0.8	2	39	10	24	37	78	53	5.6
ROSE003	Soil	277223	3743363	0.125	3	6.94	131	6.2	1	14	40	3	6	28	87	19.3
ROSE004	Soil	277223	3743363	3.61	2	8.15	77	57.7	2	47	100	8	6	67	121	34.6
ROSE005	Soil	277223	3743363	2.74	2	6.84	70	72.7	3	44	110	9	6	43	110	19.6
ROSE006	Soil	277229	3743342	1.015	1	2.86	12	43.1	<1	15	100	4	2	15	46	7.4
ROSE007	Soil	277095	3743427	0.021	4	7.33	154	<0.5	4	11	60	8	7	118	92	29.5
ROSE008	Soil	276953	3743426	0.085	2	4.69	96	1.4	2	7	80	3	6	23	100	18.2
ROBB2	Soil	277313	3742927	0.045	3	4.17	124	1	2	7	70	<1	2	33	54	14.5
BIG002	Soil	274454	3745241	0.003	4	4.55	135	<0.5	1	2	30	2	1	25	39	2.9
BIG003	Soil	274402	3745355	0.003	4	4.6	188	<0.5	<1	2	40	1	1	26	36	4.2
LP10	Soil	276130	3746543	0.013	3	5.49	127	0.5	2	5	50	11	6	28	48	10.8

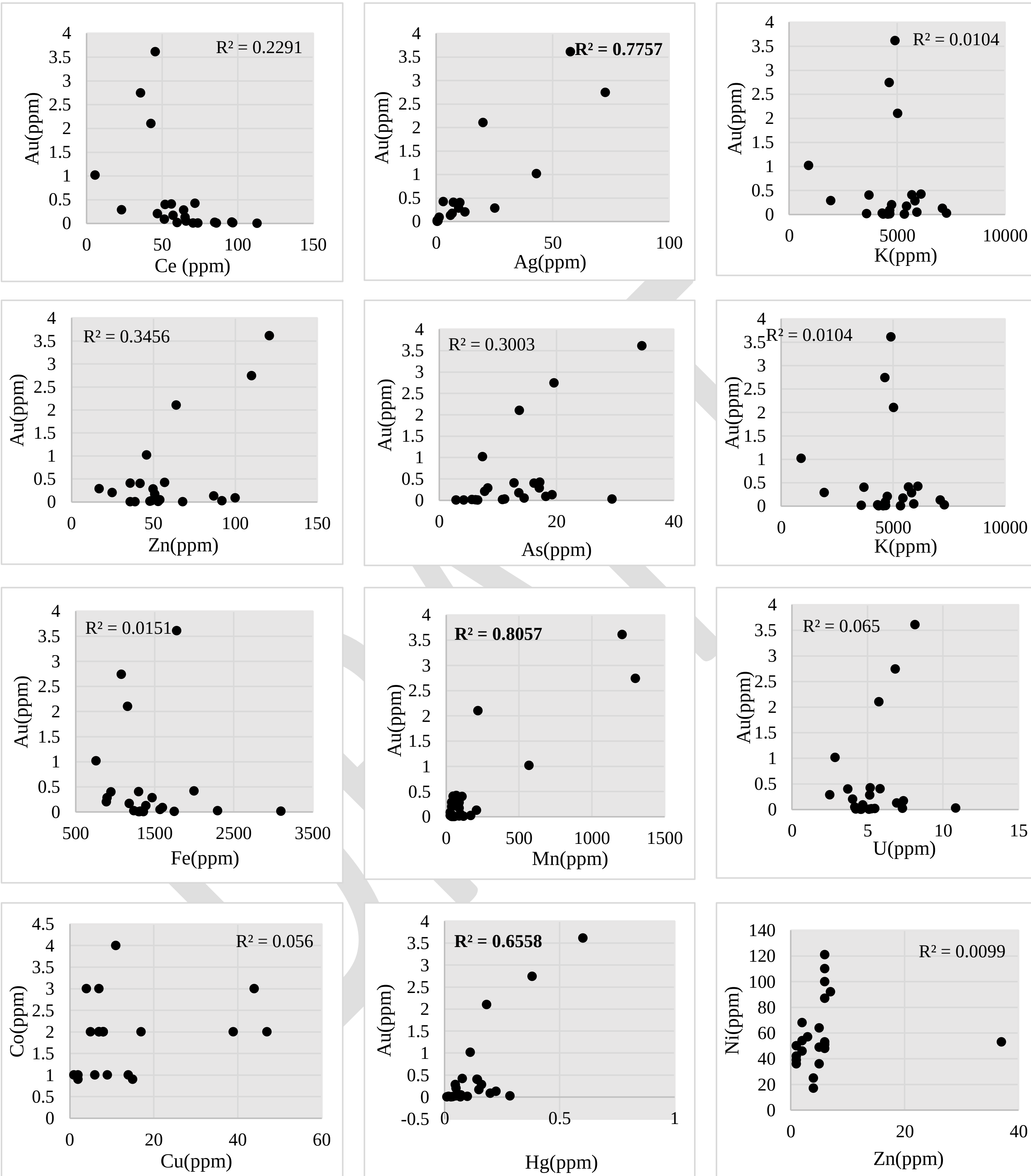

Figure 15: Correlation plots showing relationship between Au and Ag, As, Mn, K, Na, Fe, Hg, U, Ce, and Zn. The correlation between base metals such as Ni and Zn and Co and Cu.

Mineralogy

XRD Analysis

The X-Ray Diffractometer (XRD) analysis aided in determining the mineralogy of the waste rock pile that contributed to alteration and the mineral phases within the samples. Sample analysis assisted in identifying secondary mineral associated with the rock pile and their relative concentration. Determining relative number of sulfides (pyrite and sphalerite) within the waste rock piles formed a major part of the analysis. A total of sixteen (16) samples were selected for the analysis, based on hand sample observations of alteration, mineralogy and geochemical analysis results. All analyses were conducted at the NMBGMR laboratory in Socorro, New Mexico on X-Ray Diffractometer (XRD).

Detailed sample preparation for the analysis were conducted, where large volume samples were utilized to mount powdered samples (~75μ/0029 mesh) in standard milled aluminum sample holders. Samples were loaded into XRD machine to perform scans, from 2.0 degrees to 35.0 degrees 2θ, with a stepsize of 0.03 degrees and dwell time of 0.5 seconds. A forty (40) minutes mineral scan for all the samples were conducted for the analysis.

A set of 16 samples analyzed from the study area, all results showed similar patterns: high percent concentration in quartz, high in sanidine±microcline, and trace amount of pyrite and hematite. Most samples also showed noticeable amount of pyrite which indicate the presences of silver in the pyrite phase. The intensity of diffraction pattern with calculated percent composition is shown in Appendix 6.

Electron Microprobe Analysis

Electron microprobe (EMP) analyses were conducted at the NMBGMR laboratory in Socorro, New Mexico on a Cameca SX-100 electron microprobe. The analysis used for generating backscatter images, qualitative and quantitative chemical composition for polished samples from waste rock piles, as well as outcrop chip sample within alteration, veins and shear zones. Total of eight (8) representative samples were prepared specifically for electron microprobe and these were careful selected based on samples with significant geochemical Au-ICP results. Sample preparation were done using the standard petrographic grain mounts in labeled vial.

In sample analyses, the SX100 was usually operated at an accelerating voltage of 15kV and a beam current of 20nA with a focused beam. For qualitative scans, WDS Survey Spectrum (WDS Scan) reconnaissance technique was used to determine what elements are present in the samples. When the WDS mode was selected within the Quali Acqusition setup window, the WDS spectrometers are scanned over their respective wavelength ranges and a record of X-ray intensity versus spectrometer position is recorded. For cursory examination of the sample a short collection time, typically 1-3 minutes is selected. This detected all elements present in concentrations >1-5 wt% (lower limit is dependent on the element selected). The scan was set to 1000 channels and one accumulation. The resulting spectrum exhibits the characteristic X-ray peaks of the elements present at a specific point on the sample. However, in quantitative analysis, a list of calibration elements was decided based on the standards (pyrite and magnetite), crystal, background positions and slope factors that were used in the analysis. The associated detection limits and standards are presented in Table 2. Machine conditions were fully optimized based on the desired scan output. The oxides of the following elements were analyzed: Au, Al, As, Ca, Cu, Fe, K, Mg, Mn, Si, S, Ti, Zn, Zr and REE.

Table 3: Average composition (quantitative) of iron oxides (FeOx) phases (ROSE-001:10 analyses, ROSE-004: 6 analyses, ROSE-005: 11 analyses from Rosedale mine and BEL-001: 14 analyses, BEL-002: 10 analyses, BEL-003: 10 analyses, BEL-012: 9 analyses from Bell mine). Sample element with asterisk (*) showed pyrite, but the analysis was conducted on oxide phase

Element Concentration (Weight Percent)											
Al	**As**	**Au**	**Ca**	**Cu**	**Fe**	**Mg**	**Mn**	**Si**	**S**	**Ti**	**Total**
ROSE-001(FeO$_x$)											
0.97	0.11	0.61	0.12	0.03	77.65	0.03	0.16	4.33	0.06	0.08	84.15
ROSE-004 (FeO$_x$)*											
1.03	0.36	0.63	0.19	0.03	72.50	0.14	0.63	3.69	9.79*	1.08	90.06
ROSE-005 (FeO$_x$)											
2.11	0.31	0.69	0.22	0.07	76.30	0.02	0.18	4.10	0.07	0.06	84.14
BEL-001 (FeO$_x$)											
2.58	0.24	0.67	0.22	0.02	64.80	0.17	0.59	7.56	0.06	0.76	77.66
BEL-002 (FeO$_x$)											
2.19	0.34	0.72	0.25	0.04	66.80	0.08	0.32	4.83	0.09	0.21	75.87
BEL-003 (FeO$_x$)											
30.29	0.16	0.56	0.22	0.38	51.49	0.07	0.55	3.60	0.02	0.05	87.38
BEL-012 (FeO$_x$)											
0.88	0.16	0.72	0.20	0.02	67.36	0.02	0.11	5.35	0.18	0.10	75.09

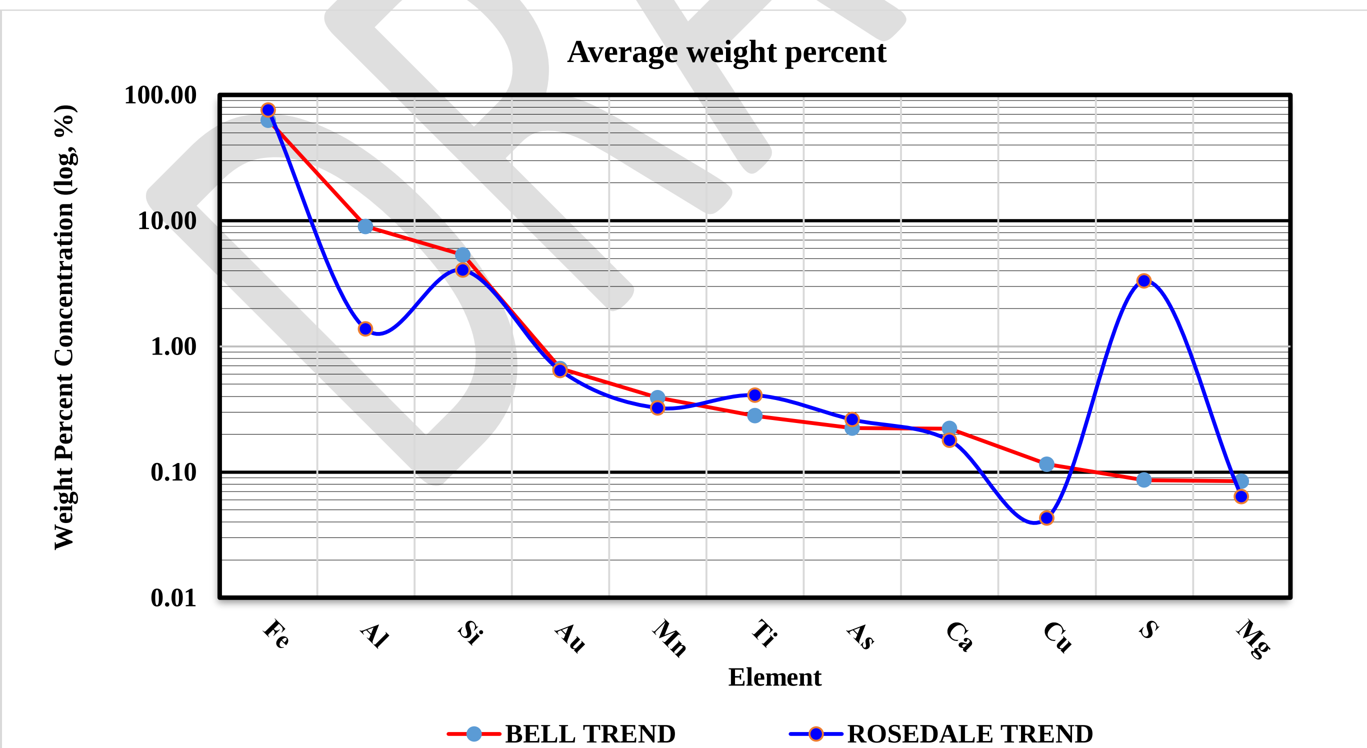

Figure 16: Plot of average weight percent of elements analyzed by electron microprobe for the Rosedale (Blue) and Bell mine (Red). Number of points analyzed for Bell (n=43) and Rosedale (n=27) samples on hematite grains. Base metal phases such as Cu was observed in both trends. Oxidized pyrite was observed in Rosedale samples.

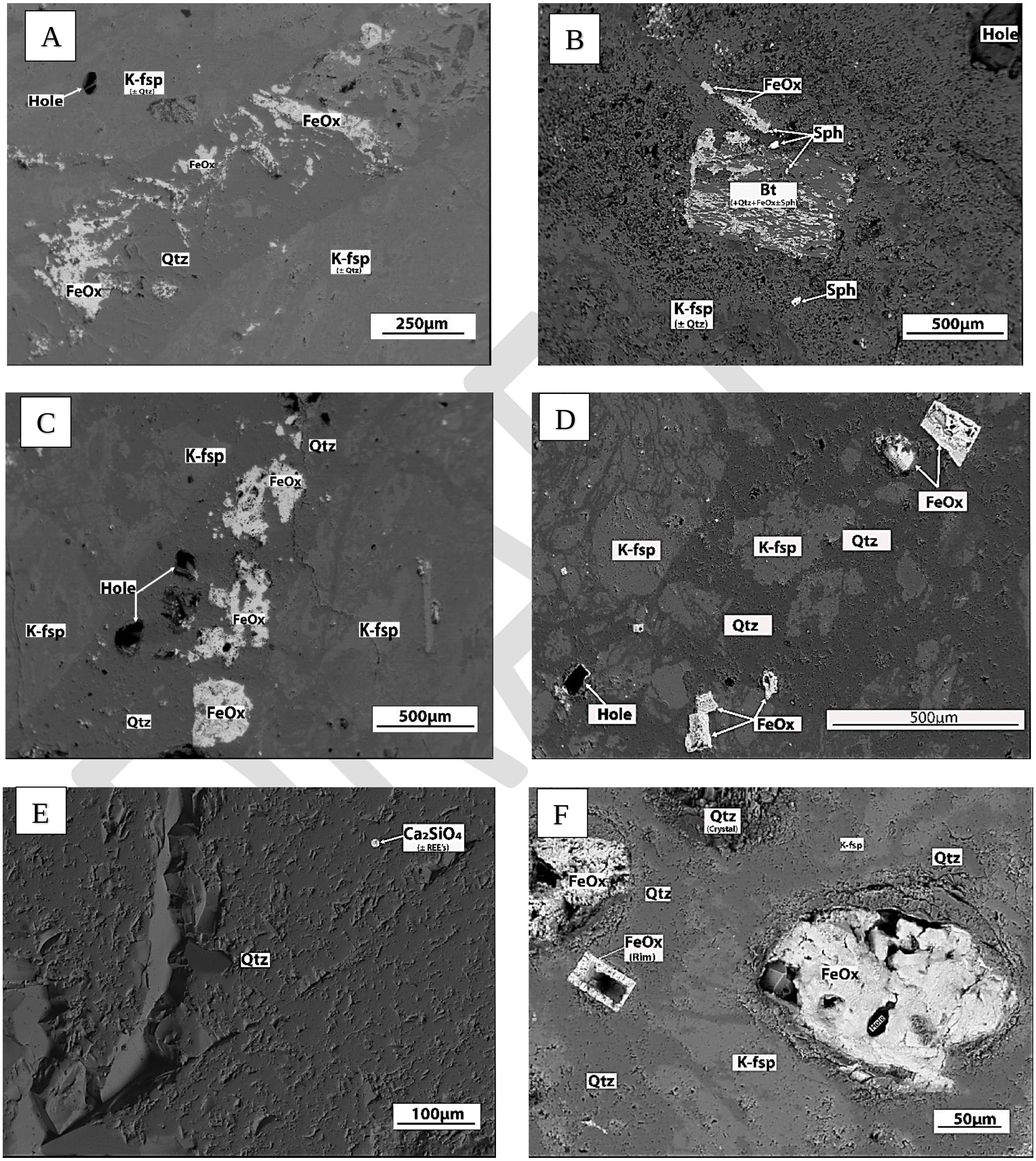

Figure 17: (A-F) BSE images of samples with gold concentrations from electron microprobe. (A) Hematite associated with quartz vein (ROSE-005). (B) Destruction and replacement of biotite by hematite and quartz. Pyrite intergrown with hematite and minor sphalerite replaced by hematite and quartz (ROSE-004). (C) Hematite within quartz vein associated with silicification

(ROSE-005) (D) Completely altered pyrite by hematite (ROSE-001). E) Observed calcium silicate with REE phase (ROSE-004). F) Destruction and replacement of pyrite by hematite (ROSE-001).

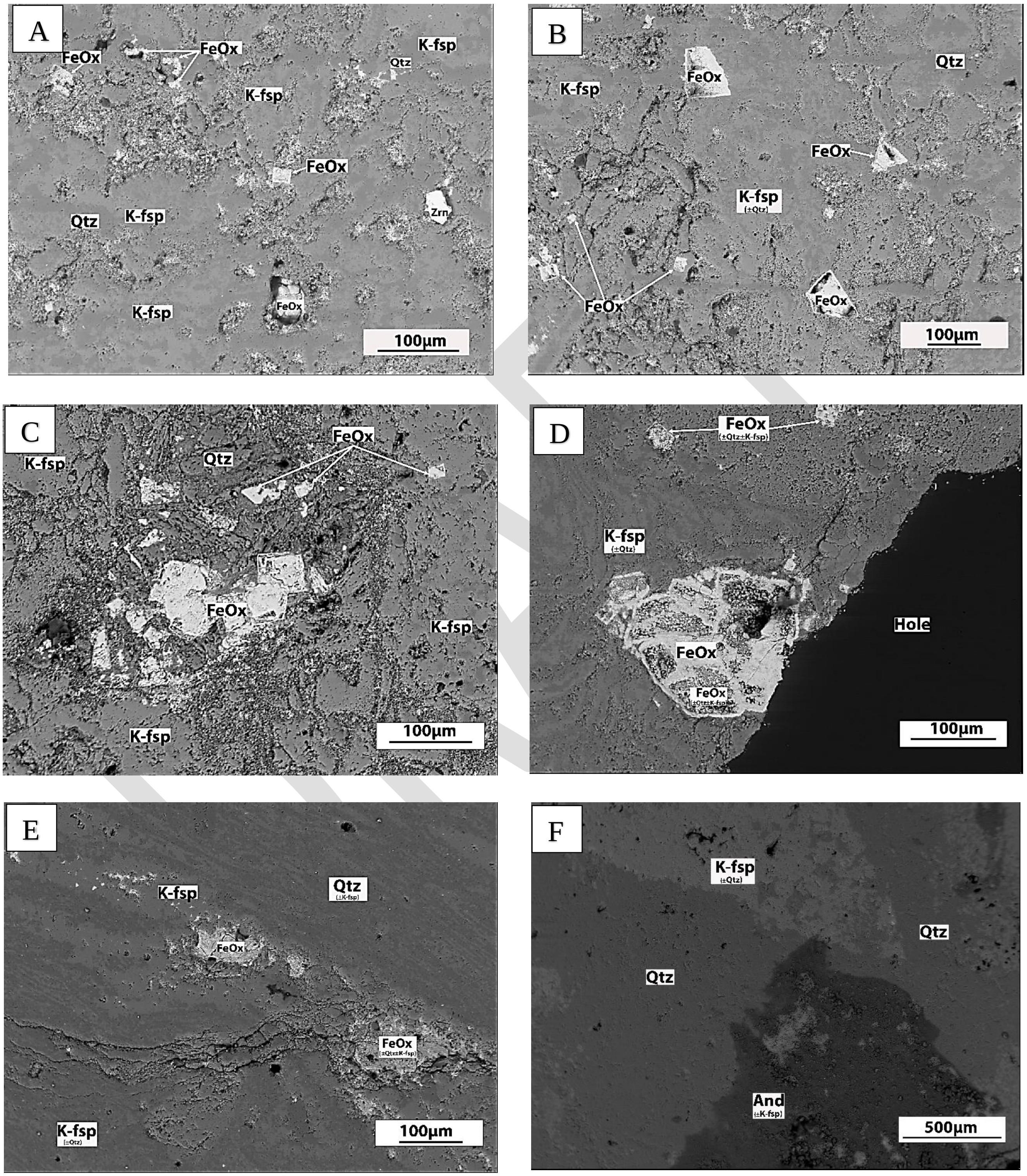

Figure 18: (A-F) BSE images of samples with gold concentrations from electron microprobe. A-E) Completely bifurcated and pyrite replaced by hematite (BEL-001, BEL-002) F) Pervasive potassium aluminum silicate in samples from Bell mine (BEL-003)

In oxidized rock samples from waste rock piles show, iron-oxide alteration after pyrite overgrowths. Most pyrite grains identified in all the samples were oxidized to hematite and contain detectable Au based results from the quantitative scan on electron microprobe analyses (Fig. 17 and 18). These hematite after pyrite are the only evidence that indicate direct confirmation of sulfide minerals existing in these rocks prior to oxidation. No fresh rock sample was analyzed for this study. In the rhyolitic breccias at fault and shear zones, iron oxide after pyrite with overgrowths are generally originate within quartz veinlets. Sphalerite is the only base metal sulfide observable in small amount in a sample from Rosedale mine analyzed and were generally replaced by hematite through oxidation. A Cu phase which occurs in minute amount was observed with Rosedale mine sample with high geochemical value (ROSE-004). McLemore (1996) documented that most low sulfidation vein deposits in New Mexico carries some concentration of Cu, but they are not enough for production. A unique assemblage of calcium silicate with REE phase was observed in at least a sample from Rosedale mine which is associated with the mineralization zones. Generally, no indication of Ag was present in any of the samples analyzed and this is typical of volcanic-epithermal deposit within Rosedale mining district (Lasky 1932, McLemore, 1994)

Gangue minerals associated with the Rosedale samples include quartz, potassium feldspar, biotite and kaolinite. Quartz and potassium feldspar are major constituents of the groundmass, where quartz forms the matrix of the sample. The destruction and replacement of biotite by hematite and quartz in some portions of the samples were observed along fractures of the biotite gradually spreading into adjacent portions.
Qualitative analysis plot for metal phases from the Rosedale and Bell mines presented in Appendix 3. The metal phases include Iron oxide, Sphalerite, Copper and Calcium silicate with REE. Table 3 above summarized the average composition (quantitative) of iron oxides (FeO_x) metal phases, including base metal stage pyrite that were analyzed for all the samples: Sample from the Rosedale mine showed a pyrite phase but the analysis was conducted on oxides phase.

CHAPTER SIX: MINERAL RESOURCES EVALUATION

Mine Features

Prior to beginning fieldwork, all available published materials regarding the Rosedale district were compiled and reviewed. Maps, reports, and databases were acquired from historical data that indicates spatial locations of mine features in the district. The data acquired from literature search provided a valuable background information on mine features and which data to collect during the study. Fieldwork observation provided information on the present state of mine features. A total of 99 mine features were accessed during fieldwork. (Table 4 and Fig. 19)

Table 4: Summary of mine features located in the Rosedale district.

Mine	No. of Mines Feature	Mine Feature	Depth of workings (ft)
Rosedale	**28**	Shafts (14 levels), Pits, Adit, Tailings, Mill Foundations, Trenches	2- ≥726
Bell	**16**	Tailings, Shafts, Adit, Mill Foundations, Pits	2 - >50
Bell South	**7**	Adit, Shafts, Pits	3 - >10
Big Rosa Canyon	**33**	Shafts, Adit, Pits, Trenches	2 - >30
Robb Prospect	**10**	Adit, Shaft	3 - 20
Lane Prospect	**4**	Shafts, Pits, Trenches	2 - >30
Oak Spring	**1**	Drillhole	-

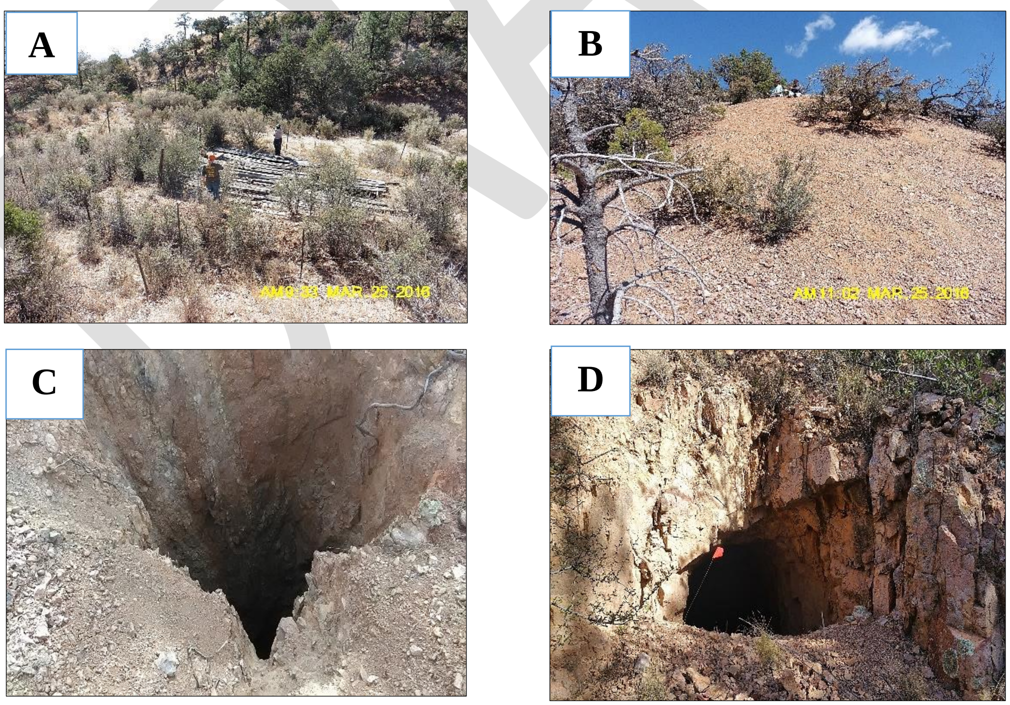

Figure 19: Mine features located at Rosedale and Bell mine: A) Shaft –Rosedale mine. B) Waste Rock pile-Rosedale mine. C) Shaft-Bell mine. D) Adit-Bell mine

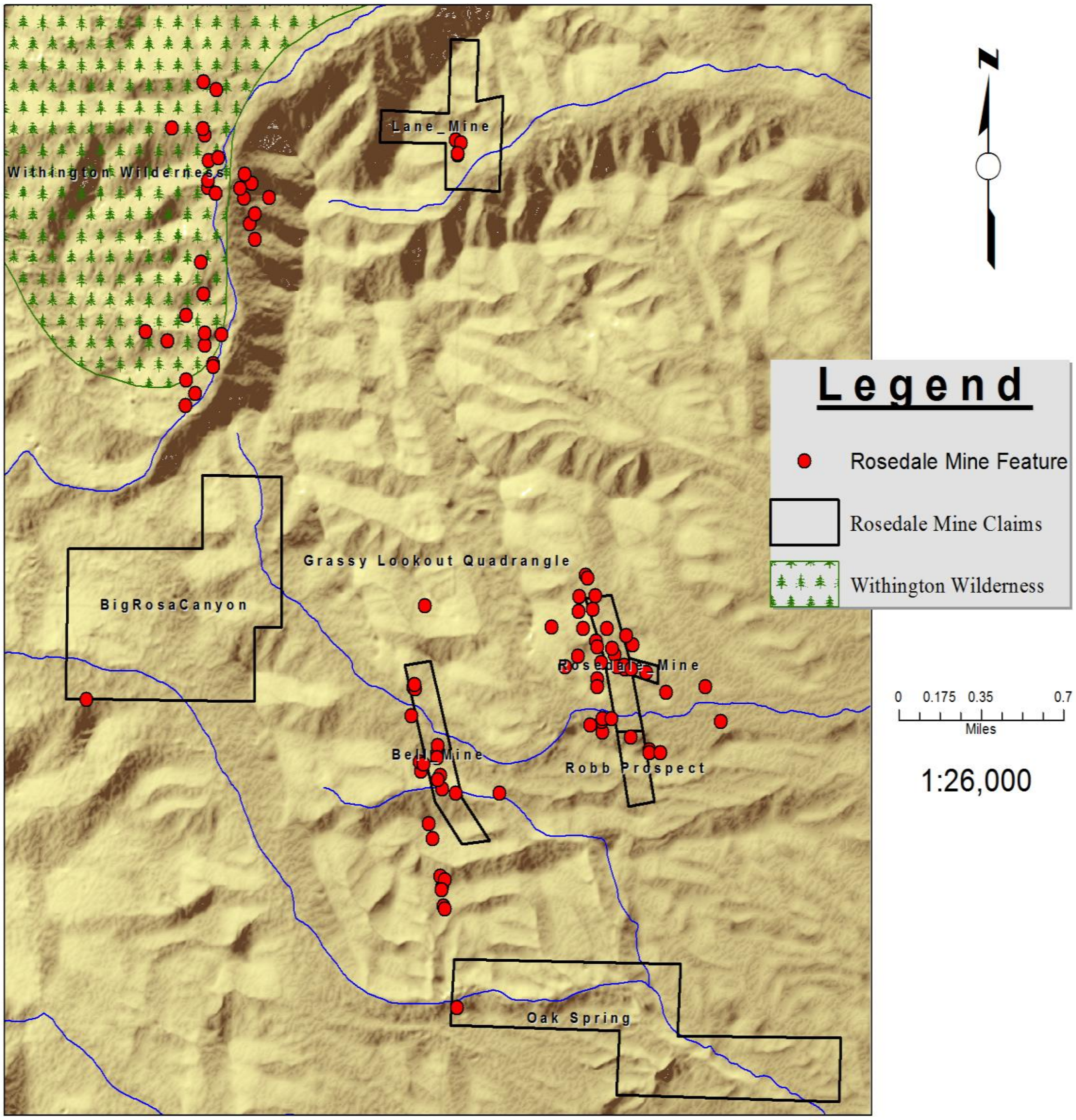

Figure 20: Location of mine features in Rosedale district.

Waste Rock pile and Rock Chip sampling

Representative samples on each waste rock piles and rock chip were collected from the study area for geochemistry, petrological and mineralogy analyzes. Geochemical analysis of these samples will be utilized to determine the chemical composition of these waste dumps and also to classify and characterize the suitability of these materials as a backfill. Depending on the mineral composition and the volume of these dumps, an economic valuation was assessed for their mineral resource potential. Sampling procedure employed for various sampling area are as follows:

Bulk Composite Sampling

- Clean shovel or stainless hand trowel used for the collection of representative multiple composite samples from waste rock piles

- Approximately 5-gallon bucket full of 20 mesh sieved material collected and split into a well labeled 4 zip-lock bags
- Sample bags are well sealed and secured to prevent moisture loss from the sample
- Labeled sample bags are stored in buckets and carefully transported to the Economic Lab at NMBGR for laboratory analysis
- Samples are prepared for shipment to ALS Lab, Reno, Nevada for geochemical analysis

Rock Chip Sampling

- Selected outcrops that represent specific rock types and alteration assemblages are sampled with a clean hammer and chisel. Clean rock surface are usually sample to avoid contamination or misrepresentation
- 3-5 kg of rock are taken with hammer and chisel
- Samples placed in labeled bags and carefully transported for lab analysis

All sampling types are photographed and geographically located using the GPS. Quality control programs are in place for all samples dispatched to the lab.

Figure 21: Bulk composite of waste rock pile and selective rock chip sampling.

Waste Rock Pile Mapping

GPS location points around the waste rock piles are recorded or dimension around the pile is measured with the measuring tape to determine the area of the piles. To calculate an estimated volume of the piles the height of these dumps is measured or estimated and shapes of the piles sketched in ArcGIS to determine the actual profile for volume calculation. Spatial locations and estimated volumes for some waste rock piles at the Rosedale and Bell mine are depicted in the Figure 20 and Table 5 respectively.

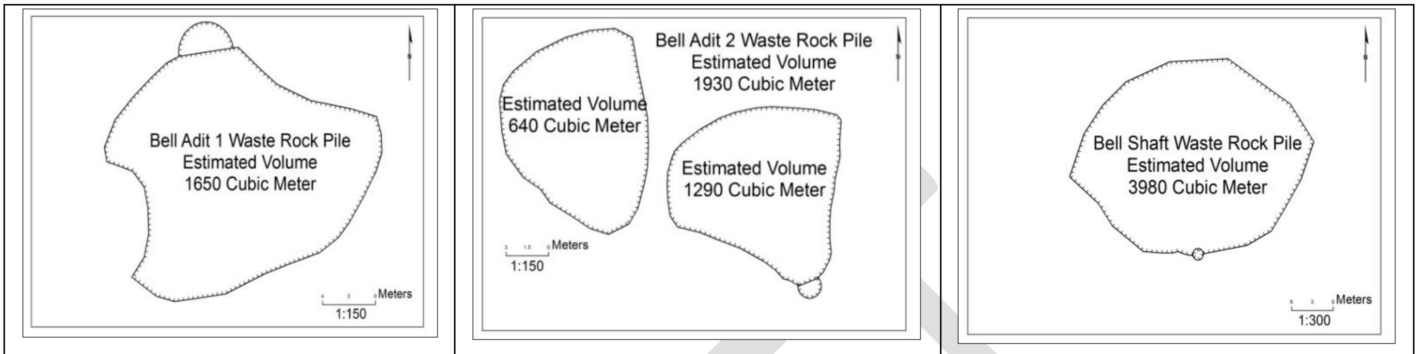

Figure 22: Estimated volumes of selected waste rock piles at Bell mine.

Table 5: Summary of estimated volume for various waste rock piles in Rosedale district.

Location	Easting	Northing	Elevation	Mine Feature	Estimated Volume (m^3)	Comment
Bell Adit 1	276018	3742604	7452	Waste rock pile	1650	Crushed rock material from mine adit
Bell Adit 2	275993	3742661	7540	Waste rock pile	1930	Material from two separate waste rock piles
Bell Adit 3	276013	3742689	7576	Waste rock pile	650	Crushed rock material from mine adit
Bell Shaft 1	275989	3742824	7552	Waste rock pile	3980	Crushed rock material from mine shaft >50ft
Bell Mill Tails	276115	3742575	7452	Tailings	77	Tailing material deposited at Bell Mill

Geological Mapping

Mineralization is structurally controlled, as mineralization occurs in a well-developed vein that is brecciated and sheared zones within the rhyolitic porphyry rock. Detailed mapping of the study area was not conducted due to limited time constrains however a few geological features at adits and shafts were examined during field work. Geological units examined and described, include lithology, structures and alteration, mostly at Rosedale and Bell mines. Geological units differentiated based on color, particle size, composition, stratigraphic position, dip, thickness and other properties. A relationship model for structures and mineralization of vein lineation within Rosedale and Bell mine area generated to define the origin and trend of gold mineralization in Rosedale district.

CHAPTER SEVEN: DISCUSSIONS

Controls on Mineralization

The Rosedale volcanic-epithermal vein deposits occur in Mogollon-Datil field and are mostly formed by complex regional and local structures that appears to control emplacement of magma and subsequent flow of hydrothermal fluids. The structural setting connected to the mineralization for the Rosedale deposit is considered to be related to the normal fault along the margins of Mt. Withington calderas, although other tectonic settings played varying roles in the mineral deposition Mineralization within the district is structurally controlled and mainly confined to open space along faults, shear zones and fractures in brecciated rhyolite-porphyry rocks. The composition of the host rocks of the deposits ranges from rhyolitic to andesitic, and ore is likely to be hosted by several different compositional units within the district. In general, the deposit is characterized by the predominance of argillic alteration, consisting of a mica-type mineral+ quartz + pyrite (oxidized) and often borders a silicified zone near the vein. Also, near the veins, fine-grained potassium feldspar is often disseminated in the wallrock.

Mineral Resource Potential

There is high mineral-resource potential of Au and Ag deposits at the Rosedale district because there is known Au production from the Rosedale and Bell mine and evidence of moderate to low grade material from surface and subsurface sampling from waste rock piles and other mine features. The Rosedale district have produced an estimated 28,000oz of gold and 10,000oz of silver mined from fourteen (14) levels of underground development (McLemore, 2017). Drilling in the district has indicated subsurface mineralization from low to high grade intercepts which will require further exploration work for economic development in the current market. Mineralogical analysis data also indicates that, there are concentrations of Au and Ag in low-sulfidation deposits. Evidence of geological mineralization controls observed during fieldwork also points to a high potential of a volcanic-epithermal vein deposits in the district. However, additional mapping and exploration drilling could locate additional trends and mineralization features at depth. Any potential exploration or subsequent mine development would have to be accessed taking into consideration the environmental effects and other mine impact assessment (McLemore, 1985).

Volcanic-Epithermal Vein Deposit Comparison

Most of the volcanic-epithermal system in Mogollon-Datil field are of low-sulfidation type except for Alum Mountain which is high-sulfidation system based on alteration mineral assemblage of the deposit (McLemore,1996). Nearly all volcanic-epithermal deposit in Mogollon-Datil field are hosted in Oligocene to Miocene volcanic and intrusive rocks. Few epithermal veins are hosted locally by Paleozoic and Mesozoic sedimentary rocks in few areas, such as Chloride, Cat Mountain and Abbe Spring, but these districts are considered as near Oligocene-Miocene volcanic center (McLemore,1994). Stratigraphic and structural relationships indicate, date of mineralization is typically indicating 5-15 Ma younger that the host rocks (McLemore, 1994). McLemore (1994) indicated that, nearly all low-sulfidation deposits in Mogollon-Datil volcanic field, such as the Rosedale shows similar characteristics with respect to vein emplacement, mineralogy, alteration and texture and these are typically related to magmatic-hydrothermal fluids. Mineralization is structurally controlled and filled spaces along faults and fractures planes which commonly form prominent outcrops and bifurcation, pinch and swell along strike. Complex vein textures, especially brecciation, banded layering and concentration by quartz and are common to most districts and locally are associated with higher concentration of metals (Buchanan, 1981; McLemore,1993),

Low-sulfidation systems in New Mexico, typically are silver rich and gold poor with gangue of quartz and calcite. However, the Rosedale district differs in the ratio of gold and silver associated with the mineralization. The district is one of the few volcanic-epithermal, precious-metal deposits that contains predominantly gold with low silver (Fig. 23; McLemore,1994). Low-sulfidation deposits with low silver to gold ratios are generally associated with native gold, native silver and electrum with rare silver sulfide and sliver sulfosalts and base metals (Hayba et. al., 1985). In contrast, the Socorro Peak district contains predominately silver with little gold (Lasky,1932). Most low-sulfidation volcanic-epithermal deposits in New Mexico contains minor amounts of base metals and base metal content typically increase with depth in many areas. The Steeple Rock district contains significant base metals along with silver and gold but not considered to be enough for production.

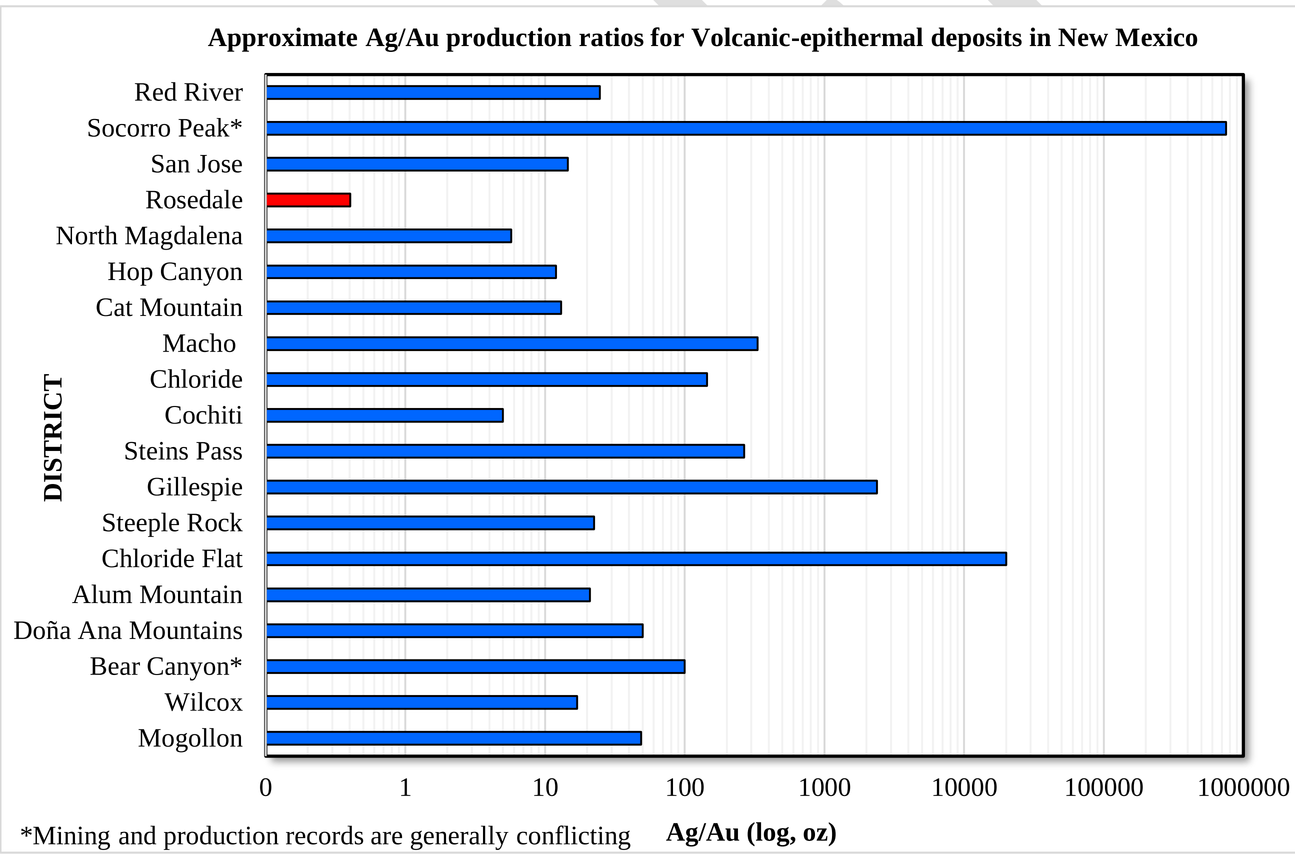

Figure 23: Approximate Ag/Au ratios for volcanic-epithermal deposit in New Mexico based on production (McLemore, 2017).

Waste Rock Piles Characterization

Most rock samples from waste rock piles exhibit iron-oxide alteration, mostly as pyrite replacements by hematite except for a sample from the Rosedale mine that showed a nominal residual pyrite phase in electron microprobe analysis. Rates of pyrite oxidation is subjected to the presence of water however, the water table at the Rosedale district was observed to be deep (723 feet). In view of that, potential of ARD of the waste rock pile is considered very low hence the material can be suitable for backfill material. Regarding potential environmental issues with Rosedale district waste rock, no ARD was observed from this material during fieldwork.

Average pH values of the mine features range between 4.9 and 6.6. The pH results indicate moderately alkaline to acidic waste rock piles (Appendix 6). Total dissolved solids (TDS) values calculated were between 5.9 and 40 mg/L and these results provide an indication of the level of dissolved solids in the stream or lakes closer to the waste rock piles

CHAPTER EIGHT: CONCLUSIONS AND RECOMMENDATIONS

The mineral-resource potential for the Rosedale district shows high certainty for a low-sulfidation, volcanic-epithermal vein system of gold and silver. Mineralization generally exist as native gold and silver with low silver to gold ratios. From geochemical analysis the ratios of gold and silver for the Rosedale and Bell mine were 0.05 and 0.03 respectively. Gold also showed positive correlation with silver and manganese for the whole rock geochemistry.

The presence of mineralization trends from surface samples and mined out volcanic-epithermal veins from the Rosedale and Bell mine suggest that additional deposits exist and probably extensive at depth. The best potential is associated with faults, shear and alteration zones within the district. Geochemical analysis results of waste rock samples from areas sampled show elevated metals, specifically for gold. From these results, samples from the Rosedale shows a more consistent elevated metal pattern averaging about 1.21 ppm while samples from the Bell mine shows low results of about 0.23 ppm.

Electron microprobe analyses reveal elevated gold content, with little or no silver, within hematite grains. Sphalerite was found in nominal amounts in a sample from the Rosedale mine and was generally replaced by hematite through oxidation. A copper phase, which occurs in trace amounts, is associated with the sample that had elevated whole-rock gold concentrations (3.61 ppm Au, ROSE-004, from the Rosedale mine).

Rosedale district shows similarities in alterations, mineralogy, lithology and structural characteristics compared to other volcanic-epithermal deposit within New Mexico

Most samples exhibited iron-oxide alteration, mostly as pyrite replacements by hematite with no potential for ARD. Therefore, can be concluded that, the waste rock piles are suitable as backfill of unprotected mine features. In addition, a borrow pit was used as cover for the Rosedale tailings, and no ARD has been observed from this material.

Detailed petrographic studies can be performed on the prepared samples for mineralogy that will ascertain the paragenesis of the Au and Ag in the waste rock pile samples.

Conducting progressive outcrop mapping and sampling of veins and other rock types will assist to define the mineralization and also to determine background metal concentration of the area. Sampling of mine features such as shafts, pits, adits and waste rock piles can be used as an effective tool for exploration in the district.

Detailed mapping within Rosedale mining district will assist to define major alteration zones and structural trends that controls mineralization in northern and southern extension of Rosedale and Bell mines. There are possible parallel trends which is thought to represent major eruptive phases that may tapped progressively deeper and less evolved material from a sub-caldera magma chamber.

CHAPTER NINE: REFERENCES

Anderson E. C.(1957), The Metal Resources of New Mexico and Their Economic Features Through 1954 , Bulletin 39 , A revision of Bulletin 7, by Lasky and Wootton, with detailed information for the years 1932-1954, State Bureau of Mines and Mineral Resources, New Mexico Institute of Mining & Technology Campus Station Socorro, New Mexico, pp. 140- 150

Anderson G. B. (1907), History of New Mexico: It's Resources and People (in two volumes). Los Angeles, CA: Pacific States Publishing Company, pp. 960-961

Batchelder J. H. (1910). Report on the Rosedale Mine , Rosedale, New Mexico, Unpublished Report , pp. 16.

Blakestad R. (1975), Rosedale Prospect: Summary of work to date, Socorro County, New Mexico, Perry, Knox, Kaufman Inc. Study Report of Rosedale Prospect, Unpublished, 6 pp.

Buchanan, L. J.(1981), Precious Metal Deposits Associated with Volcanic Environments in the Southwest, in Dickinson, W. R., and Payne, W. D. (eds.), Relations of Tectonics to Ore Deposits in the South Cordillera, Arizona Geological Society Digest, Vol. XIV, pp. 237-261.

Cather S. M., McIntosh W. C. and Chapin E. C. (1987), Stratigraphic, Age, and Rates of Deposition of Datil Group(Upper Eocene-Lower Oligocene), West-Central New Mexico, New Mexico Bureau of Geology and Mineral Resources, 6 pp

Chapin, C. E., Chamberlin, R. M., Osburn, G. R., Sanford, A. R., and White, D. L., (1978), Exploration framework of the Socorro geothermal area, New Mexico; ln Chapin, C. E., and Elston, W. E. (eds.), Field guide to selected cauldrons and mining districts of the Datil-Mogollon volcanic field, New Mexico: New Mexico Geological Society, Special Publication 7, p. l15-129.

Chapin, C. E., Chamberlin, R. M., Osburn, G. R., Sanford, A. R., and White, D. L., (1979), Geological Investigation of the Socorro Geothermal Area, New Mexico Bureau of Mines and Mineral Resources, p. 15 - 53

Chapin, C. E. (1979), Evolution of the Rio Grande Rift: A Summary: in Riecker, R. E., Rio Grande Rift: tectonics and magmatism: American Geophysical Union, pp. 1-5.

Chapin, C. E., Wilks, M., and McIntosh, W. C. (2004), Space-Time Patterns Of Late Cretaceous To Present Magmatism In New Mexico—Comparison with Andean Volcanism and Potential for Future Volcanism; in Cather, S. M., McIntosh, W. C., and Kelley, S. A., Tectonics, geochronology, andvolcanism in the southern Rocky Mountains and Rio Grande rift: New Mexico Bureau of Geology and Mineral Resources, Bulletin 160, pp. 13-41.

Cox D. P. and Singer D. A. editor, (1986), Mineral Deposit Model, United States Geological Survey, Bullettin 1693, p. 168-169

Deal E. G. (1973), Geology of the northern part of San Mateo Mountains, Socorro County, New Mexico: A study of the rhyolite ash-flow tuff cauldron and the role of laminar flow in the ash-flow tuffs : Unpublished Ph.D Dissertation, University of New Mexico, Albuquerque, New Mexico, pp. 108-109

Eggleston, T. L. (1982), Geology of the Central Chupadera Mountains, Socorro County, New Mexico: New Mexico Bureau of Mines and Mineral Resources, Open-file Rept. 141, 162 pp.

Elston W. E, Damon P. E., Coney P. J., Rhodes R. C., Smith E. I. And Bikerman M. (1973), Tertiary Volcanic Rocks, Mogollon-Datil Province, New Mexico, and Surrounding Region: K-Ar Dates, Patterns of Eruption, and Periods of Mineralization, Geological Society of America Bulletin v. 84, pp. 2259-2274

Elston, W. E., (1978), Mid-Tertiary cauldrons and their relationship to mineral resources in southwestern New Mexico-a brief review; in Chapin, C. E., and Elston, W. E., eds., Field guide to selected cauldrons and mining districts of the Datil-Mogollon volcanic field, New Mexico: New Mexico Geological Society, Special Publication 7, p. 107–113.

Elston, W. E., (1994), Siliceous volcanic centers as guides to mineral exploration: review and summary: Economic Geology, v. 89, p. 1662–1686

Ferguson C. A. (1986), Geology of the East-Central San Mateo Mountains, Socorro County, New Mexico, New Mexico Bureau of Mines and Mineral Resources, Open-File Report 252, pp. 26 – 99

Ferguson C. A. (1991), Stratigraphic and Structural Studies in the Mt. Withington Caldera, Grassy Lookout Quadrangle, Socorro County, New Mexico, Department of Geology and Geophysics, University of Calgary, Alberta, Canada, 6 p.

Ferguson, C.A., and Osburn, G.R. (1993), Geology of the Mt. Withington 7.5’ Quadrangle, Socorro County, New Mexico: New Mexico Bureau of Mines and Mineral Resources, Open-file Report 403, 1: 24,000 scale

Goudarzi, G. H., (1984), Guide to preparation of mineral survey reports on public lands: U. S. Geological Survey, Open-file Report 84-787, 50 p.

Hayba, D. O. (1983), A Compilation of Fluid-Inclusion and Stable-Isotope Data on Selected Precious- and Base-Metal Epithermal Deposits, U.S. Geological Survey, Open-File Report 83-450, 24 p.

Hayba, D. O., Bethke P. M., Heald P. and Foley N. K. (1985), Geologic, Mineralogic, and Geochemical Characteristics of Volcanic-Hosted Epithermal Precious-Metal Deposits, in Geology and Geochemistry of Epithermal Systems, Vol. 2, Society of Economic Geologists, pp. 129-162.

Hedge, C.E., Z.E. and Peterman, et al. (1968), Precambrian Geochronology of the Northwestern Uncompahgre Plateau, Utah And Colorado, in Geological Survey Research 1968, U.S. Geol. Survey. Prof. Paper 600-C, C91-C96, 1968.

Osburn G. R., and Chapin C. E., (1983), Ash-Flow Tuffs and Cauldrons in the Northeast Mogollon-Datil Volcanic Field-A summary; Socorro Region II, Chapin, C. E.; Callender, J. F.; [eds.], New Mexico Geological Society 34th Annual Fall Field Conference Guidebook, pp. 197-204

Osburn, G. R., and Chapin, C. E. (1983), Nomenclature for Cenozoic Rocks of Northeast Mogollon-Datil Volcanic Field, New Mexico: New Mexico Bureau of Mines and Mineral Resources, Stratigraphic Chart 1, 7 pp., I sheet.

Johnson, M.G. (1972), Placer gold deposits of New Mexico: U.S. Geological Survey, Bulletin 1348, 46 p.

Jones, F. A. (1904), New Mexico mines and minerals: Santa Fe, The New Mexican Printing Co., 346 p.

Koschmann, A.H., and Bergendahl, M.H. (1968) Principal gold-producing districts of the United States: U.S. Geological Survey, Professional Paper 610, pp. 211

Lasky S. G. (1932), The Ore Deposits of Socorro County, New Mexico, New Mexico Bureau of Mines & Mineral Resources, A Division of New Mexico Institute of Mining & Technology, Bulletin 8, pp. 94 - 98

Lindgren W., Graton L. C. and Gordon C. H. (1910). The Ore Deposit of New Mexico, United States Geological Survey, p. 190-204

Lipman, P. W. (1976), Caldera-Collapse Breccias in the Western San Juan Mountains, Colorado: Geological Society of America, Bulletin, v. 87, pp. 1397-7470

McDowell, T.W., and Claubaugh, S.E. (1979), Ignimbrites of the Sierra Madre Occidental and their relation to the tectonic history of western Mexico: Geological Society of America, Special Paper 180, pp. 113-124.

McIntosh W. C., Chapin C. E., Ratté J. C., Sutter J. F.,(1992a), Time-Stratigraphic Framework for the Eocene-Oligocene Mogollon-Datil Volcanic Field, Southwest New Mexico: Geological Society of America Bulletin, Vol. 104, pp. 851-871

McLemore, V. T., Hoffman, G., Smith, M, Mansell, M., and Wilks, M., 2005a, Mining districts of New Mexico: New Mexico Bureau of Geology and Mineral Resources, Open-file Report 494, CD-ROM.

McLemore, V. T., Krueger, C. B., Johnson, P., Raugust, J. S., Jones, G. E., Hoffman, G. K. and Wilks, M., 2005b, New Mexico Mines Database: Society of Mining, Exploration, and Metallurgy, Mining Engineering, February, p. 42–47.

McLemore V. T., Price L. G., Bland D., Barker J. M. (2005). Mining in New Mexico: The Environment, Water, Economics, and Sustainable Development. New Mexico Bureau of Geology and Mineral Resources and division of New Mexico Institute of Mining and Technology. Decision makers Field Guide. p. 133 – 156

McLemore V. T. (1984). Preliminary Report on the Geology and Mineral-Resource Potential of Torrance County, New Mexico, New Mexico Bureau of. Mines and Mineral Resources, Open-file Report 192, United States Department of the Interior, p. 94 – 200

McLemore, V. T. (1985), Evaluation of mineral-resource potential in New Mexico: New Mexico Geology, v. 7, p. 50-53.

McLemore V. T. (1996), Volcanic-epithermal, precious-metals deposits in New Mexico, New Mexico Bureau of Mines and Mineral Resources, p. 951-969

McLemore, V.T. (2001), Silver and gold resources in New Mexico: New Mexico Bureau of Mines and Mineral Resources, Resource Map 21, 60 pp.

McLemore, V.T., (2012), Mining Districts in the San Mateo Mountains, Socorro and Sierra Counties, New Mexico: New Mexico Geological Society, Guidebook 63, p. 85-87.

McLemore V. T. (2012), Geology of the Southern San Mateo Mountains, Socorro And Sierra Counties, New Mexico, New Mexico Geological Society, Guidebook 63, p. 261-272.

McLemore V. T. and North R. (1986), Silver and Gold Occurrence In New Mexico, New Mexico Bureau of Mines and Mineral Resources, Resource Map 15, 32 pp

McLemore V. T. (1993), Geology and Geochemistry of the Mineralization and Alteration in the Steeple Rock district, Grant County, New Mexico and Greenlee County, Arizona (Ph.D. dissertation); University of Texas at El Paso, Open File Report 397, pp.

McLemore V. T. (1994), Volcanic-epithermal deposits in the Mogollon-Datil volcanic field, west-central, New Mexico, New Mexico Geological Society 45th Annual Fall Field Conference Guidebook, p. 299-309

McLemore, V.T., Smith, K.S., Russell, C.C., editors (2014), Management Technologies for Metal Mining Influenced Water, volume 6: Sampling and monitoring for the mine life cycle: Society for Mining, Metallurgy, and Exploration, Inc., Littleton, CO.

Milligan M. H. (1967), Three Page Letter to Mr. Harry Ralston, Albuquerque, New Mexico, August 11, 1967, Re: “A Summary of an Examination of the Rosedale Property on August 6, 1967.” Río Bravo Exploration Co., Albuquerque, New Mexico (Photocopy made available through the courtesy of Senior Mining Engineer Robert W. Eveleth, New Mexico Bureau of Geology and Mineral Resources, Socorro).

Munroe, E. A. (1999), Geology and geochemistry of waste rock piles in the Hillsboro mining district, Sierra County, New Mexico: M.S. thesis, New Mexico Institute of Mining and Technology, Socorro, 144 p.

North R. (1983), History and Geology of the Precious Metal Occurrences In Socorro County, New Mexico, New Mexico Bureau of Mines and Mineral Resources, New Mexico Geological Society 34th Annual Fall Field Conference Guidebook 344p, pp. 261-268

North, R.M., and McLemore, V.T., 1988, A classification of the precious metal deposits of New Mexico, in Schafer, R.W., Cooper, J.J., and Vikre, P. G., eds., Bulk mineable precious-metal deposits of the western United States: Reno, Geological Society of Nevada, p. 625–659.

Neubert J. T. (1983), Mineral Investigation of the Apache Kid and Withington Wilderness Areas, Socorro County, New Mexico, US Department of Interior, Bureau of Mines, MLA 72-83, p. 6 -11

Scott D. (1991), Geochemical Survey of Rosedale Mining District, Socorro County, New Mexico, GEOC 471: Exploration Geochemistry Report prepared for David I. Norman, Unpublished Report, 110 pp

Smith, K.S., Ramsey, C.A., and Hageman, P.L. (2000b), Sampling Strategy for Rapid Screening of Mine-Waste Dumps on Abandoned Mine Lands, In ICARD 2000, Proceedings of the Fifth International Conference on Acid Rock Drainage, Denver, Colorado, May 21-24, 2000, v. II, p. 1453-1461. Available online at http://crustal.usgs.gov/projects/minewaste/pdfs/kathy.pdf

Smith K. S., Hageman P. L., Ramsey C.A., Wildeman T. R., and Ranville J. F. (2005), Reconnaissance Sampling and Characterization of Mine-Waste Material, U.S. EPA Hard Rock Mining 2006 Conference, Tucson, Arizona, 14 pp

Wells, E.H., and Wootton, T.P. (1940), Gold Mining and Gold Deposits in New Mexico: New Mexico Bureau of Mines and Mineral Resources, Circular 5, 25 p.

White, D.L., (19780), Rb-Sr Isochron Ages of Some Precambrian Plutons in South-Central New Mexico, Isochron/West, 21, p 8-14

APPENDICES

Appendix 1: Selected sketches and photographs of waste rock piles and estimated volumes

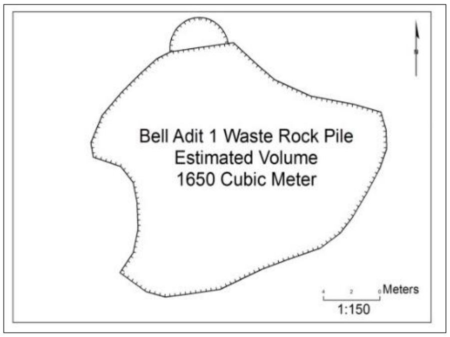

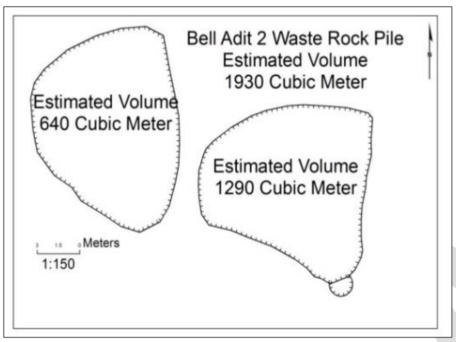

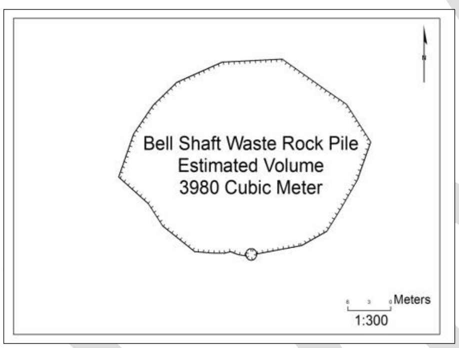

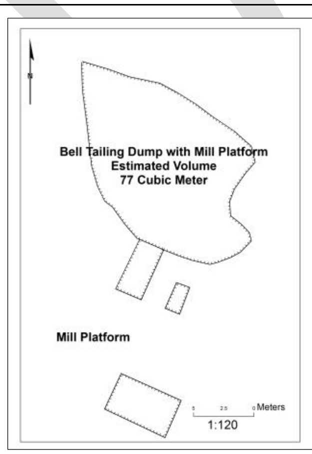

Appendix 2: Petrographic descriptions of samples. Location of samples in Appendix 4. Note: HT=hydrothermal alteration. Mod=moderate. Plag=plagioclase

Sample Number	Rock Frag-ments %	Clast Shape	Rank of HT Alt.	Intensity of HT Alt.	Weather-ing	Mineralogy	Description of Quartz	Descrip-tion of Feldspar	Descrip-tion of Oxides	Comments
ROSE1	40% of total sample, mostly rhyolite	Angular	Silicic	low	oxidized spots	quartz, feldspar, oxides	glassy prismatic, milky massive	plag in clasts	Single black grains and in clasts	
ROSE2	50% of tot., mostly rhyolite	Angular	Silicic	low	oxidized spots	quartz, feldspar, oxides	glassy prismatic, milky massive	plag in clasts	clasts show spots of oxidation	
ROSE3	50% of tot., mostly rhyolite	Angular	Silicic	low	oxidized spots	quartz, feldspar, oxides	glassy prismatic, milky massive	Some free plag	clasts show spots of oxidation	
ROSE4	50% of tot., mostly rhyolite, some solid gray clasts (andesite ?)	Angular	Silicic	low	oxidized spots	quartz, feldspar, oxides	glassy prismatic, milky massive	Some free plag	clasts show spots of oxidation	Weakly-cemented clumps dissolved during washing
ROSE5	50% of tot., mostly rhyolite, some clasts have black crust, rest is qtz+feld. Sand	Angular	Silicic	low	oxidized spots	quartz, feldspar, oxides	glassy prismatic, milky massive	Plag in sand	Present as black crusts on some clasts	Weakly-cemented clumps dissolved during washing
ROSE6	20% of tot. rest is sand	Angular	Silicic	low	oxidized spots	quartz, feldspar, oxides	glassy prismatic, milky massive	Plag in sand	Soft, subround black lumps of unk. Oxide	black lumps easily crush to powder between fingers
ROSE7	60% of tot, Mostly rhyolitic tuff	Angular	Argillic	mod	oxidized mod	quartz, feldsper, FeOx,MnO_2	glassy quartz, prismatic	Plag	Moderate Fe stains, MnO_2	Rhyolitic tuff fragment show moderate FeOx stains and MnO2 spots

Sample Number	Rock Frag-ments %	Clast Shape	Rank of HT Alt.	Intensity of HT Alt.	Weather-ing	Mineralogy	Description of Quartz	Descrip-tion of Feldspar	Descrip-tion of Oxides	Comments
ROSE8	30% of Tot, oxidized rhyolite with some tuff	Angular	Sicilic	low	Oxidized	Quartz, feldspar, FeOx, MnO_2	Milky to glassy.Moderate oxidation	plag	Moderate Fe stains, MnO2	Mostly quartz fragment with Tuff and Rhyolite, Moderate MnO_2 stringers
BEL003	10% of tot., mostly rhyolite (broken-down), some andesite	Angular	Silicic	low	oxidation on clasts	quartz, feldspar, oxides	glassy prismatic, milky massive	present in clasts	Single black grains and in clasts	
BEL002	50% of tot, Rhyolite	Angular	Silicic	mod	Mod	quartz, feldspar, FeOx	Milky to glassy quartz	present in clasts	Moderate Fe stains, MnO_2	Mostly rhyolite fragments with quartz
BEL008	10% of tot, rhyolite fragment	Angular	Silicic	mod	Mod	quartz,MnO_2, FeOx	Milky to glassy quartz	Plag	Low Fe stains, MnO_2 spots	Mostly silicified quartz fragments with minor rhyolite,
BEL009	70% of tot, Rhyolitic breccia	angular-subangular	Silicic	mod	Mod	quartz,MnO_2, FeOx	prismatic, Milky quartz	plag	Pervasive Fe stains, MnO2 stringers	Leached minerals forming vesicles in rhyolite, crystal quartz grains in rhyolite with low silicification
BEL012	20% of tot. rhyolite	Angular	Silicic	mod	Mod	quartz, FeOx	Milky to glassy quartz	Plag	Moderate Fe stains	Silicified rhyolite with moderate amount of iron stains. Spots of oxidized minerals
BEL015	70% of tot, Rhyolitic Tuff	angular-subangular	Argillic	mod	Moderate	quartz, feldspar, FeOx, MnO_2	glassy prismatic, milky massive	plag	Low Fe stains, MnO2 spots	Moderate amount of argilic alteration on rhyolitic tuff. MnO2 spots
ROBB2	60% in total, Rhyolite fragment with quartz	Angular	Silicic, Argillic	mod	Oxidized spots	quartz, feldspar, iron oxide	glassy to milky quartz	Plag in porphyry rhyolite	Moderate Fe stains	Silicified rhyolite porphry with some argillic alteration. Moderate amount of iron stains

Appendix 3: Qualitative analysis plot for metal phases in the Rosedale district

Qualitative analysis plot for metal phases at the Rosedale mine

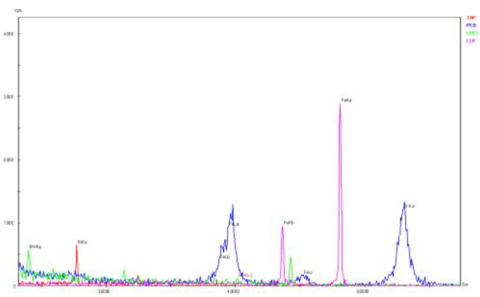

Hematite Phase

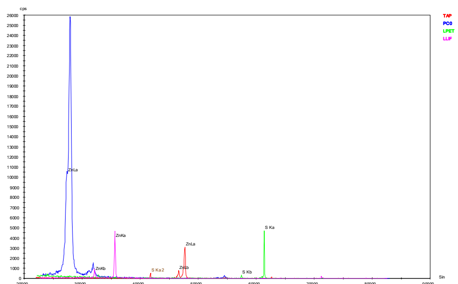

Sphalerite (ZnS) Phase

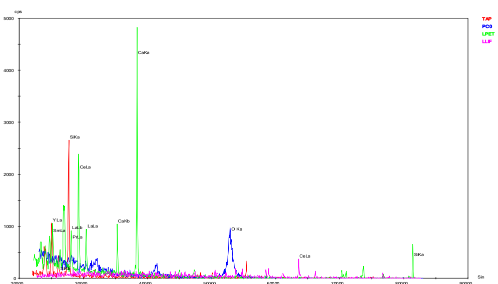

Calcium Silicate (Ca_2SiO_4) with REE's Phase

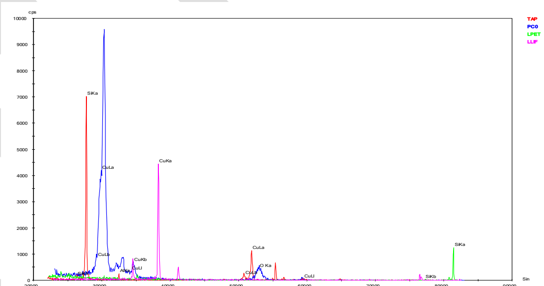

Copper (Cu) Phase

Qualitative analysis plot for metal phases at the Bell mine

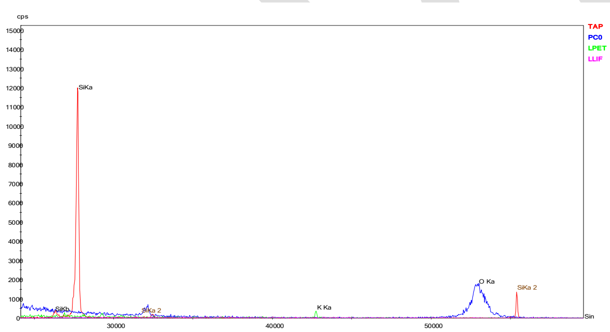

Quartz Phase

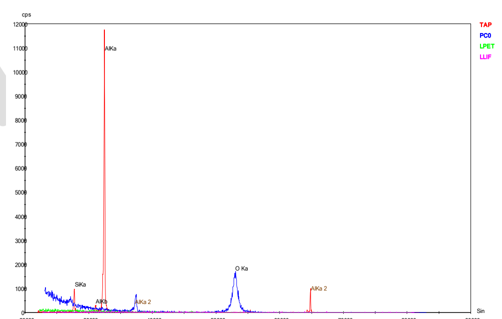

Aluminium Oxide Phase

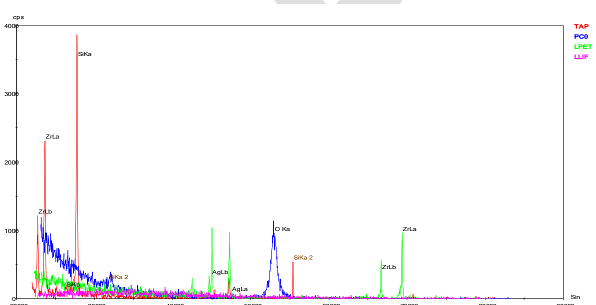

Zircon (Silver-bearing) Phase

Appendix 4: Whole rock geochemical analysis results for Rosedale district (Historical and present)

Historical geochemical results of Grassy Lookout conducted by Charles Ferguson (1990)

Samp. ID	Au(oz/t)	Ag(oz/t)	UTM Easting	UTM Northing
NM-89-1	0.00	0.44	275981	3742641
NM-89-10	0.00	0.20	278445	3747518
NM-89-10b	0.00	0.00	278439	3747526
NM-89-13	0.00	0.00	274544	3745310
NM-89-16	0.00	0.04	276228	3746360
NM-89-16a	0.00	0.12	276231	3746351
NM-89-16b	0.00	0.00	276235	3746366
NM-89-16d	0.00	0.00	276234	3746357
NM-89-17	0.00	0.00	275955	3746998
NM-89-18	0.00	0.00	275885	3746931
NM-89-19a	0.00	0.64	276069	3746629
NM-89-19b	0.00	0.12	276064	3746635
NM-89-19c	0.00	0.90	276072	3746638
NM-89-2	0.00	0.00	275974	3742636
NM-89-20	0.04	0.04	276138	3746611
NM-89-23a	0.00	0.78	277458	3748348
NM-89-23b	0.00	0.34	277467	3748346
NM-89-23h	0.00	0.12	277466	3748339
NM-89-24	0.00	0.08	277460	3748341
NM-89-29	0.00	0.00	272258	3748982
NM-89-33	0.00	0.04	273329	3746922
NM-89-34	0.00	0.22	276342	3748162
NM-89-35	0.00	0.00	271436	3745377
NM-89-36	0.00	0.00	269657	3745034
NM-89-9	0.00	0.04	275179	3746083
NM90.14	0.00	0.02	272490	3737073
NM90.22	0.00	0.00	269384	3739742
NM90.45	0.00	0.00	271624	3738736
T-89-11	0.00	0.00	274448	3745401
T-89-42a	0.00	0.26	274360	3746243
T-89-43	0.00	0.10	274360	3746243
T-89-XXX	0.00	0.00	279603	3749234

Whole rock geochemistry results for rock chip sampling conducted by Sunshine Mining Company

Samp. ID	UTM E	UTM N	Samp Type	ICP (ppm)														
				Ag	**As**	**Au**	**Cu**	**Hg**	**Mo**	**Pb**	**Sb**	**Tl**	**Zn**	**Bi**	**Cd**	**Ga**	**Se**	**Te**
287	275838	3741408	Rock Chip	0.112	14	0.012	4.71	0.1	9.88	7.62	4.17	0.499	28.3	0.25	0.125	1.02	0.998	0.499
289	275892	3741411	Rock Chip	0.045	1.85	0.002	5.75	0.098	9.97	11.6	2.99	0.488	34.9	0.244	0.153	1.85	0.977	0.488
299	275956	3741417	Rock Chip	0.05	5.35	0.0005	3.89	0.1	9.65	9.02	1.35	0.499	37.6	0.25	0.117	1.33	0.998	0.499
324	276015	3741424	Rock Chip	0.03	29.5	0.018	5.12	0.093	11.5	11.1	9.07	0.466	36.4	0.223	0.131	2.45	0.931	0.466
336	276083	3741429	Rock Chip	0.016	7.8	0.0005	2.65	0.095	7.7	10.6	5.82	0.475	29.3	0.238	0.115	1.96	0.951	0.475
340	275825	3741481	Rock Chip	0.014	16.8	0.004	2.04	0.096	7.71	8.43	2.06	0.479	14.5	0.239	0.096	0.861	1	0.479
420	275883	3741487	Rock Chip	0.022	7.83	0.006	3	0.099	7.63	6.75	0.86	0.497	43.2	0.249	0.101	1.72	0.994	0.497
427	276069	3741507	Rock Chip	6.18	9.03	0.51	7.03	0.096	32.9	5.42	8.43	0.481	16.2	0.314	0.096	1.32	0.962	0.481
456	276556	3741219	Rock Chip	6.06	3.13	0.173	8.6	0.099	31.4	13	4.29	0.72	8.35	0.249	0.101	0.664	0.994	0.497
458	276572	3741133	Rock Chip	6.99	0.197	3.32	0.049	0.543	8.3	1.13	0.493	19.4	0.19	0.162	0.968	0.247	0.059	
460	276578	3741042	Rock Chip	2.97	4.74	1.48	1.65	0.02	1.71	6.65	0.938	0.495	13.5	0.134	0.109	0.56	0.247	0.066
461	276590	3740951	Rock Chip	5.59	10.6	2.63	2.83	0.042	0.72	14.6	2.95	0.488	20.9	0.158	0.181	1.32	0.244	0.049
051	276034	3742024	Rock Chip	0.099	10	0.047	3.12	0.096	8.74	10.9	4.36	0.481	30.6	0.24	0.141	1.59	0.962	0.481
052	275916	3742014	Rock Chip	0.029	4.02	0.0005	4.2	0.093	10.1	12.9	1.06	0.466	36.3	0.233	0.39	1.97	0.931	0.466
053	275787	3742000	Rock Chip	0.03	3.94	0.0005	4.21	0.097	5.4	12.3	4.27	487	17.3	0.248	0.145	1.93	0.975	0.487
054	276024	3742095	Rock Chip	0.184	18	0.073	4.56	0.097	11.3	10.6	3.41	0.486	16.3	0.257	0.098	2.24	0.973	0.486
055	275911	3742083	Rock Chip	0.036	2.71	0.0005	3.18	0.099	7.1	9.98	0.705	0.496	26	0.248	0.111	1.96	0.992	0.96
056	275785	3742071	Rock Chip	0.036	3.85	0.0005	3.6	0.097	13.3	15.6	1.67	0.486	32.7	0.286	0.148	1.42	0.973	0.486
057	276128	3742103	Rock Chip	0.063	10.4	0.066	4.27	0.098	7.67	8.33	4.48	0.491	22.3	0.246	0.098	2.27	0.982	0.491
058	276258	3742117	Rock Chip	0.096	6.66	0.0009	8.75	0.099	11.4	24.9	1.75	0.494	84.5	0.247	0.117	1.85	0.988	0.494
059	276389	3742129	Rock Chip	0.056	4.97	0.0008	5.97	0.092	13.6	8.2	1.22	0.462	45.2	0.231	0.128	1.19	0.924	0.462
060	276505	3742144	Rock Chip	0.07	8.81	0.0005	4.28	0.1	8.75	13.8	2.09	0.481	34.9	0.24	0.096	1.71	0.962	0.481
061	276625	3742149	Rock Chip	0.05	7.9	0.002	6.13	0.097	12.5	9.58	2.88	0.487	41.1	0.244	0.097	1.82	0.975	0.487
062	276010	3742168	Rock Chip	0.057	4.11	0.0006	5.93	0.099	8.14	16.4	0.419	0.493	51.7	0.247	0.11	1.23	0.986	0.493
063	275901	3742160	Rock Chip	0.041	4.33	0.0005	5.16	0.098	10.9	12	0.851	0.49	46.7	0.245	0.127	1.61	0.98	0.49
170	276143	3742035	Rock Chip	0.475	20.3	0.025	5.62	0.096	16.6	11.6	3.04	0.479	32.3	0.239	0.113	1.8	0.958	0.479
171	276213	3742041	Rock Chip	0.045	14.2	0.003	4.94	0.094	11.6	18.9	1.22	0.471	27.4	0.235	0.182	1.94	942	0.471
172	276275	3742048	Rock Chip	0.045	7.59	0.0006	4.69	0.099	8.31	10.7	1.32	0.493	30.9	0.247	0.099	1.94	0.986	0.493
173	276333	3742053	Rock Chip	0.036	16.3	0.0005	4.85	0.097	15.9	6.22	2.24	0.484	38.9	0.242	0.097	1.17	0.969	0.484
174	276397	3742060	Rock Chip	0.044	9.41	0.0006	5.02	0.092	9.08	10.1	2.07	0.461	43.1	0.231	0.092	1.78	0.923	0.461
175	276456	3742066	Rock Chip	0.04	9.08	0.0007	5.91	0.092	16.9	8.85	2.52	0.461	48.9	0.231	0.096	1.99	0.923	0.461
176	276513	3742071	Rock Chip	0.052	13.7	0.0005	5.42	0.099	9.68	26.8	4.39	0.494	47.5	0.247	0.128	2.52	0.988	0.494
177	276577	3742075	Rock Chip	0.025	12.9	0.002	5.65	0.094	11.1	10.2	2.43	0.589	41.7	0.234	0.094	2.11	0.936	0.468

178	276635	3742080	Rock Chip	0.047	13	0.001	5.74	0.097	11.3	9.14	2.45	0.544	59.5	0.243	0.097	1.44	0.971	0.485
179	276692	3742087	Rock Chip	0.029	9.65	0.0005	6.48	0.096	18.2	8.68	1.74	0.48	43.8	0.24	0.096	1.88	0.96	0.48
180	275799	3741926	Rock Chip	0.036	11.3	0.001	4.36	0.093	9.48	12.1	8.56	0.466	34.3	0.233	0.152	2.97	0.931	0.466
181	275867	3741933	Rock Chip	0.03	5.01	0.002	4.44	0.1	12	12.6	3.48	0.537	26.5	0.25	0.159	1.72	1	0.5
182	275922	3741938	Rock Chip	0.043	5.43	0.002	7.05	0.1	9.34	11.5	3.86	0.499	28.6	0.276	0.155	1.99	0.998	0.499
183	275982	3741945	Rock Chip	2.35	23.2	0.423	8.77	0.097	39.5	6.27	9.96	0.942	28.8	0.243	0.114	1.2	0.971	0.485
184	276046	3741950	Rock Chip	0.064	10.5	0.004	6.54	0.092	11.2	12.2	4.13	0.46	62.5	0.23	0.122	2	0.921	0.46
185	276097	3741957	Rock Chip	0.061	9.49	0.003	5.56	0.099	17.1	18.1	5.59	0.494	63.3	0.247	0.134	1.55	0.988	0.494
186	276159	3741963	Rock Chip	0.056	12.5	0.01	6.1	0.099	11.7	9.77	3.17	0.493	21.1	0.247	0.108	1.27	0.986	0.493
187	276228	3741974	Rock Chip	0.044	18.8	0.038	6.33	0.094	14.2	11.8	7.29	0.472	26.9	0.236	0.167	1.43	0.943	0.472
188	276286	3741976	Rock Chip	0.033	8.81	0.0005	5.18	0.098	8.02	6.57	0.976	0.489	25.1	0.245	0.135	1.32	0.978	0.489
189	276343	3741981	Rock Chip	0.026	12.4	0.002	5.33	0.092	8.95	8.51	2.97	0.46	41.5	0.23	0.102	1.7	0.921	0.46
190	276408	3741990	Rock Chip	0.184	36.4	0.076	8.22	0.478	7.93	81.3	5.5	0.49	69.1	0.245	0.266	1.15	0.98	0.49
191	276465	3741993	Rock Chip	0.055	6.76	0.001	8.48	0.099	6.49	7.93	2.5	0.497	42.7	0.249	0.101	1.07	0.994	0.497
194	276189	3741744	Rock Chip	0.059	10.7	0.005	5.19	0.093	9.46	8.67	5.72	0.467	45.5	0.234	0.177	1.49	0.935	0.467
195	276246	3741750	Rock Chip	0.037	16.9	0.002	3.43	0.097	9.63	11.6	6.08	0.486	28.1	,.243	0.145	1.6	0.973	0.486
196	276305	3741756	Rock Chip	0.095	13.3	0.0006	6.03	0.097	10.6	13.1	6.31	0.484	42.9	0.242	0.208	1.58	0.967	0.484
197	276362	3741761	Rock Chip	0.043	11.8	0.001	5.13	0.094	11	15.6	2.87	0.468	52.8	0.253	0.137	1.9	0.936	0.468
198	276426	3741767	Rock Chip	0.031	12	0.002	5.76	0.092	7.85	8.27	2.84	0.458	43.9	0.229	0.1	1.26	0.916	0.458
199	276489	3741773	Rock Chip	0.035	16.2	0.0009	5.28	0.094	8.38	10.2	3.64	0.47	50	0.235	0.097	1.68	0.94	0.47
2152	275879	3741455	Rock Chip	0.014	5.98	0.0008	3.3	0.093	9.01	17.2	1.65	0.466	38.4	0.233	0.101	2.05	0.931	0.466
2153	275944	3741455	Rock Chip	0.017	8.56	0.001	3.29	0.093	5.75	18.1	6.79	0.466	28.4	0.233	0.143	2.05	0.931	0.466
2154	276009	3741448	Rock Chip	0.014	6.09	0.0005	3.28	0.093	7.54	13.8	2.58	0.471	34.3	0.235	0.113	1.72	0.942	0.471
2155	276072	3741446	Rock Chip	0.016	32.8	0.0005	3.64	0.096	10.6	10.8	20.7	0.482	41.7	0.241	0.131	2.56	0.963	0.482
2156	276131	3741435	Rock Chip	0.022	12	0.008	3.39	0.1	9.81	8.53	3.91	0.498	20.7	0.249	0.187	1.76	0.996	0.498
2157	276192	3741440	Rock Chip	0.238	82.8	0.02	5.66	0.098	31.3	24.5	2.85	2.96	32.6	0.265	1.19	2.18	0.98	0.49
2158	276255	3741447	Rock Chip	0.016	27.9	0.0008	3.2	0.092	45.3	10.8	2.54	0.46	30.1	0.412	0.195	2.14	0.921	0.46
2159	276322	3741453	Rock Chip	0.015	20.8	0.0005	2.88	0.098	6.9	12.3	2.59	0.49	29.3	0.245	0.155	2.05	0.98	0.49
2160	276381	3741459	Rock Chip	0.014	12.7	0.0005	2.23	0.096	8.53	10.4	0.445	0.478	13.3	0.239	0.22	1.51	0.956	0.478
2161	276436	3741463	Rock Chip	0.024	27.1	0.0005	3.38	0.099	5.52	11.9	1.99	0.493	25.9	0.247	0.246	1.57	0.986	0.493
2162	276497	3741469	Rock Chip	0.015	8.32	0.0005	2.88	0.097	6.33	7.99	0.714	0.484	34.8	0.242	0.112	1.43	0.969	0.484
2164	275833	3741709	Rock Chip	0.123	34.5	0.242	9.13	0.106	20.9	26.8	2.04	7.62	178	0.244	2.47	1.76	0.977	0.488
2165	275897	3741717	Rock Chip	0.015	10.6	0.0005	4.01	0.098	10.6	11.7	12.7	0.49	27.1	0.245	0.17	3.17	0.98	0.49
2166	275956	3741722	Rock Chip	0.014	5.92	0.0005	3.06	0.098	5.35	9.05	4.03	0.48	14.9	0.24	0.096	1.49	0.96	4.8

2167	276016	3741728	Rock Chip	0.018	6.48	0.002	4.03	0.097	9.81	10.6	7.65	0.486	31.3	0.253	0.104	1.78	0.973	0.486
2168	276070	3741732	Rock Chip	0.028	3.75	0.001	2.68	0.093	11.1	26.2	0.895	0.464	17.9	0.269	0.134	1.7	0.928	0.464
2169	276126	3741738	Rock Chip	0.233	10.8	0.03	4.37	0.17	14.5	12.9	4.4	0.476	36.8	0.306	0.18	1.91	0.952	0.476
259	275857	3742007	Rock Chip	0.084	6.16	0.026	3.41	0.099	7.67	13.8	5.76	0.494	33.4	0.247	0.11	2.12	0.988	0.494
260	276113	3741589	Rock Chip	0.039	8.38	0.004	3.4	0.099	7.95	15.1	4.05	0.493	36.6	0.247	0.174	1.69	1.28	0.493
261	276053	3741582	Rock Chip	0.203	7.97	0.0005	2.68	0.099	8.19	9.83	2.8	0.493	34.8	0.247	0.099	1.6	0.986	0.493
262	275992	3741575	Rock Chip	0.018	3.14	0.027	2.73	0.094	6.18	11	1.69	0.47	34.3	0.235	0.151	1.75	0.94	0.47
263	275932	3741570	Rock Chip	0.022	3.52	0.0005	3.8	0.099	8.28	12	0.452	0.497	34.9	0.249	0.099	1.63	1.38	0.497
264	275872	3741564	Rock Chip	0.015	9.6	0.0005	2.35	0.093	4.48	16.6	1.35	0.466	42.2	0.233	0.093	2.89	0.933	0.466
265	275811	3741558	Rock Chip	0.014	7.35	0.0005	3.12	0.095	7.26	20.8	6.19	0.476	34.1	0.238	0.16	2.21	0.952	476
266	275790	3741560	Rock Chip	0.016	5.64	0.0005	5.74	0.097	11.2	10.6	0.549	0.484	34.3	0.242	0.122	1.96	0.969	0.484
267	276173	3741597	Rock Chip	0.077	9.32	0.001	2.7	0.099	6	7.94	1.51	0.495	14.4	0.248	0.099	1.24	0.99	0.495
268	276232	3741602	Rock Chip	0.039	8.33	0.009	2.03	0.138	5.31	6.85	1.28	0.465	10.1	0.232	0.093	1.16	0.929	0.465
269	276293	3741609	Rock Chip	0.033	16.5	0.0005	1.82	0.099	11.3	11.7	1.83	0.46	14.1	0.23	0.142	1.78	0.919	0.46
270	276355	3741616	Rock Chip	0.029	22.4	0.002	2.86	0.098	8.58	6.28	3.71	0.491	35.8	0.246	0.202	1.49	0.982	0.491
271	276415	3741622	Rock Chip	0.021	9.05	0.0005	2.21	0.1	4.95	6.75	0.868	0.498	26.2	0.249	0.1	1.06	1.02	0.498
272	276470	3741627	Rock Chip	0.021	17.1	0.0005	6.12	0.095	7.59	8.15	2.05	0.473	28.7	0.236	0.108	1.09	0.945	0.473
273	276482	3741614	Rock Chip	0.029	29.2	0.0005	2.6	0.093	9.05	8.55	2	0.466	31.4	0.233	0.111	1.34	0.931	0.466
274	276118	3741808	Rock Chip	0.065	14.2	0.01	3.23	0.096	7.08	9.01	4.17	0.479	32.5	0.239	0.207	1.55	0.958	0.479
275	276182	3741815	Rock Chip	0.027	5.62	0.0005	2.08	0.095	4.82	9.22	0.504	0.475	14.6	0.238	0.095	1.12	0.951	0.475
276	276242	3741821	Rock Chip	0.023	11.9	0.003	2.89	0.093	8.55	8.89	1.5	0.467	24.2	0.234	0.145	1.92	0.935	0.467
277	276300	3741826	Rock Chip	0.016	9.65	0.0005	2.51	0.094	6.61	10.3	1.44	0.471	37.9	0.235	0.117	1.19	0.942	0.471
278	276360	3741831	Rock Chip	0.026	9.32	0.007	2.72	0.094	6.89	8.93	1.02	0.47	33.3	0.235	0.105	1.72	1.05	0.47
279	276423	3741839	Rock Chip	0.034	10.8	0.0005	2.26	0.095	6.73	9	1.96	0.473	44.9	0.236	0.106	1.33	0.95	0.473
280	276481	3741845	Rock Chip	0.02	10.6	0.028	2.7	0.093	7.05	8.31	2.86	0.465	39.9	0.232	0.095	1.52	0.929	0.465
281	276061	3741804	Rock Chip	0.223	8.1	0.003	2.97	0.098	9.63	8.67	3.29	0.492	22.7	0.246	0.098	1.21	0.984	0.492
282	276001	3741797	Rock Chip	0.03	2.82	0.004	2.85	0.094	7.17	9.9	6.02	0.472	16.6	0.236	0.094	1.4	0.943	0.472
283	275943	3741791	Rock Chip	0.026	1.79	0.0005	2.36	0.092	7.2	8.09	3.59	0.461	29.8	0.231	0.092	1.43	0.923	0.461
284	275880	3741786	Rock Chip	0.015	4.39	0.0005	2.36	0.1	6.54	12.8	14.4	0.498	19.8	0.249	0.1	2.05	0.996	0.498
288	275975	3742017	Rock Chip	0.394	15.4	0.079	7.84	0.094	12.4	8.99	3.46	0.47	40.3	0.235	0.094	2.32	0.94	0.47
290	276089	3742029	Rock Chip	0.15	6.26	0.01	6.41	0.097	22.4	3.26	2	0.483	15.6	0.241	0.097	1.9	0.965	0.483
291	276079	3742100	Rock Chip	0.028	13.9	0.0005	4.83	0.092	9.23	8.88	2	0.459	26.5	0.229	0.096	1.25	0.917	0.459
292	275964	3742089	Rock Chip	0.034	4.51	0.0005	3.98	0.098	8.16	8.71	2.2	0.488	22.4	0.244	0.098	1.66	0.977	0.488
293	275851	3742077	Rock Chip	0.036	3.56	0.0005	5.48	0.092	9.94	14.1	1.01	0.836	49.1	0.231	0.303	1.69	0.924	0.462

294	276194	3742107	Rock Chip	0.053	5.8	0.0005	5.17	0.095	8.44	8.93	1.08	0.473	36.3	0.236	0.121	1.36	0.945	0.473
295	276323	3742122	Rock Chip	0.037	4.26	0.0005	4.65	0.098	8.85	6.95	1.05	0.488	27.6	0.244	0.098	1.33	0.977	0.488
296	276445	3742134	Rock Chip	0.049	9.23	0.0005	4.38	0.091	9.55	7.62	2.91	0.457	36.9	0.229	0.109	1.18	0.914	0.457
297	276564	3742145	Rock Chip	0.028	5.45	0.0005	3.21	0.1	7.4	5.59	1.75	0.498	31.1	0.249	0.1	0.881	0.996	0.498
298	276684	3742155	Rock Chip	0.061	4.21	0.0005	4.7	0.099	13.5	10.2	1.3	0.494	24.8	0.247	0.099	1.01	0.988	0.494
300	275950	3742163	Rock Chip	0.032	3.34	0.0005	2.79	0.099	8.19	9.36	1.52	0.494	33.8	0.247	0.102	1.19	0.988	0.494
312	276224	3740921	Rock Chip	0.059	15.6	0.006	10.8	0.097	9.36	12.4	3.04	0.486	36	0.489	0.157	1.68	0.973	0.486
313	276165	3740914	Rock Chip	0.038	7.09	0.006	8.11	0.097	10.6	5.52	2.22	0.486	35.1	0.29	0.097	1.8	0.973	0.486
314	276107	3740910	Rock Chip	0.037	10.3	0.005	7.66	0.093	11.3	9.07	3.27	0.466	30.9	0.326	0.21	1.85	0.933	0.466
315	276044	3740904	Rock Chip	0.048	3.77	0.054	8.13	0.097	6.98	20.3	1.54	0.483	26.9	0.328	0.127	1.74	0.965	0.483
316	275988	3740900	Rock Chip	0.08	8.48	0.102	15.7	0.095	6.67	13.5	2.98	0.476	31.9	0.885	0.171	2.11	0.952	0.476
317	275924	3740898	Rock Chip	0.027	8.47	0.006	5.14	0.097	8.92	10.1	1.37	0.486	34.3	0.243	0.131	2.3	0.973	0.486
318	275911	3740989	Rock Chip	0.035	8.12	0.0006	13.9	0.097	5.97	10.9	2.62	0.486	33	0.289	0.122	2.28	0.973	0.486
319	275975	3740994	Rock Chip	0.047	5.99	0.004	15.9	0.099	8.93	13.6	2.07	0.494	32.9	0.294	0.139	2.24	0.988	0.494
320	276035	3740999	Rock Chip	0.059	13.5	0.005	6.03	0.093	10.5	10.3	19.5	0.467	28.1	0.297	0.157	2.33	0.935	0.467
321	276100	3741019	Rock Chip	0.032	9.32	0.0008	4.26	0.097	12.7	6.74	2.39	0.484	23	0.242	0.097	1.58	0.969	0.484
322	276166	3741030	Rock Chip	0.043	15.3	0.0008	5.09	0.094	8.01	10.9	4.44	0.469	43.2	0.407	0.102	2.2	0.938	0.469
323	276214	3741012	Rock Chip	0.066	3.58	0.0005	4.26	0.1	10.6	8	1.01	0.5	23.4	0.38	0.1	1.63	1	0.5
325	276182	3741309	Rock Chip	0.158	17.4	0.019	5.74	0.091	18	11.4	7.15	0.456	37.8	0.228	0.168	1.9	0.912	0.456
326	276245	3741315	Rock Chip	0.077	30.1	0.036	5.21	0.092	11.2	9.54	11.4	0.461	45	0.231	0.188	1.3	0.923	0.461
327	276306	3741300	Rock Chip	0.024	15.8	0.0005	2.49	0.097	16.4	7.15	3.83	0.483	22.5	0.241	0.104	1.17	0.965	0.483
328	276364	3741326	Rock Chip	0.035	4.59	0.0005	2.42	0.094	6.26	6.44	2.35	0.471	11.2	0.235	0.094	1.15	0.942	0.471
329	276420	3741332	Rock Chip	0.028	25.1	0.0005	3.58	0.096	12.4	8.7	5.29	0.481	33.4	0.24	0.112	1.36	0.962	0.481
330	276480	3741323	Rock Chip	0.028	19.4	0.0005	3.68	0.1	8.88	9.52	1.84	0.499	39	0.25	0.16	1.35	0.998	0.499
331	276542	3741328	Rock Chip	0.025	13.7	0.005	4.91	0.095	11.9	9.31	1.35	0.473	43.2	0.236	0.095	1.4	0.945	0.473
332	276262	3741405	Rock Chip	0.014	5.23	0.0005	2.14	0.095	5.65	4.64	1.53	0.474	20.5	0.237	0.095	0.544	0.949	0.474
333	276216	3741395	Rock Chip	0.048	12.9	0.008	2.3	0.094	14.7	6.34	2.02	0.471	9.44	0.235	0.098	1.14	0.942	0.471
334	276184	3741373	Rock Chip	0.343	37.6	0.137	3.84	0.093	10.6	8.06	11.3	0.463	31.5	0.231	0.139	1.29	0.926	0.463
335	276209	3741362	Rock Chip	0.165	22.8	0.328	3.02	0.096	9.97	8.58	6.06	0.48	14	0.24	0.096	1.21	0.96	0.48
337	275998	3741362	Rock Chip	0.017	6.04	0.0005	3.78	0.097	6.27	11.8	6.22	0.484	27.4	0.242	0.097	1.89	0.969	0.484
338	275956	3741362	Rock Chip	0.018	4.84	0.0005	3.27	0.091	5.25	13.9	2.79	0.457	36.6	0.229	0.091	1.53	0.914	0.457
339	275894	3741354	Rock Chip	0.014	5.17	0.0005	2.88	0.096	7.48	10.7	3.9	0.479	26.6	0.239	0.144	1.16	0.958	0.479
341	276122	3741358	Rock Chip	0.707	18.4	0.006	3.01	0.099	8.49	7.88	7.66	0.495	25.1	0.248	0.132	1.2	0.99	0.495
408	276135	3741664	Rock Chip	0.054	7.82	0.003	7.38	0.092	9.6	10.9	4.74	0.458	20.4	0.229	0.095	1.84	0.916	0.458

409	276079	3741657	Rock Chip	0.053	9.3	0.002	2.94	0.097	4.93	8.31	3.16	0.484	32.9	0.242	0.097	1.8	0.969	0.484
410	276017	3741653	Rock Chip	0.043	17.5	0.002	3.15	0.099	12.6	16.8	5.77	0.497	63.9	0.302	0.152	2.06	0.994	0.497
411	275960	3741645	Rock Chip	0.015	4.56	0.0005	2.86	0.099	7.44	17	7.33	0.497	15.2	0.325	0.099	2.14	0.994	0.497
412	275897	3741639	Rock Chip	0.016	6.14	0.0005	1.73	0.097	5.97	9.18	4.84	0.484	33.4	0.242	0.097	2.2	0.969	0.484
413	275838	3741634	Rock Chip	0.021	4.24	0.0005	2.73	0.099	7.04	10.6	1.17	0.497	24.8	0.249	0.102	1.91	0.994	0.497
414	276196	3741671	Rock Chip	0.083	9.09	0.002	2.43	0.097	4.46	14.5	1.4	0.484	16.7	0.242	0.097	2.46	0.969	0.484
415	276258	3741677	Rock Chip	0.027	22	0.0005	2.84	0.095	42.3	7.98	3.49	0.473	24.9	0.376	0.154	1.98	0.947	0.473
416	276315	3741684	Rock Chip	0.016	8.37	0.0005	2.73	0.094	3.43	7.51	1.83	0.47	43.4	0.235	0.128	1.99	0.94	0.47
417	276380	3741691	Rock Chip	0.024	11.2	0.0005	2.85	0.098	7.69	8.63	2.01	0.491	36.8	0.246	0.135	1.84	0.982	0.491
418	276440	3741698	Rock Chip	0.016	20.9	0.0005	2.82	0.096	4.59	6.71	2	0.48	39.8	0.24	0.123	1.55	1.19	0.48
419	276496	3741704	Rock Chip	0.033	11.5	0.015	3.71	0.098	7.84	11.7	4.17	0.488	24.9	0.244	0.098	2.67	1.17	0.488
421	276108	3741883	Rock Chip	0.023	3.07	0.0005	3.21	0.093	14.1	8.8	0.337	0.465	21.8	0.232	0.124	2.13	0.929	0.465
422	276053	3741877	Rock Chip	0.027	11.7	0.007	3.92	0.098	5.88	12.1	4.45	0.489	36.5	0.245	0.109	2.48	0.978	0.489
423	275990	3741872	Rock Chip	0.027	2.7	0.0005	3.2	0.097	9.07	9.29	1.73	0.487	12.2	0.244	0.097	2.04	0.975	0.487
424	275926	3741865	Rock Chip	0.024	4.34	0.017	2.81	0.096	3.71	8.98	1.95	0.482	36.8	0.241	0.096	1.97	0.963	0.482
425	275870	3741861	Rock Chip	0.019	2.68	0.0005	3.23	0.094	5.92	8.83	2.31	0.469	25.4	0.235	0.094	1.33	0.938	0.469
426	275814	3741854	Rock Chip	0.028	2.49	0.0006	2.49	0.097	5.21	10.9	3.8	0.483	22	0.241	0.098	1.79	0.965	0.483
428	276172	3741890	Rock Chip	0.021	3.15	0.0005	3.13	0.099	8.95	7.06	0.594	0.493	11.9	0.247	0.099	1.38	0.986	0.493
429	276234	3741895	Rock Chip	0.043	10.6	0.001	2.33	0.092	7.5	8.16	2.1	0.459	13.7	0.229	0.093	1.48	0.917	0.459
430	276293	3741901	Rock Chip	0.025	7.77	0.007	2.76	0.099	9.03	6.83	0.707	0.496	27.6	0.248	0.124	1.84	0.992	0.496
431	276352	3741906	Rock Chip	0.041	5.39	0.0005	2.34	0.095	7.98	7.72	1.08	0.473	34.3	0.237	0.095	1.5	0.947	0.473
432	276414	3741911	Rock Chip	0.017	11.7	0.0005	2.71	0.095	5.63	7.64	2.9	0.476	35.1	0.238	0.11	1.46	0.952	0.476
433	276472	3741917	Rock Chip	0.027	9.9	0.0005	4.08	0.097	7.51	8.36	2.96	0.484	40.3	0.242	0.102	1.79	0.967	0.484
434	276290	3740925	Rock Chip	0.017	10.7	0.0005	2.99	0.097	5.5	9.32	1.13	0.483	39.3	0.241	0.097	1.5	0.98	0.483
435	276351	3740931	Rock Chip	0.014	9.57	0.0005	3.74	0.092	8.73	9.16	1.84	0.458	39.3	0.229	0.092	1.71	0.916	0.458
436	276424	3740936	Rock Chip	0.017	10.3	0.0005	3.36	0.093	7.57	10.2	1.46	0.465	37.8	0.268	0.093	1.47	0.929	0.465
437	276470	3740940	Rock Chip	0.043	14.6	0.0007	2.4	0.093	5.98	11.4	4.81	0.466	37.5	0.233	0.093	0.96	0.933	0.466
438	276532	3740947	Rock Chip	0.027	11.5	0.0005	3.05	0.099	4.87	13.6	2.72	0.493	33.7	0.247	0.099	1.54	0.986	0.493
439	276516	3741037	Rock Chip	0.016	12.5	0.0005	3.1	0.097	9	12.1	0.954	0.483	30.2	0.241	0.097	1.34	0.965	0.483
440	276458	3741032	Rock Chip	0.02	9.08	0.0005	2.77	0.095	8.31	11.1	3.51	0.475	39.8	0.239	0.095	1.45	0.951	0.475
441	276409	3741028	Rock Chip	0.016	15.7	0.0005	3.09	0.098	6.43	12.2	5.76	0.488	41.7	0.367	0.098	2.22	0.977	0.488
442	276335	3741023	Rock Chip	0.059	7.58	0.0005	2.47	0.1	5.02	10.9	1.89	0.498	25.5	0.251	0.1	1.43	0.996	0.498
443	276277	3741018	Rock Chip	0.02	7.92	0.0005	2.4	0.091	8.38	11.4	2.48	0.456	28.7	0.302	0.091	1.33	0.912	0.456
444	276203	3741100	Rock Chip	0.019	15.2	0.0005	3.09	0.095	6.37	11	4.83	0.473	40.2	0.236	0.095	1.74	0.945	0.473

445	276266	3741104	Rock Chip	0.014	10.8	0.0005	2.5	0.092	5.01	7.78	3.96	0.461	41	0.231	0.092	1.58	0.923	0.461
446	276327	3741110	Rock Chip	0.023	15.7	0.0005	2.37	0.093	4.98	10.8	4.8	0.463	36	0.284	0.093	0.858	0.926	0.463
447	276390	3741115	Rock Chip	0.015	10	0.0005	2.06	0.098	7.49	7.91	1.08	0.491	28.6	0.246	0.098	0.995	0.982	0.491
448	276449	3741122	Rock Chip	0.014	4.33	0.0005	5.69	0.095	6.67	10.3	0.838	0.473	39.3	0.236	0.095	1.53	0.945	0.473
449	276509	3741128	Rock Chip	0.015	8.15	0.0005	3.25	0.099	6.33	9.49	0.699	0.496	38.7	0.248	0.099	1.61	0.992	0.496
466	276124	3741512	Rock Chip	0.095	13.5	0.021	3.53	0.097	10.5	6.75	2.21	0.486	29.5	0.243	0.102	1.79	0.973	0.486
467	276007	3741501	Rock Chip	0.035	4.05	0.002	6.94	0.1	5.7	14.7	2.03	0.498	32.8	0.314	0.232	2.38	0.996	0.498
468	275946	3741494	Rock Chip	0.028	3.28	0.002	3.84	0.092	6.13	9.21	1.49	0.462	34.4	0.231	0.146	1.93	0.924	0.462
469	275790	3741475	Rock Chip	0.03	2.24	0.003	3.51	0.095	4.67	9.94	1.36	0.473	30.9	0.237	0.116	1.76	0.947	0.473
470	275688	3741471	Rock Chip	0.028	3.24	0.003	3.5	0.092	4.94	10.2	2.39	0.459	36.7	0.229	0.104	1.99	0.917	0.459
471	275609	3741464	Rock Chip	0.044	4.36	0.0006	3.45	0.099	6.13	11.6	2.14	0.497	42	0.249	0.1	2.28	0.994	0.497
474	276307	3741531	Rock Chip	0.033	6.88	0.003	4.8	0.095	5.31	9.67	1.51	0.473	26.1	0.237	0.174	2.11	0.947	0.473
475	276369	3741539	Rock Chip	0.03	12.8	0.001	3.54	0.095	6.04	8.99	1.67	0.475	34	0.238	0.119	1.91	0.951	0.475
476	276426	3741544	Rock Chip	0.025	11.3	0.0007	3.73	0.099	4.9	8.4	1.53	0.494	33.2	0.247	0.126	1.86	0.988	0.494
477	276537	3741577	Rock Chip	0.027	15.9	0.003	2.76	0.094	5.53	7.02	1.97	0.485	34.7	0.235	0.094	1.55	0.938	0.469
481	275999	3741293	Rock Chip	0.015	7.1	0.0005	3.49	0.094	5.84	10.3	1.35	0.471	31.2	0.316	0.094	1.76	0.942	0.471
482	276001	3741278	Rock Chip	0.015	7.78	0.0005	3.62	0.097	8.87	11.6	4.23	0.487	34.7	0.244	0.132	2.1	0.975	0.487
483	275938	3741285	Rock Chip	0.016	6.66	0.0005	3.41	0.098	6.19	10.9	1.79	0.492	38.1	0.246	0.098	1.74	0.984	0.492
484	275880	3741280	Rock Chip	0.014	13.3	0.0005	2.88	0.097	5.8	13.7	4.35	0.483	40.6	0.241	0.097	1.76	0.972	0.483
485	275894	3741160	Rock Chip	0.022	10.1	0.0005	3.03	0.094	6.59	11.9	2.46	0.472	30.4	0.342	0.094	1.54	0.943	0.472
486	275960	3741166	Rock Chip	0.017	9.54	0.0008	2.96	0.092	9.41	11.2	3.5	0.46	30.2	0.276	0.092	1.47	0.919	0.46
487	276024	3741170	Rock Chip	0.014	8.14	0.0006	3.13	0.096	8.5	11.6	2.31	0.482	35.7	0.241	0.096	1.86	1.21	0.482
488	276076	3741175	Rock Chip	0.014	9.89	0.0005	3.11	0.093	8.19	11.6	2.43	0.464	34.7	0.339	0.093	2.17	0.928	0.464
489	276137	3741182	Rock Chip	0.015	8.13	0.0005	3.34	0.099	5.66	11	1.76	0.495	28.4	0.248	0.099	2.06	0.99	0.495
490	276195	3741185	Rock Chip	0.057	15	0.009	5.18	0.095	24.8	10.1	7.27	0.473	24.9	0.27	0.097	1.45	0.947	0.473
491	276257	3741192	Rock Chip	0.039	6.51	0.002	3.37	0.095	7.91	11.8	2.77	0.474	32.8	0.237	0.095	2.01	0.949	0.474
492	276317	3741197	Rock Chip	0.014	7.48	0.0005	3.76	0.092	9.18	11.1	1.71	0.46	29.4	0.23	0.092	1.81	0.921	0.46
493	276375	3741203	Rock Chip	0.015	12.5	0.0005	2.59	0.099	4.94	8.41	2.21	0.496	25.7	0.248	0.099	1.3	0.992	0.496
494	276440	3741210	Rock Chip	0.014	10.2	0.0005	3.61	0.091	10.1	7.74	1.28	0.456	38	0.228	0.091	1.4	0.912	0.456
495	276498	3741214	Rock Chip	0.118	9.42	0.008	3.77	0.099	8.69	8.98	3.73	0.494	26.2	0.247	0.099	1.74	0.988	0.494
496	276153	3741093	Rock Chip	0.018	9.96	0.0005	3.29	0.096	7.56	11.2	2.54	0.482	36.2	0.318	0.096	1.82	0.963	0.482
497	276085	3741086	Rock Chip	0.015	12.7	0.0005	3.59	0.099	6.59	13.6	3.29	0.493	39.1	0.263	0.099	2.54	0.986	0.493
498	276029	3741081	Rock Chip	0.015	8.1	0.0005	3.22	0.098	5.59	10.8	2.53	0.488	29.6	0.27	0.098	1.89	0.977	0.488
499	275968	3741076	Rock Chip	0.015	7.18	0.0005	3.65	0.098	9.56	12.4	3.68	0.491	32.6	0.246	0.098	2.66	0.982	0.491
500	275904	3741071	Rock Chip	0.014	8.54	0.0005	3.79	0.091	7.3	14	0.839	0.456	37.8	0.228	0.107	2.91	0.912	0.456

Geochemical Results for stream sediment sampling conducted by Sunshine Mining Company

Samp ID	Samp. Type	UTME	UTMN	Ag	As	Au	Cu	Hg	Mo	Pb	Sb	Tl	Zn	Bi	Cd	Ga	Se	Te
404	Stream Sed	277790.6717	3740913.91	5.18	5.64	0.197	1.45	0.117	1.67	20.5	2.2	0.494	43.7	0.78	0.128	2.01	0.247	0.056
406	Stream Sed	277423.0324	3741763.885	7.66	5.77	3	2.39	0.031	0.491	17.1	1.41	0.934	21.7	0.832	0.141	1.07	0.244	0.049
311	Stream Sed	276078.1872	3742808.101	41.5	3.93	2.87	9.42	0.027	0.982	12.9	0.575	0.494	37	0.237	0.161	2.93	0.247	0.049
464R	Stream Sed	277124.9963	3743298.851	0.223	8.03	0.038	16.5	0.1	4.44	47.8	1.58	0.499	56.3	0.25	0.649	1.66	0.998	0.499
2251	Stream Sed	275998.2554	3741272.108	14.9	5.87	0.197	4.59	0.075	1.39	14.9	1.88	0.494	31.4	0.485	0.244	1.74	0.247	0.049
2252R	Stream Sed	276120.4931	3741309.414	15.4	5.53	2.36	8.47	0.094	28.3	8.74	9.53	0.469	14.8	0.235	0.137	1.16	0.938	0.469
2253	Stream Sed	276099.8556	3741419.745	34.4	8.82	5.05	9.16	0.073	1.45	18.9	2.46	0.489	40.7	0.271	0.335	2.65	0.244	0.049
2254	Stream Sed	275974.0459	3741653.241	7.69	6.02	0.195	2.19	0.052	0.64	10.3	2.73	0.488	33.4	0.198	0.206	1.55	0.244	0.059
2255	Stream Sed	276066.6503	3741825.22	32.7	10.2	5.67	5.75	0.098	2.43	18.2	4.27	0.564	35.4	0.318	0.308	2.87	0.463	0.058
2256R	Stream Sed	276074.5878	3741817.283	13.1	10.8	1.47	12.3	0.097	28.6	36.8	7	0.486	24.6	0.243	0.421	0.754	0.973	0.486
2257	Stream Sed	276281.6247	3741434.033	11.3	24.3	0.918	3.33	0.06	8.27	12.9	3.12	0.492	20	0.22	0.23	1.13	0.246	0.049
2258	Stream Sed	276507.0431	3741364.496	11.8	11.3	0.198	4.07	0.054	0.326	15.3	3.42	0.495	36.2	0.201	0.337	1.26	0.247	0.049
2259R	Stream Sed	277045.1184	3742509.663	1.26	3.62	0.133	9.55	0.092	12.2	13	5.53	0.809	18.1	0.229	0.189	1.8	0.917	0.459
301	Stream Sed	278423.0712	3742613.777	2.91	5.36	1.29	1.52	0.019	0.601	7.12	1.24	0.485	16.8	0.155	0.073	0.768	0.243	0.065
302	Stream Sed	278513.5589	3742786.021	4.11	4.5	1.62	1.31	0.019	0.617	7.36	1.27	0.486	14.3	0.134	0.083	0.69	0.243	0.049
303	Stream Sed	277860.0367	3742898.602	72.5	3.32	75.9	1.6	0.02	1.37	6.81	1.64	0.496	22.7	0.104	0.058	1.17	0.248	0.051
304	Stream Sed	278284.2705	3743287.064	19.9	3.88	2.56	4.28	0.02	0.497	9.8	0.787	0.492	25.1	0.123	0.203	0.885	0.246	0.054
305	Stream Sed	277781.8522	3743432.532	24.9	3.6	3.17	4.78	0.051	0.548	10.4	0.627	0.495	24.3	0.121	0.198	1.19	0.247	0.049
306	Stream Sed	277749.8376	3743188.321	399	4.24	151	3.37	0.1	3.15	9.28	8.63	0.488	51.7	0.068	0.062	1.02	0.244	0.063
307	Stream Sed	277565.0257	3743005.097	6.67	6.16	1.95	3.46	0.105	0.502	11.2	1.23	0.495	25.2	0.183	0.139	1.43	0.248	0.06
308	Stream Sed	277734.3594	3743059.998	2.96	3.12	1.55	0.902	0.02	0.525	5.75	0.613	0.493	13.4	0.098	0.05	0.534	0.247	0.049
309	Stream Sed	276728.0411	3743365.473	2.97	5.99	1.29	6.69	0.02	2.19	6.14	1.19	0.494	14.7	0.124	0.083	0.612	0.247	0.049
310R	Stream Sed	279188.7504	3743162.273	1106	6.63	177	13	0.295	6.61	20.7	15.9	0.487	68.2	0.237	0.151	6.79	0.243	0.049
401	Stream Sed	276940.2991	3741380.371	12.9	8.88	0.198	4.4	0.056	0.325	12.4	1.14	0.495	38.7	0.157	0.131	1.15	0.248	0.05
402	Stream Sed	277044.016	3741433.817	8.57	49.98	0.2	2.07	0.059	0.344	9.71	1.44	0.499	29.3	0.185	0.162	1.19	0.25	0.05
403	Stream Sed	276897.4366	3741562.405	11.9	9.21	0.195	2.78	0.091	0.45	10.9	2.45	0.485	39.8	0.22	0.214	1.73	0.243	0.049
405	Stream Sed	277376.7302	3741548.249	5.52	3.79	0.197	3.47	0.047	0.331	19	0.781	0.494	23.9	2.61	0.136	1.24	0.247	0.073
407	Stream Sed	277218.0461	3742042.717	12.3	7.95	0.199	3.95	0.054	0.387	15.5	1.41	0.496	32	0.261	0.186	1.41	0.248	0.05
451	Stream Sed	275935.0771	3743079.476	9.61	4.19	1.75	9.42	0.061	1.04	16.8	0.728	0.494	27.9	0.393	0.348	1.04	0.247	0.084
452	Stream Sed	276566.9519	3742913.432	2.92	3.54	1.98	0.82	0.019	0.842	5.87	0.652	0.4986	12.4	0.113	0.039	0.543	0.243	0.071
453	Stream Sed	275870.5054	3742690.762	11.7	11.3	1.99	3.06	0.095	1.93	12.1	3.31	0.497	54.5	0.197	0.214	2.32	0.249	0.084
454	Stream Sed	275875.1357	3742589.559	2.96	7.62	1.58	4.29	0.043	0.881	6.64	1.52	0.493	53	0.093	0.115	1.85	0.247	0.099
455R	Stream Sed	276003.8487	3742644.601	0.436	8.49	0.078	7.51	0.097	8.14	15.4	3.27	2.34	72.4	0.244	0.587	1.21	0.975	0.487

456R	Stream Sed	276006.6268	3742615.629	6.06	3.13	0.173	8.6	0.099	31.4	13	4.29	0.72	8.35	0.249	0.101	0.664	0.994	0.497
457	Stream Sed	276724.7294	3742278.461	18.8	10.4	0.199	5.9	0.101	1.87	15	2.11	0.498	33.2	0.307	0.286	1.66	0.249	0.078
459	Stream Sed	276585.8229	3742456.394	6.04	7.32	0.198	1.98	0.042	0.658	7.08	1.29	0.494	21.7	0.177	0.118	0.992	0.366	0.054
463R	Stream Sed	277108.4598	3743400.716	0.092	13.4	0.002	11.2	0.094	11.6	59.1	1.41	1.4	105	0.235	0.594	2.13	0.938	0.469
465	Stream Sed	277207.1496	3743344.888	3648	16.7	336	20.6	0.452	7.93	40.5	38.4	0.698	91.6	0.277	0.245	5.98	0.294	0.127
480	Stream Sed	276628.8178	3742372.388	0.035	4.46	0.0008	5.46	0.099	7.86	12.1	1.94	0.724	44	0.38	0.147	1.9	0.99	0.495

Geochemical ICP results conducted for this study

Date	Samp. No.	Mine Name	Samp type	UTM E	UTM N	Au-ICP21 (ppm)	ME-XRF26 (%)															S-IR08 (%)	C-IR07 (%)
						Au	Al_2O_3	BaO	CaO	Cr2O3	Fe2O3	K2O	MgO	MnO	Na2O	P2O5	SiO2	SrO	TiO2	LOI 1000	Total	S	C
11/20/2016	BEL001	Bell	Rock	276018	3742604	0.024	12.06	0.02	0.64	<0.01	1.24	7.3	0.2	0.03	1.32	0.03	74.8	0.01	0.19	1.34	99.27	0.02	0.18
11/20/2016	BEL002	Bell	Soil	276018	3742604	0.403	8.76	0.02	0.11	0.01	1.3	5.69	0.08	0.05	0.31	0.01	82.82	<0.01	0.14	0.81	100.15	0.01	0.13
11/20/2016	BEL003	Bell	Soil	276018	3742604	0.168	8.59	0.02	0.41	0.01	1.18	5.45	0.15	0.09	0.38	0.01	81.48	<0.01	0.13	1.37	99.34	0.01	0.31
11/20/2016	BEL004	Bell	Rock	276018	3742604	0.201	6.99	0.02	0.08	0.01	0.89	4.75	0.03	0.04	0.13	0.01	86.54	<0.01	0.1	0.59	100.2	0.01	0.03
11/20/2016	BEL005	Bell	Soil	276115	3742575	0.006	11.61	0.03	0.53	<0.01	1.75	4.67	0.24	0.12	2.23	0.03	73.21	<0.01	0.3	4.61	99.41	0.02	2.05
11/20/2016	BEL006	Bell	Rock	276018	3742620	0.283	3.63	0.01	0.12	0.01	0.9	1.93	0.04	0.04	0.07	<0.01	91.6	<0.01	0.05	0.69	99.13	0.02	0.05
11/20/2016	BEL007	Bell	Rock	276018	3742620	<0.001	12.84	0.02	0.3	<0.01	1.36	5.34	0.15	0.06	3.3	0.01	75.76	<0.01	0.21	0.65	100.05	0.01	0.02
12/14/2016	BEL008	Bell	Soil	275993	3742661	0.397	5.52		0.12		0.95	3.71	0.09	0.11	0.23	0.01	88.35		0.08	0.71	94.36	0.01	0.12
12/14/2016	BEL009	Bell	Soil	275988	3742824	0.281	8.51		0.09		1.47	5.84	0.09	0.09	0.46	0.01	80.84		0.11	0.71	89.71	0.01	0.17
12/14/2016	BEL012	Bell	Soil	276000	3742845	0.418	9.7		0.13		2	6.11	0.2	0.07	0.37	0.02	79.74		0.17	1.26	90.07	0.01	0.24
3/25/2016	ROSE001	Rosedale	Soil	277223	3743363	2.1	7.15	0.03	0.24	0.01	1.16	5.03	0.09	0.22	0.29	0.01	83.63	0.01	0.1	1.1	99.13	0.01	0.34
3/25/2016	ROSE002	Rosedale	Soil	277223	3743363	0.011	11.78	0.04	0.12	0.01	3.1	4.66	0.46	0.05	0.94	0.05	74.7	0.01	0.2	2.31	99.61	0.48	0.07
3/25/2016	ROSE003	Rosedale	Soil	277223	3743363	0.125	10.66	0.03	0.12	0.01	1.39	7.11	0.11	0.21	0.49	0.02	78.18	0.01	0.16	0.97	99.56	0.01	0.07
3/25/2016	ROSE004	Rosedale	Soil	277223	3743363	3.61	7.6	0.08	0.3	<0.01	1.78	4.91	0.1	1.21	0.22	0.01	81.62	0.01	0.1	1.13	99.24	0.01	0.06
3/25/2016	ROSE005	Rosedale	Soil	277223	3743363	2.74	6.8	0.14	0.97	0.01	1.08	4.64	0.1	1.3	0.12	0.01	83.64	0.02	0.09	1.19	100.3	0.01	0.02
3/25/2016	ROSE006	Rosedale	Soil	277229	3743342	1.015	1.84	0.06	0.52	0.01	0.76	0.9	0.04	0.57	0.04	<0.01	94.42	0.01	0.02	0.69	99.98	0.02	0.02
3/11/2017	ROSE007	Rosedale	Soil	277095	3743427	0.021	12.98		0.44		2.3	4.32	0.49	0.17	0.85	0.04	75.3		0.24	2.61	86.76	<0.01	0.22
3/11/2017	ROSE008	Rosedale	Soil	276953	3743426	0.085	8.9		0.11		1.6	4.66	0.21	0.03	0.23	0.02	82.03		0.14	1.72	90.75	<0.01	0.19
6/30/2017	ROBB2	Rosedale	Soil	277313	3742927	0.045	9.66		0.13		1.57	5.93	0.19	0.1	0.94	0.01	79.5		0.16	1.14	89.67	<0.01	0.29
6/24/2017	BIG002	Big Rosa	Soil	274454	3745241	0.003	12.48		0.23		1.31	4.36	0.33	0.05	0.71	0.02	77.75		0.16	2.35	87.27	<0.01	0.22
6/24/2017	BIG003	Big Rosa	Soil	274402	3745355	0.003	12.54		0.22		1.3	4.57	0.24	0.04	0.97	0.02	76.87		0.21	2.86	87.3	<0.01	0.3
6/30/2017	LP10	Lane	Soil	276130	3746543	0.013	10.26		0.18		1.32	3.59	0.18	0.09	0.32	0.02	81.42		0.17	2.48	89.77	0.01	0.51

Date	Samp. No.	ME-MS81 (ppm)																		
		Ba	Ce	Cr	Cs	Dy	Er	Eu	Ga	Gd	Ge	Hf	Ho	La	Lu	Nb	Nd	Pr	Rb	Sm
11/20/2016	BEL001	155	96.2	40	4.97	7.88	5.5	0.49	20.8	6.95	<5	6.1	1.77	46.8	0.84	33.6	36.9	11.15	353	8.4
11/20/2016	BEL002	88.1	56.3	40	10.25	6.07	4.11	0.3	16.4	4.81	<5	4.3	1.29	25.2	0.63	23.1	20.6	6.16	304	5.23
11/20/2016	BEL003	114	57.4	30	13	6.55	4.33	0.32	17.8	5.29	<5	4.3	1.48	26	0.7	23.4	22.3	6.4	292	5.57
11/20/2016	BEL004	55.1	47	100	9.52	5.35	3.52	0.29	15.9	4.27	<5	3.5	1.13	20.5	0.5	22.4	18.5	5.31	255	4.43
11/20/2016	BEL005	191	70.6	20	7.09	7.94	4.85	0.64	16.8	6.65	<5	8.8	1.69	31.6	0.7	27.5	30.3	8.34	194.5	7.35
11/20/2016	BEL006	26.1	23.2	70	8.48	3.01	1.86	0.15	17.7	2.44	<5	1.8	0.62	11	0.26	9.5	9.3	2.72	124	2.62
11/20/2016	BEL007	57.1	113	20	8.95	10.75	6.5	0.61	20.4	9.97	<5	8	2.26	50.2	0.89	31.6	47.6	13.35	208	11.55
12/14/2016	BEL008	89	52.1	30	10.8	5.91	3.91	0.25	17.1	5.25	<5	2.7	1.15	16.8	0.45	12.3	18.6	4.69	214	4.34
12/14/2016	BEL009	102.5	64.3	20	12.85	8.21	5.28	0.34	15.8	7.26	<5	4.5	1.68	26.5	0.67	21.1	25.6	6.95	326	6.63
12/14/2016	BEL012	155	71.9	20	9.08	7.29	4.65	0.36	15.8	6.1	<5	4.5	1.53	28.3	0.63	22.6	25.4	7.02	319	5.55
3/25/2016	ROSE001	191.5	42.7	30	11.9	5.04	3.14	0.27	13.1	3.85	<5	3.3	1.07	19.6	0.48	16.8	15.7	4.62	244	3.79
3/25/2016	ROSE002	369	96.9	110	3.12	8.34	5.44	0.41	25.1	7.2	<5	9.6	1.79	49.1	0.8	34.8	39.7	10.95	156.5	8.43
3/25/2016	ROSE003	148	65.3	30	10.1	6.92	4.74	0.36	18.1	5.44	<5	5.3	1.54	30.4	0.72	27.6	25.4	7.41	345	6.04
3/25/2016	ROSE004	677	45.5	40	11.25	5.71	3.48	0.36	17.3	4.41	<5	2.9	1.17	20.8	0.52	16.8	18	5.16	239	4.28
3/25/2016	ROSE005	1255	35.9	30	10.25	4.53	2.94	0.2	16.2	3.78	<5	2.6	1.02	16.8	0.45	13.8	14.4	4.12	230	3.56
3/25/2016	ROSE006	598	5.8	60	5.55	1.23	0.6	0.09	13.7	1.02	<5	0.4	0.24	2.6	0.09	2.1	3.1	0.75	55.1	1.05
3/11/2017	ROSE007	122.5	84.9	20	18.75	7.92	5.81	0.42	23.5	6.4	<5	6	1.74	36.2	0.9	32.7	27.9	8.25	236	6.25
3/11/2017	ROSE008	79	51.7	30	14.7	5.74	3.78	0.27	18.9	4.79	<5	3.5	1.24	24.6	0.56	19.4	20.8	6.02	261	4.79
6/30/2017	ROBB2	155	66	20	20.3	6.9	4.64	0.45	14.4	5.69	<5	4.5	1.49	29.3	0.67	23.5	24.9	7.17	306	5.87
6/24/2017	BIG002	60.1	73.8	10	15.85	6.38	4.5	0.3	20.3	5.26	<5	5.9	1.39	36.3	0.74	33.5	25	7.65	219	5.09
6/24/2017	BIG003	76.9	86	10	3.33	9.87	6.46	0.44	18.9	8.4	<5	7	2.17	40.6	0.99	31.2	37.3	10.4	185.5	8.15
6/30/2017	LP10	69.6	60	20	11.9	6.03	4.29	0.38	19.7	4.53	<5	5.1	1.35	26.4	0.73	29.4	19.9	5.71	217	4.49

Date	Samp. No.	Sn	Sr	Ta	Tb	Th	Tm	U	V	W	Y	Yb	Zr	Ag	Cd	Co	Cu	Li	Mo	Ni	Pb	Sc	Zn
11/20/2016	BEL001	4	55.3	2.3	1.33	26.7	0.88	10.85	19	6	51.4	5.67	153	0.9	<0.5	3	4	20	1	5	20	3	49
11/20/2016	BEL002	3	43.2	1.6	0.87	17.35	0.65	5.84	12	5	40	4.09	107	7.5	<0.5	2	8	70	14	5	24	2	36
11/20/2016	BEL003	3	46	1.6	0.99	17.35	0.71	7.38	16	7	44	4.6	105	6.9	<0.5	2	8	70	19	6	30	2	51
11/20/2016	BEL004	2	34.2	1.3	0.78	14	0.58	4.03	11	3	34.5	3.52	83	12.4	<0.5	1	6	90	24	4	16	1	25
11/20/2016	BEL005	4	62.3	1.8	1.24	14.8	0.7	4.23	18	2	46.5	4.64	286	<0.5	<0.5	3	7	30	1	6	24	3	53
11/20/2016	BEL006	2	21.2	0.6	0.44	6.57	0.32	2.51	23	2	18.5	1.94	47	25.2	<0.5	1	9	100	55	4	8	1	17
11/20/2016	BEL007	3	17.6	2.2	1.68	21.5	0.98	5.11	7	3	62.1	6.05	236	<0.5	<0.5	1	1	30	1	2	23	3	68
12/14/2016	BEL008	2	32	0.7	0.91	12.45	0.5	3.7	9	5	36.2	3.21	68	10.2	<0.5	2	8	100	6	1	65	0.7	42
12/14/2016	BEL009	2	38.5	1.5	1.28	16.6	0.74	5.16	9	5	49.6	4.66	119	9.7	0.5	2	8	60	4	1	119	0.7	50
12/14/2016	BEL012	3	54.9	1.5	1.08	17.1	0.74	5.19	16	7	44.4	4.66	119	3.1	<0.5	2	7	50	3	3	39	1.1	57
3/25/2016	ROSE001	2	49	1.2	0.77	13.15	0.48	5.76	9	17	32.3	3.21	82	20.2	<0.5	2	17	80	6	5	26	1	64
3/25/2016	ROSE002	4	73.2	2.1	1.27	13.6	0.84	5.27	21	5	49.3	5.22	311	0.8	<0.5	2	39	10	24	37	78	2	53
3/25/2016	ROSE003	3	68.7	1.8	1.05	21.3	0.72	6.94	11	12	45.2	4.69	131	6.2	<0.5	1	14	40	3	6	28	2	87
3/25/2016	ROSE004	2	124	1	0.87	13.05	0.52	8.15	13	71	36.7	3.44	77	57.7	<0.5	2	47	100	8	6	67	2	121
3/25/2016	ROSE005	2	165.5	0.9	0.68	10.85	0.45	6.84	12	100	30.8	2.88	70	72.7	<0.5	3	44	110	9	6	43	1	110
3/25/2016	ROSE006	1	59.2	0.1	0.19	1.74	0.11	2.86	5	30	7.9	0.68	12	43.1	<0.5	<1	15	100	4	2	15	<1	46
3/11/2017	ROSE007	4	51.2	2.2	1.18	24.5	0.81	7.33	19	8	52.8	5.78	154	<0.5	<0.5	4	11	60	8	7	118	0.9	92
3/11/2017	ROSE008	2	54.9	1.3	0.87	16.25	0.54	4.69	19	11	35.6	3.6	96	1.4	<0.5	2	7	80	3	6	23	1.2	100
6/30/2017	ROBB2	3	33.3	1.7	1.04	17.95	0.71	4.17	7	12	43.9	4.49	124	1	<0.5	2	7	70	<1	2	33	0.9	54
6/24/2017	BIG002	4	37.4	2.4	0.96	26	0.69	4.55	7	6	43.7	4.99	135	<0.5	<0.5	1	2	30	2	1	25	0.8	39
6/24/2017	BIG003	4	50.6	2.3	1.54	22.6	1.02	4.6	8	3	60.4	6.58	188	<0.5	<0.5	<1	2	40	1	1	26	1.2	36
6/30/2017	LP10	3	65.8	2.1	0.86	21.1	0.7	5.49	12	6	42.1	4.74	127	0.5	<0.5	2	5	50	11	6	28	0.6	48

Date	Samp. No.	ME-MS42 (ppm)									
		As	Bi	Hg	In	Re	Sb	Sc	Se	Te	Tl
11/20/2016	BEL001	11.2	0.14	0.049	0.03	<0.001	3.66	0.7	<0.2	<0.01	0.23
11/20/2016	BEL002	12.8	0.12	0.141	0.024	<0.001	11.5	0.4	<0.2	0.02	0.13
11/20/2016	BEL003	13.6	0.12	0.15	0.022	0.001	10.95	0.5	<0.2	0.01	0.29
11/20/2016	BEL004	7.8	0.1	0.05	0.018	0.001	3.89	0.3	<0.2	0.01	0.28
11/20/2016	BEL005	6.2	0.15	0.036	0.025	<0.001	1.08	1	<0.2	0.01	0.08
11/20/2016	BEL006	8.3	0.06	0.047	0.011	0.001	5.01	0.2	<0.2	<0.01	0.31
11/20/2016	BEL007	6.6	0.07	0.011	0.029	<0.001	1.02	1.2	<0.2	<0.01	0.03
12/14/2016	BEL008	16.2	0.71	0.143			9.3		0.3	0.02	0.29
12/14/2016	BEL009	17.1	4.17	0.161			10.5		0.2	0.16	0.26
12/14/2016	BEL012	17.2	0.46	0.077			11		<0.2	<0.01	0.16
3/25/2016	ROSE001	13.7	0.1	0.183	0.023	<0.001	38.3	0.8	<0.2	0.04	0.19
3/25/2016	ROSE002	5.6	2.12	0.018	0.127	0.001	0.55	0.5	0.6	0.81	0.24
3/25/2016	ROSE003	19.3	0.12	0.224	0.033	<0.001	42.3	1	0.2	<0.01	0.11
3/25/2016	ROSE004	34.6	0.12	0.602	0.025	<0.001	126	1.1	0.3	0.06	0.65
3/25/2016	ROSE005	19.6	0.08	0.381	0.02	0.001	61.9	0.9	0.3	0.05	0.47
3/25/2016	ROSE006	7.4	0.02	0.112	<0.005	0.001	33.5	0.4	<0.2	<0.01	0.34
3/11/2017	ROSE007	29.5	0.35	0.285			1.58		<0.2	<0.01	0.34
3/11/2017	ROSE008	18.2	0.18	0.199			21.9		0.2	0.01	0.11
6/30/2017	ROBB2	14.5	0.47	0.071			16		<0.2	0.02	0.09
6/24/2017	BIG002	2.9	0.42	0.069			0.57		<0.2	<0.01	0.07
6/24/2017	BIG003	4.2	0.33	0.028			0.63		0.2	<0.01	0.12
6/30/2017	LP10	10.8	0.37	0.099			1.21		<0.2	<0.01	0.24

Appendix 5: XRD Analysis data for Rosedale district

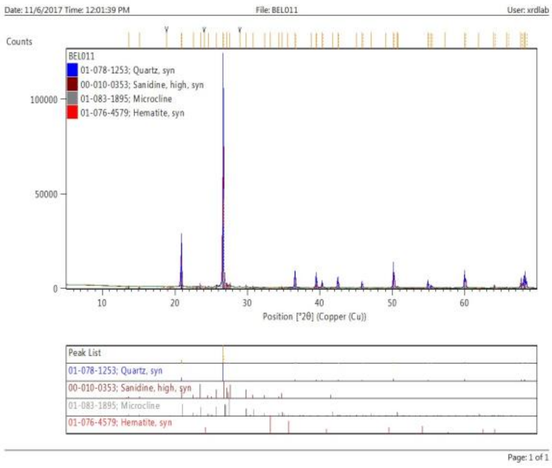

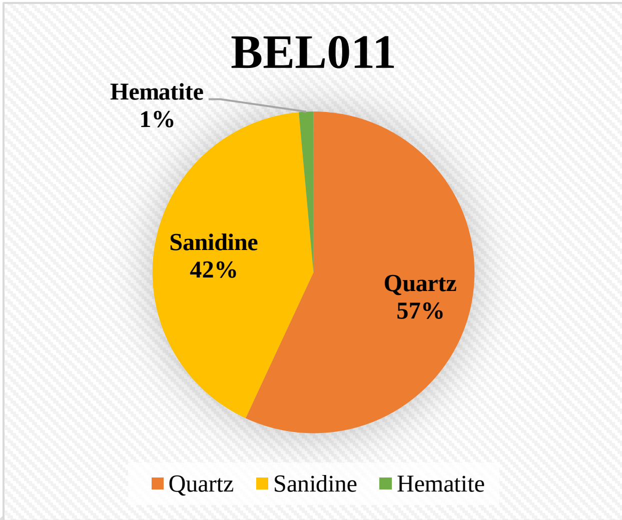

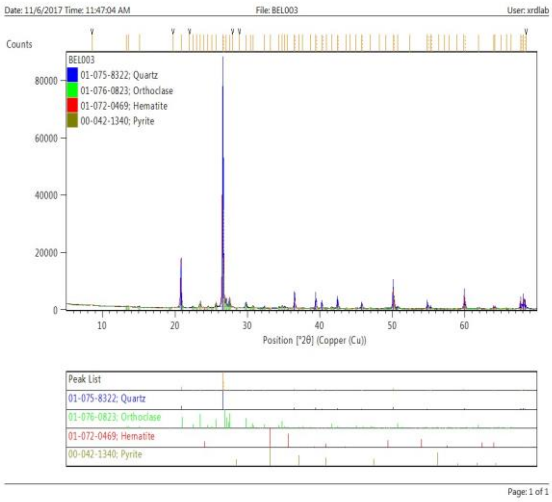

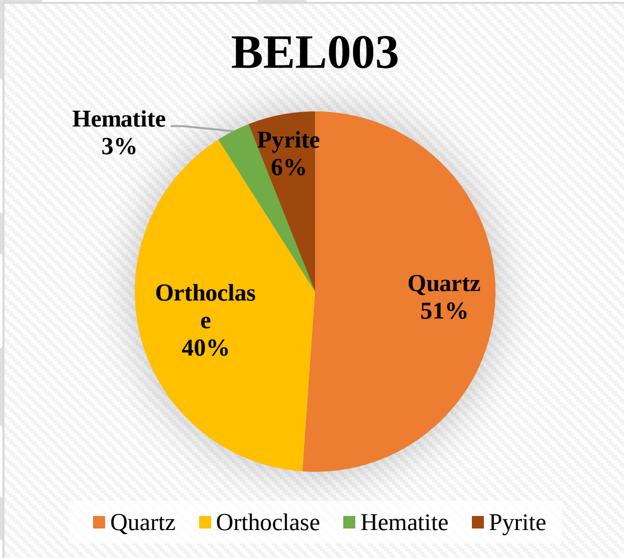

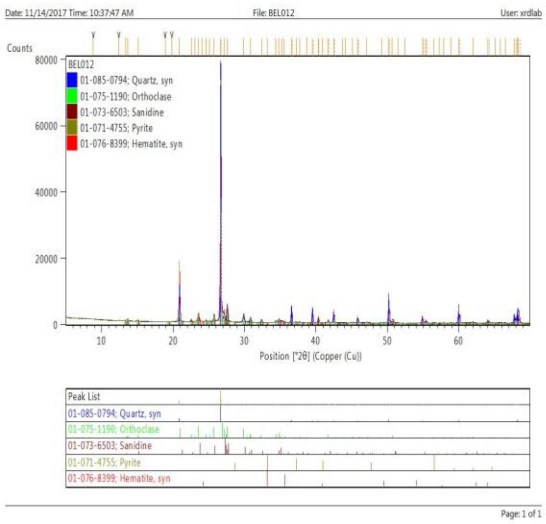

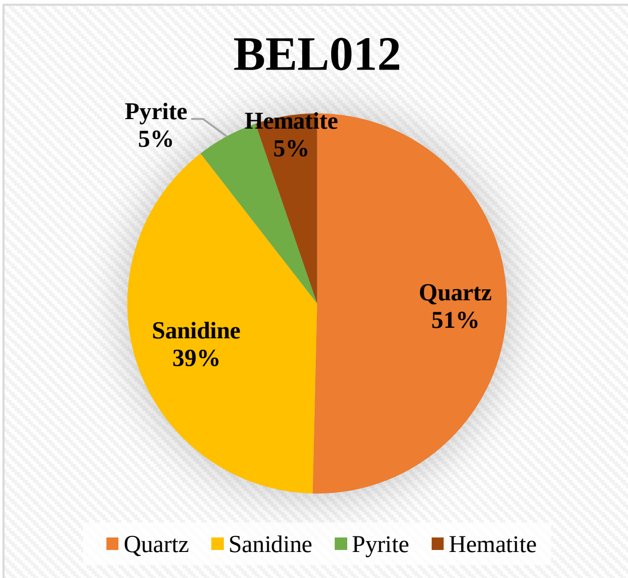

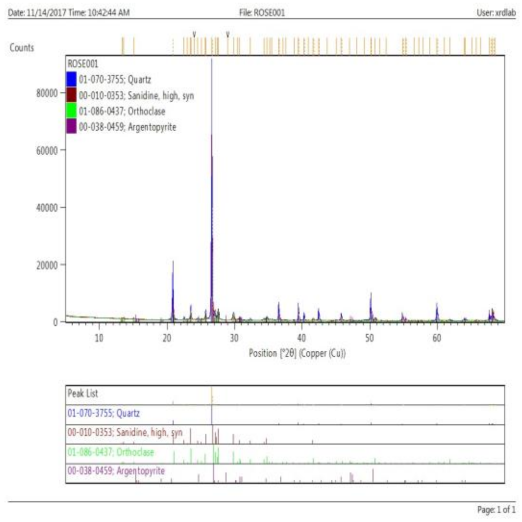

Date: 11/14/2017 Time: 10:42:44 AM
File: ROSE001
User: xrdlab
Counts
ROSE001
01-070-3755; Quartz
00-010-0353; Sanidine, high, syn
01-086-0437; Orthoclase
00-038-0459; Argentopyrite
80000
60000
40000
20000
0
10
20
30
40
50
60
Position [°2θ] (Copper (Cu))
Peak List
01-070-3755; Quartz
00-010-0353; Sanidine, high, syn
01-086-0437; Orthoclase
00-038-0459; Argentopyrite
Page: 1 of 1

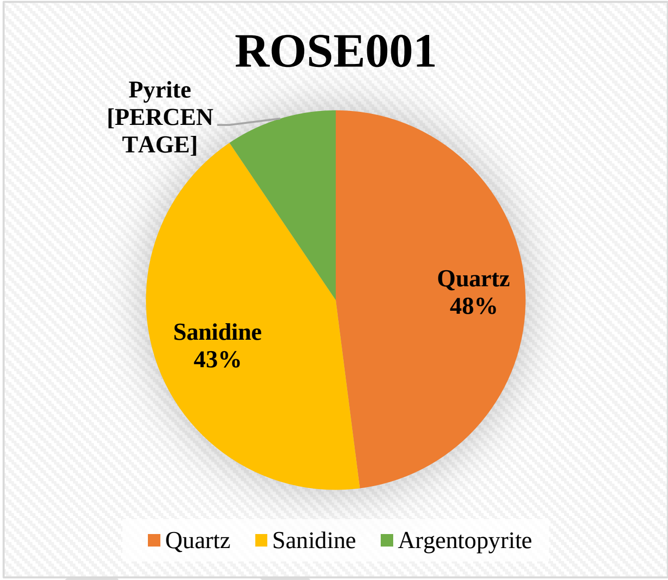

ROSE001
Pyrite [PERCENTAGE]
Quartz 48%
Sanidine 43%
Quartz
Sanidine
Argentopyrite

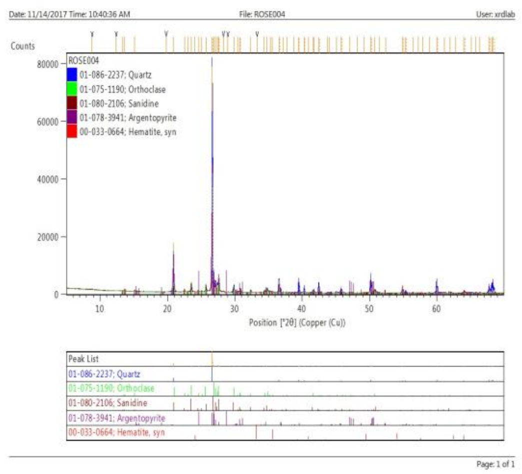

Date: 11/14/2017 Time: 10:40:36 AM
File: ROSE004
User: xrdlab
Counts
ROSE004
01-086-2237; Quartz
01-075-1190; Orthoclase
01-080-2106; Sanidine
01-078-3941; Argentopyrite
00-033-0664; Hematite, syn
80000
60000
40000
20000
0
10
20
30
40
50
60
Position [°2θ] (Copper (Cu))
Peak List
01-086-2237; Quartz
01-075-1190; Orthoclase
01-080-2106; Sanidine
01-078-3941; Argentopyrite
00-033-0664; Hematite, syn
Page: 1 of 1

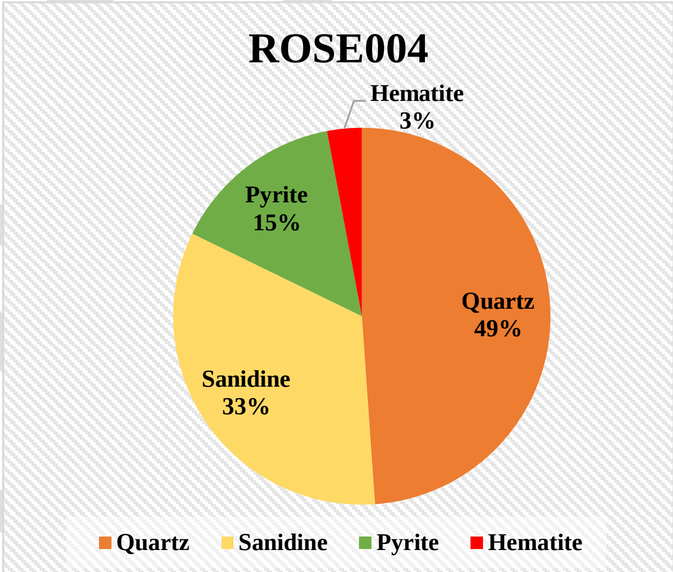

ROSE004
Hematite 3%
Pyrite 15%
Quartz 49%
Sanidine 33%
Quartz
Sanidine
Pyrite
Hematite

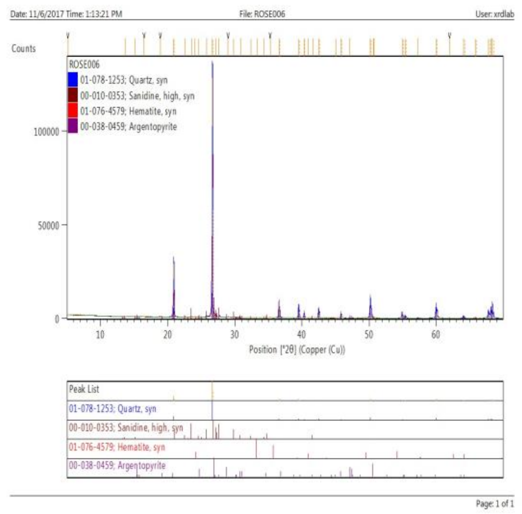

Date: 11/6/2017 Time: 1:13:21 PM
File: ROSE006
User: xrdlab
Counts
ROSE006
01-078-1253; Quartz, syn
00-010-0353; Sanidine, high, syn
01-076-4579; Hematite, syn
00-038-0459; Argentopyrite
100000
50000
0
10
20
30
40
50
60
Position [°2θ] (Copper (Cu))
Peak List
01-078-1253; Quartz, syn
00-010-0353; Sanidine, high, syn
01-076-4579; Hematite, syn
00-038-0459; Argentopyrite
Page: 1 of 1

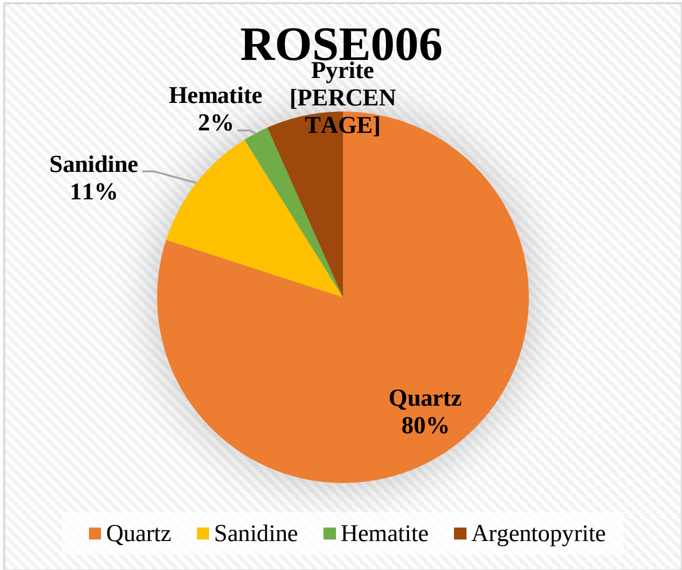

ROSE006
Pyrite [PERCENTAGE]
Hematite 2%
Sanidine 11%
Quartz 80%
Quartz
Sanidine
Hematite
Argentopyrite

Appendix 6: Net Neutralization Potential (NNP) for selected samples from the Rosedale district

Sample	S (%)	C (%)	AP (Kg CaCO3)	NP (total C)	NNP	NPR	NAGpH	ABA classification
ROSE1	0.01	0.34	0.31	28.32	28.01	90.63	6.23	Non-acid forming
ROSE2	0.48	0.07	15.00	5.83	-9.17	0.39	5.64	uncertain
ROSE3	0.01	0.07	0.31	5.83	5.52	18.66	6.04	Non-acid forming
ROSE4	0.01	0.06	0.31	5.00	4.69	15.99	6.15	Non-acid forming
ROSE5	0.01	0.02	0.31	1.67	1.35	5.33	5.73	Non-acid forming
ROSE007	0.01	0.22	0.31	18.33	18.01	58.64	6.34	Non-acid forming
ROSE008	0.01	0.19	0.31	15.83	15.51	50.65	4.92	Non-acid forming
BEL002	0.01	0.13	0.31	10.83	10.52	34.65	5.86	Non-acid forming
BEL003	0.01	0.31	0.31	25.82	25.51	82.63	5.39	Non-acid forming
BEL005	0.02	2.05	0.63	170.77	170.14	273.22	6.08	Non-acid forming
BEL008	0.01	0.12	0.31	10.00	9.68	31.99	5.36	Non-acid forming
BEL009	0.01	0.17	0.31	14.16	13.85	45.32	5.61	Non-acid forming
BEL012	0.01	0.24	0.31	19.99	19.68	63.97	5.11	Non-acid forming
ROBB2	0.01	0.29	0.31	24.16	23.84	77.30	5.69	Non-acid forming
BIG002	0.01	0.22	0.31	18.33	18.01	58.64	5.61	Non-acid forming
BIG003	0.01	0.3	0.31	24.99	24.68	79.97	6.27	Non-acid forming
LP10	0.01	0.51	0.31	42.48	42.17	135.95	6.67	Non-acid forming